Please check! Page 1 of 2

Review Your Abstract Before Submitting

This is how your work will appear to the public on the World Wide Web and in the printed book of abstracts.

Adsorption and diffusion of benzene in the nanoporous catalysts FAU, ZSM-5 and MCM-22: A molecular dynamics study

Ratana Rungsirisakun, Tanin Nanok, and **Jumras Limtrakul**, Department of Chemistry, Kasetsart University, Department of Chemistry, Faculty of Science, Kasetsart University, Phaholyothin Rd., Ladyao, Jatujak, Bangkok 10900, Thailand, Fax: 662-9428900 ext 324, rmuayy@yahoo.com, fscijrl@ku.ac.th

Molecular dynamics (MD) simulations of benzene in siliceous zeolites (FAU, ZSM-5, and MCM-22) were performed at loadings of 1, 2, 4, 8, and 16 molecules per unit cell. The potential energy functions for these simulations were constructed in a semi-empirical way from existing potentials and experimental energetic data. The MD simulations were employed to analyze the dynamic properties of the benzene-zeolite systems. The adsorption energies of benzene/siliceous zeolite complexes increase with increasing loading number, due to the intermolecular attraction between benzene molecules. The self-diffusion coefficient of benzene in siliceous zeolites decreases with increasing loading due to the steric hindrance between the sorbates passing each other. From the zeolite-benzene radial distribution functions it was found that the benzene molecules are relatively far from each other, about 5.2 Å for siliceous FAU, 5.2 Å for siliceous ZSM-5, and 4.8 Å for siliceous MCM-22. In the case of FAU, the benzene molecules prefer to be adsorbed parallel to the surface of the sodalite cage above the six-membered-ring. In ZSM-5, we found a T structure of the benzene molecules at loadings 2, 4, and 8 molecules per unit cell. At loadings of 16 molecules per unit cell, the molecules are lined up along the straight channel and their movement is highly correlated. For MCM-22 we found adjacent benzene molecules at a loading of 4 molecules with an orientation similar to the stacked conformation of benzene dimer in the gas phase.

not yet rated

Abstract ID#: 934099 **Password:** 699089

Program Selection: Division of Inorganic Chemistry

Topic Selection: Computational Chemistry

Title: Adsorption and diffusion of benzene in the nanoporous catalysts FAU, ZSM-5 and MCM-22: A molecular

dynamics study

Lead Presenter's Email: fscijrl@ku.ac.th

Invited: N

Presentation Format: Poster Only

Consider for Sci-Mix: N Conforms to Bylaw 6: Y

First Author

Ratana Rungsirisakun
Department of Chemistry
Kasetsart University
Department of Chemistry, Faculty of Science, Kasetsart University
Phaholyothin Rd., Ladyao, Jatujak
Bangkok, 10900
Thailand

Phone Number: 662-9428900 ext 329 Fax Number: 662-9428900 ext 324 Publishable Email: rmuayy@yahoo.com

Second Author

Tanin Nanok Department of Chemistry Please check! Page 2 of 2

Kasetsart University

Department of Chemistry, Faculty of Science, Kasetsart University

Phaholyothin Rd., Ladyao, Jatujak

Bangkok, 10900

Thailand

Phone Number: 662-942-8900 ext 323 **Fax Number:** 662-942-8900 ext 324 **Publishable Email:** g4384022@ku.ac.th

Third Author

Presenting

Jumras Limtrakul
Department of Chemistry
Kasetsart University
Department of Chemistry, Faculty of Science, Kasetsart University
Phaholyothin Rd., Ladyao, Jatujak
Bangkok, 10900
The item d

Thailand

Phone Number: 662-942-8900 ext 323 Fax Number: 662-942-8900 ext 324 Publishable Email: fscijrl@ku.ac.th

1. CHECK THAT:

- Your abstract title is in **Sentence case**. An example: Engineering gene expression of *Escherichia coli* by mRNA: Applications in molecular biology
- Your title does not begin with "The" (this will be removed during editing).
- Your title does not end with a period.

2. MAKE NECESSARY CORRECTIONS:

- Click any value in the Abstract Control Panel you want to change (e.g., Title, Author names)
- Edit the information and click the submit button.

3. AFTER PROOFING AND MODIFYING YOUR ABSTRACT, SUBMIT IT TO YOUR PROGRAM OFFICIALS FOR REVIEW:

After submitting, your paper can be viewed by your session organizer and program chair. You can make changes up until the call for papers deadline date. After this, it will be reviewed and scheduled.

4. CLICK HERE TO PRINT THIS PAGE NOW.

Submit to Program Officials

Please check! Page 1 of 2

Review Your Abstract Before Submitting

This is how your work will appear to the public on the World Wide Web and in the printed book of abstracts.

Periodic study of the interactions of rhodium (110) and (111) surfaces of ceria

Somkiat Nokbin¹, Kersti Hermansson², and **Jumras Limtrakul**¹. (1) Department of Chemistry, Kasetsart University, Department of Chemistry, Faculty of Science, Kasetsart University, Phaholyothin Rd., Ladyao, Jatujak, Bangkok 10900, Thailand, Fax: 662-942-8900 ext 324, somkiat.nokbin@gmail.com, fscijrl@ku.ac.th, (2) Materials Chemistry, Uppsala University

The interactions of $Rh/CeO_2(110)$ and $Rh/CeO_2(111)$ systems have been studied by means of periodic plane-wave density functional calculations using the VASP code and PAW method. The adsorption site dependence as well as the coverage dependence of such surfaces has been studied. Three types of interaction energies have been calculated to help characterize the metal-oxide interaction: the energy of adsorption of Rh atoms (E_{ads}), the energy of adhesion of a Rh overlayer (Eadh) and the formation-of-the-Rh-layer energy (E_{form}). As for adsorption site dependence, the 1 ML coverage of Rh overlayer was selected to study for all cases. Two adsorption sites, the surface oxygen (O_s) and the surface cerium (Ce_s) sites, were explored for (110) orientation and three adsorption sites for (111) surfaces, i.e., the surface oxygen (O_s) , the subsurface cerium (Ce_{ss}) and the subsurface oxygen (O_{ss}) , were investigated as well. As a result, we find that the adsorption site preferences are in the order $O_{s} > Ce_{s}$ and $O_s > O_{ss} > Ce_{ss}$ for (110) and (111) orientations, respectively. In case of coverage dependence, 1/2 and 1 ML coverages of Rh were studied at Os adsorption site for both (110) and (111) surfaces. We find that, at the high coverage, the metal-metal interactions within the Rh overlayer give the largest contribution to the stabilization of the Rh/CeO₂ interface, given rise of adsorption energy with the increasing surface coverage, while, naturally, the Rh-oxide interaction dominates at low coverage. The electronic properties, e.g., the density of states (DOS), electron density difference plot, spin density and the electron localization function (ELF), are presented in this study.

not yet rated

Abstract ID#: 934079 **Password:** 749875

Program Selection: Division of Inorganic Chemistry

Topic Selection: Inorganic Catalysts

Title: Periodic study of the interactions of rhodium (110) and (111) surfaces of ceria

Lead Presenter's Email: fscijrl@ku.ac.th

Invited: N

Presentation Format: Poster Only

Consider for Sci-Mix: N Conforms to Bylaw 6: Y

First Author

Somkiat Nokbin
Department of Chemistry
Kasetsart University
Department of Chemistry, Faculty of Science, Kasetsart University
Phaholyothin Rd., Ladyao, Jatujak
Bangkok, 10900
Thailand

Phone Number: 662-942-8900 ext 323 **Fax Number:** 662-942-8900 ext 324

Publishable Email: somkiat.nokbin@gmail.com

Please check! Page 2 of 2

Second Author

Kersti Hermansson Materials Chemistry Uppsala University The Ångström Laboratory Box 538 Uppsala, SE-751 21 Sweden

Phone Number: +46 18 4713767 **Fax Number:** +46 18 513548

Publishable Email: kersti@mkem.uu.se

Third Author

Presenting

Jumras Limtrakul
Department of Chemistry
Kasetsart University
Department of Chemistry, Faculty of Science, Kasetsart University
Phaholyothin Rd., Ladyao, Jatujak
Bangkok, 10900
Thailand

Phone Number: 662-942-8900 ext 323 Fax Number: 662-942-8900 ext 324 Publishable Email: fscijrl@ku.ac.th

1. CHECK THAT:

- Your abstract title is in **Sentence case**. An example: Engineering gene expression of *Escherichia coli* by mRNA: Applications in molecular biology
- Your title does not begin with "The" (this will be removed during editing).
- Your title does not end with a period.

2. MAKE NECESSARY CORRECTIONS:

- Click any value in the Abstract Control Panel you want to change (e.g., Title, Author names)
- Edit the information and click the submit button.

3. AFTER PROOFING AND MODIFYING YOUR ABSTRACT, SUBMIT IT TO YOUR PROGRAM OFFICIALS FOR REVIEW:

After submitting, your paper can be viewed by your session organizer and program chair. You can make changes up until the call for papers deadline date. After this, it will be reviewed and scheduled.

4. CLICK HERE TO PRINT THIS PAGE NOW.

Submit to Program Officials

Please check! Page 1 of 2

Review Your Abstract Before Submitting

This is how your work will appear to the public on the World Wide Web and in the printed book of abstracts.

Reaction mechanisms of nitrous oxide decomposition on carbon nanotubes

Supawadee Namuangruk, Pipat Khongpracha, and **Jumras Limtrakul**, Department of Chemistry, Kasetsart University, Department of Chemistry, Faculty of Science, Kasetsart University, Phaholyothin Rd., Ladyao, Jatujak, Bangkok 10900, Thailand, Fax: 662-9428900 ext 324, dakojung@hotmail.com, fscijrl@ku.ac.th

The reaction mechanisms of nitrous oxide decomposition on the sidewall of armchair (5,5)-SWNTs have been investigated by ONIOM(B3LYP/6-31G(d):AM1) calculation. The stepwise and concerted mechanisms have been proposed. For the stepwise mechanism, the predicted activation barrier for the cycloaddition (35.94 kcal/mol) is found to be higher than that for the releasing of the nitrogen molecule to form an epoxy adduct (22.60 kcal/mol) and is expected to be the rate-determining step. This reaction is exothermic by -39.34 kcal/mol and is predicted to be a thermochemical reaction. For the concerted mechanism which involves the single step, the activation barrier is evaluated to be 50.82 kcal/mol. Therefore, the nitrous oxide decomposition on the sidewall of armchair (5,5)-SWNTs favors to proceeding via the stepwise mechanism.

not yet rated

Abstract ID#: 934000 **Password:** 264426

Program Selection: Division of Inorganic Chemistry

Topic Selection: Computational Chemistry

Title: Reaction mechanisms of nitrous oxide decomposition on carbon nanotubes

Lead Presenter's Email: fscijrl@ku.ac.th

Invited: Y

Presentation Format: Poster Only

Consider for Sci-Mix: N Conforms to Bylaw 6: Y

First Author

Supawadee Namuangruk Department of Chemistry Kasetsart University

Department of Chemistry, Faculty of Science, Kasetsart University

Phaholyothin Rd., Ladyao, Jatujak

Bangkok, 10900

Thailand

Phone Number: 662-9428900 ext 323 **Fax Number:** 662-9428900 ext 324

Publishable Email: dakojung@hotmail.com

Second Author

Pipat Khongpracha
Department of Chemistry
Kasetsart University
Department of Chemistry, Faculty of Science, Kasetsart University
Phaholyothin Rd., Ladyao, Jatujak
Bangkok, 10900
Thailand

Phone Number: 662-9428900 ext 323 Fax Number: 662-9428900 ext 324 Publishable Email: jiko_yo@hotmail.com Please check! Page 2 of 2

Third Author

Presenting

Jumras Limtrakul
Department of Chemistry
Kasetsart University
Department of Chemistry, Faculty of Science, Kasetsart University
Phaholyothin Rd., Ladyao, Jatujak
Bangkok, 10900
Thailand

Phone Number: 662-942-8900 ext 323 Fax Number: 662-942-8900 ext 324 Publishable Email: fscijrl@ku.ac.th

1. CHECK THAT:

- Your abstract title is in **Sentence case**. An example: Engineering gene expression of *Escherichia coli* by mRNA: Applications in molecular biology
- Your title does not begin with "The" (this will be removed during editing).
- Your title does not end with a period.

2. MAKE NECESSARY CORRECTIONS:

- Click any value in the Abstract Control Panel you want to change (e.g., Title, Author names)
- Edit the information and click the submit button.

3. AFTER PROOFING AND MODIFYING YOUR ABSTRACT, SUBMIT IT TO YOUR PROGRAM OFFICIALS FOR REVIEW:

After submitting, your paper can be viewed by your session organizer and program chair. You can make changes up until the call for papers deadline date. After this, it will be reviewed and scheduled.

4. CLICK HERE TO PRINT THIS PAGE NOW.

Submit to Program Officials

Please check! Page 1 of 2

Review Your Abstract Before Submitting

This is how your work will appear to the public on the World Wide Web and in the printed book of abstracts.

Effect of the zeolite framework on the adsorption of alkenes to ZSM-5 zeolite: An ONIOM study

Supawadee Namuangruk¹, Duangkamol Tantanak², and **Jumras Limtrakul**¹. (1) Department of Chemistry, Kasetsart University, Department of Chemistry, Faculty of Science, Kasetsart University, Phaholyothin Rd., Ladyao, Jatujak, Bangkok 10900, Thailand, Fax: 662-942-8900 ext 324, dakojung@hotmail.com, fscijrl@ku.ac.th, (2) Chemistry Department, Faculty of Science, King Mongkut's Institute of Technology Ladkrabang

The structures and energetics associated with the adsorption of ethene and 4 butene isomers on HZSM-5 zeolite have been studied using a 46T cluster and calculated at ONIOM2(B3LYP/6-311++G (d,p):UFF) level. The adsorption energy for ethylene-zeolite complex is predicted to be -8.17 kcal/mol, which is in good agreement with the experimental data of -9.0 kcal/mol. The trend of the calculated adsorption energies (kcal/mol) for the butene isomers is; 1-butene (-16.06) > cis-2-butene (-13.62) \approx trans-2-butene (-13.25) > isobutene (-6.96). The isobutene-zeolite complex is the least stable due to the most steric repulsion between the methyls substituted around the C=C bond and zeolite framework, the more substituted the more steric and the lower the adsorption energy that is found. Although the ONIOM results indicate that isobutene hardly approaches the acid site and have a poorer bind interaction with the zeolite framework, but NBO analysis shows that it has the most electron density transfer and the largest overlapping stabilization energy. These findings relate the reason why ZSM-5 is selective towards isobutene from n-butene and indicate that acidic proton from the zeolite is easy to transfer to isobutene. Thus, further catalytic conversion of isobutene would be more facile.

not yet rated

Abstract ID#: 933860 **Password:** 551274

Program Selection: Division of Inorganic Chemistry

Topic Selection: Nanoscience - Application

Title: Effect of the zeolite framework on the adsorption of alkenes to ZSM-5 zeolite: An ONIOM

study

Lead Presenter's Email: fscijrl@ku.ac.th

Invited: N

Presentation Format: Poster Only

Consider for Sci-Mix: N Conforms to Bylaw 6: Y

First Author

Supawadee Namuangruk
Department of Chemistry
Kasetsart University
Department of Chemistry, Faculty of Science, Kasetsart University
Phaholyothin Rd., Ladyao, Jatujak
Bangkok, 10900
Thailand

Publishable Email: dakojung@hotmail.com

Please check! Page 2 of 2

Second Author

Duangkamol Tantanak Chemistry Department, Faculty of Science King Mongkut's Institute of Technology Ladkrabang Bangkok, 10520 Thailand

Phone Number: (662) 3264111 ext 6234

Fax Number: (662) 3264415

Publishable Email: ktduangk@kmitl.ac.th

Third Author

Presentina

Jumras Limtrakul
Department of Chemistry
Kasetsart University
Department of Chemistry, Faculty of Science, Kasetsart University
Phaholyothin Rd., Ladyao, Jatujak
Bangkok, 10900
Thailand

Phone Number: 662-942-8900 ext 323 Fax Number: 662-942-8900 ext 324 Publishable Email: fscijrl@ku.ac.th

1. CHECK THAT:

- Your abstract title is in **Sentence case**. An example: Engineering gene expression of *Escherichia coli* by mRNA: Applications in molecular biology
- Your title does not begin with "The" (this will be removed during editing).
- Your title does not end with a period.

2. MAKE NECESSARY CORRECTIONS:

- Click any value in the Abstract Control Panel you want to change (e.g., Title, Author names)
- Edit the information and click the submit button.

3. AFTER PROOFING AND MODIFYING YOUR ABSTRACT, SUBMIT IT TO YOUR PROGRAM OFFICIALS FOR REVIEW:

After submitting, your paper can be viewed by your session organizer and program chair. You can make changes up until the call for papers deadline date. After this, it will be reviewed and scheduled.

4. CLICK HERE TO PRINT THIS PAGE NOW.

Submit to Program Officials

Please check! Page 1 of 3

Review Your Abstract Before Submitting

This is how your work will appear to the public on the World Wide Web and in the printed book of abstracts.

Oxidative dehydrogenation of propane over a nanostructured Fe-ZSM-5 catalyst for propylene production: A combined QM/MM pathway analysis

Suwat Pabchanda, Tanin Nanok, Supawadee Namuangruk, Pilin Limtrakul, and **Jumras Limtrakul**, Department of Chemistry, Kasetsart University, Department of Chemistry, Faculty of Science, Kasetsart University, Phaholyothin Rd., Ladyao, Jatujak, Bangkok 10900, Thailand, Fax: 662-942-8900 ext 324, pabchanda@rocketmail.com, fscijrl@ku.ac.th

The reaction mechanism of oxidative dehydrogenation of propane over Fe-ZSM-5 zeolite for propylene production has been investigated using a 46T nanocluster of Fe-ZSM-5 zeolite by the ONIOM2(B3LYP/6-311+G (3df,2p):UFF) method. Stepwise and concerted mechanisms of propane oxydehydrogenation on the iron active site of Fe-ZSM-5 zeolite, [FeO₂]⁺, are considered. The adsorption energy of propane is evaluated to be -13.5 kcal/mol. For the stepwise mechanism, the secondary C-H bond dissociation of propane has an activation energy of 11.1 kcal/mol, which is lower than the hydrogen abstraction of primary carbon with an energy barrier of 14.7 kcal/mol, which agrees relatively well with the homolytic bond dissociation energies. The reaction for both then proceeds preferably via a rapid recombination of the propyl radical and the a-oxygen (O- species) which forms the highly stable proproxide which in turn is strongly adsorbed on the iron active site. Subsequently, the propylene product can be formed by the other C-H bond dissociation with an activation energy of 56.4 kcal/mol, which is the rate-limiting step of the stepwise mechanism. For the concerted mechanism, the oxidative dehydrogenation of propane takes place in a single reaction step without the proproxide formation. The primary and the secondary C-H bond dissociations occur simultaneously with an energy barrier of 29.4 kcal/mol, which is close to the summation of the activation energies of the initial hydrogen abstraction at the primary carbon and at the secondary carbon. The propylene produced can be desorbed and requires an energy of 16.8 kcal/mol.

not yet rated

Abstract ID#: 948288 Password: 340136

Program Selection: Division of Petroleum Chemistry

Topic Selection: Chemistry of Petroleum and Emerging Technologies

Title: Oxidative dehydrogenation of propane over a nanostructured Fe-ZSM-5 catalyst for propylene production:

A combined QM/MM pathway analysis **Lead Presenter's Email:** fscijrl@ku.ac.th

Invited: Y

Presentation Format: Oral Consider for Sci-Mix: N Conforms to Bylaw 6: Y

First Author

Suwat Pabchanda
Department of Chemistry
Kasetsart University
Department of Chemistry, Faculty of Science, Kasetsart University
Phaholyothin Rd., Ladyao, Jatujak
Bangkok, 10900
Thailand

Phone Number: 662-942-8900 ext 323 **Fax Number:** 662-942-8900 ext 324

Publishable Email: pabchanda@rocketmail.com

Second Author

Tanin Nanok
Department of Chemistry
Kasetsart University
Department of Chemistry, Faculty of Science, Kasetsart University
Phaholyothin Rd., Ladyao, Jatujak
Bangkok, 10900

http://oasys.acs.org/acs/231nm/petr/upload/saveupload.cgi

Please check! Page 2 of 3

Thailand

Phone Number: 662-942-8900 ext 323 **Fax Number:** 662-942-8900 ext 324 **Publishable Email:** g4384022@ku.ac.th

Third Author

Supawadee Namuangruk
Department of Chemistry
Kasetsart University
Department of Chemistry, Faculty of Science, Kasetsart University
Phaholyothin Rd., Ladyao, Jatujak
Bangkok, 10900
Thailand

Phone Number: 662-9428900 ext 323 Fax Number: 662-9428900 ext 324 Publishable Email: dakojung@hotmail.com

Fourth Author

Pilin Limtrakul
Department of Chemistry
Kasetsart University
Department of Chemistry, Faculty of Science, Kasetsart University
Phaholyothin Rd., Ladyao, Jatujak
Bangkok, 10900
Thailand
Publishable Email: frscpll@ku.ac.th

Fifth Author

Presenting

Jumras Limtrakul
Department of Chemistry
Kasetsart University
Department of Chemistry, Faculty of Science, Kasetsart University
Phaholyothin Rd., Ladyao, Jatujak
Bangkok, 10900
Thailand

Phone Number: 662-942-8900 ext 323 Fax Number: 662-942-8900 ext 324 Publishable Email: fscijrl@ku.ac.th

1. CHECK THAT:

- Your abstract title is in **Sentence case**. An example: Engineering gene expression of *Escherichia coli* by mRNA: Applications in molecular biology
- Your title does not begin with "The" (this will be removed during editing).
- Your title does not end with a period.

2. MAKE NECESSARY CORRECTIONS:

- Click any value in the Abstract Control Panel you want to change (e.g., Title, Author names)
- Edit the information and click the submit button.

3. AFTER PROOFING AND MODIFYING YOUR ABSTRACT, SUBMIT IT TO YOUR PROGRAM OFFICIALS FOR REVIEW:

After submitting, your paper can be viewed by your session organizer and program chair. You can make changes up until the call for papers deadline date. After this, it will be reviewed and scheduled.

4. CLICK HERE TO PRINT THIS PAGE NOW.

Submit to Program Officials

Please check! Page 1 of 2

Review Your Abstract Before Submitting

This is how your work will appear to the public on the World Wide Web and in the printed book of abstracts.

Cycloaddition reactions between benzo-fused five-membered ring dienes and single-wall carbon nanotubes: A QM/MM study

Suwassa Bamrungsap and **Jumras Limtrakul**, Department of Chemistry, Kasetsart University, Department of Chemistry, Faculty of Science, Kasetsart University, Phaholyothin Rd., Ladyao, Jatujak, Bangkok 10900, Thailand, Fax: 662-9428900 ext 324, suwussa@hotmail.com, fscijrl@ku.ac.th

The transition states and products of the cycloaddition reactions between different types of benzo-fused five membered ring dienes and (5,5) single-wall carbon nanotubes (SWNTs) have been investigated by using the our-Own-N-layered-Integrated molecular Orbital and molecular Mechanics (ONIOM) approaches utilizing the two layered ONIOM scheme (B3LYP/6-31G(d):AM1). The reactivity of the cycloaddition reactions are evaluated on the basis of Frontier Molecular Orbital (FMO) energy gaps between reactants and the aromaticity of dienes. The results have been performed so that the reactivity of cycloaddition reaction of benzo-fused diene and SWNT is correlated to the aromaticity of the dienes. The reactivity of these reactions is less kinetically and thermodynamically favourable than the reactions between these dienes and ethylene which are the typical reactions. In order to enhance the viability of the cycloaddition reaction, the metal cation is introduced into the center of the SWNT. The increasing of the reactivity of Na@SWNT is due mainly to the stabilized LUMO orbital of the SWNT.

not yet rated

Abstract ID#: 934095 Password: 207411

Program Selection: Division of Inorganic Chemistry

Topic Selection: Nanoscience - Application

Title: Cycloaddition reactions between benzo-fused five-membered ring dienes and single-wall carbon nanotubes:

A QM/MM study

Lead Presenter's Email: fscijrl@ku.ac.th

Invited: N

Presentation Format: Poster Only

Consider for Sci-Mix: N Conforms to Bylaw 6: Y

First Author

Suwassa Bamrungsap Department of Chemistry Kasetsart University Department of Chemistry, Faculty of Science, Kasetsart University Phaholyothin Rd., Ladyao, Jatujak Bangkok, 10900 Thailand

Phone Number: 662-9428900 ext 323 Fax Number: 662-9428900 ext 324 Publishable Email: suwussa@hotmail.com

Second Author

Presenting

Jumras Limtrakul
Department of Chemistry
Kasetsart University
Department of Chemistry, Faculty of Science, Kasetsart University
Phaholyothin Rd., Ladyao, Jatujak

Please check! Page 2 of 2

Bangkok, 10900

Thailand

Phone Number: 662-942-8900 ext 323 Fax Number: 662-942-8900 ext 324 Publishable Email: fscijrl@ku.ac.th

1. CHECK THAT:

- Your abstract title is in **Sentence case**. An example: Engineering gene expression of *Escherichia coli* by mRNA: Applications in molecular biology
- Your title does not begin with "The" (this will be removed during editing).
- Your title does not end with a period.

2. MAKE NECESSARY CORRECTIONS:

- Click any value in the Abstract Control Panel you want to change (e.g., Title, Author names)
- Edit the information and click the submit button.

3. AFTER PROOFING AND MODIFYING YOUR ABSTRACT, SUBMIT IT TO YOUR PROGRAM OFFICIALS FOR REVIEW:

After submitting, your paper can be viewed by your session organizer and program chair. You can make changes up until the call for papers deadline date. After this, it will be reviewed and scheduled.

4. CLICK HERE TO PRINT THIS PAGE NOW.

Submit to Program Officials

การประชุมวิชาการวิทยาศาสตร์และ เทคโนโลยีแห่งประเทศไทย ครั้งที่ 32 จำนวน 7 เรื่อง

การศึกษาการเปลี่ยนแปลงอันตรกิริยาของคู่เบส อะดีนีน-ใทมีน กับอะตอมและใจออนของทอง The Alterations of the Adenine-Thymine Base Pairs on Interactions with Neutral and Charged Gold Atoms

พิพัฒน์ คงประชา^{1,2}, พรรณวิกา พรรณ โณภาศ^{1,2}, กรวิการ์ ตั้งปอง^{1,2}, จำรัส ลิ้มตระกูล^{1,2*} Pipat Khongpracha^{1,2}, Panvika Pannopard, Kornvika Tangpong, Jumras Limtrakul^{1,2*}

¹Laboratory for Computational & Applied Chemistry, Department of Chemistry, Faculty of Science, Kasetsart University, Bangkok 10900, Thailand ²Center of Nanotechnology, Kasetsart University Research and Development Institute, Kasetsart University, Bangkok 10900, Thailand ^{*}Corresponding author: Tel. 662-5705047, Fax 662-942-8900 ext 324, E-mail: jumras.l@ku.ac.th

บทคัดย่อ: จากการศึกษาอันตรกิริยาของคู่เบส อะดีนีน-ไทมีน กับอะตอมของทองที่เป็นกลาง เป็น ใอออนบวก และ ใอออนลบ ด้วยระเบียบวิธี Density Functional Theory (B3LYP/6-31G(d,p)) พบว่า อะตอมของทองที่เป็นกลางและ ใอออนบวกจะลดความแข็งแรงของพันธะ ใฮโดรเจนที่ตำแหน่ง N1-N3 แต่เพิ่มความแข็งแรงของพันธะ ใฮโดรเจนที่ตำแหน่ง O4-N6 ในขณะที่ ใอออนลบให้ผลในทางตรงข้าม โดยค่าพลังงานดึงดูดระหว่างคู่เบส อะดีนีน-ไทมีนเมื่อ ใด้รับอิทธิพลจากอะตอมของทองที่เป็นกลาง ใอออนบวก และ ใอออนลบ มีค่า -13.305 -18.216 และ -9.666 กิโลแคลอรีต่อโมลตามลำดับ

Abstract: The interactions of a Watson-Crick (WC) adenine-thymine (A-T) base pairs with an Au atom, Au⁺ cation and Au⁻ anion are investigated by means of density functional theory method (B3LYP/6-31G(d,p)). Au⁺ weakens the strength of N1-N3 hydrogen bonding but strengthens the O4-N6 hydrogen bonding in the T-A base pairing. The interaction performs in a similar manner with Au^o but conversely with Au⁻. The interaction energies of the thymine base with the adenine base bound with Au^o, Au⁺ and Au⁻ are -13.305, -18.216 and -9.666 kcal/mol, respectively.

Introduction: Biological molecular recognition, for instance in the Watson-Crick nucleoside base pairing, is always at head of the line of attention from experimentalists as well as theoretical scientists. Since nature always intelligently and reproducibly assembles biological compounds with a marvelous demeanor, materials composing Watson-Crick nucleoside bases have recently been publicized as one of the most suitable candidates for implementing in the building-block assembly. This constructive thought assists the development of "bottom-up" approaches in nanofabrication of nanoscale devices for more efficient and economic microelectronics, optics, and sensors. Interaction of adenine-thymine (A-T) and guanine-cytosine (G-C) base pairs with various metals (M) and cations (Mn⁺) were studied by experimental techniques as well as by ab initio calculations. Especially, there are a number of studies of the interactions of DNA bases with Au surfaces, Au clusters, Au ions, and Au electrodes. The purpose of the present study is to investigate

the interactions of an ordinary adenine-thymine (A-T) base pairs with an Au atom, Au atom, Au atom and Au anion by means of the rigorous density functional theory (DFT) method. These outcomes would reveal concealed phenomena and perhaps recompense experimental observations.

Methodology:All computations of the complexes formed either between the DNA bases or the Watson-Crick (WC) DNA base pairs and gold species were conducted using the

Gaussian 03 package of quantum chemical programs with hybrid density functional B3LYP level. The basis set 6-31G(d,p) was chosen for the DNA bases and the Lanl2dz basis set in combination with Hay and Wadt's relativistic effective core potential (RECP) was used for gold atoms. Geometries of the complexes studied were fully optimized with constraint to the planar.

Results Discussion and Conclusion:In the Watson-Crick thymine-adenine (T-A) base pairs, it is well known that there are two hydrogen bonding interactions, named here as the N3-H3^{···}N1 and the N6-H6[·]...O4 interactions. The optimized geometries of complexes of gold species (Au^o, Au⁺, and Au⁻) with the Watson-Crick thymine-adenine (T-A) base pairs are documented in Figure 1.

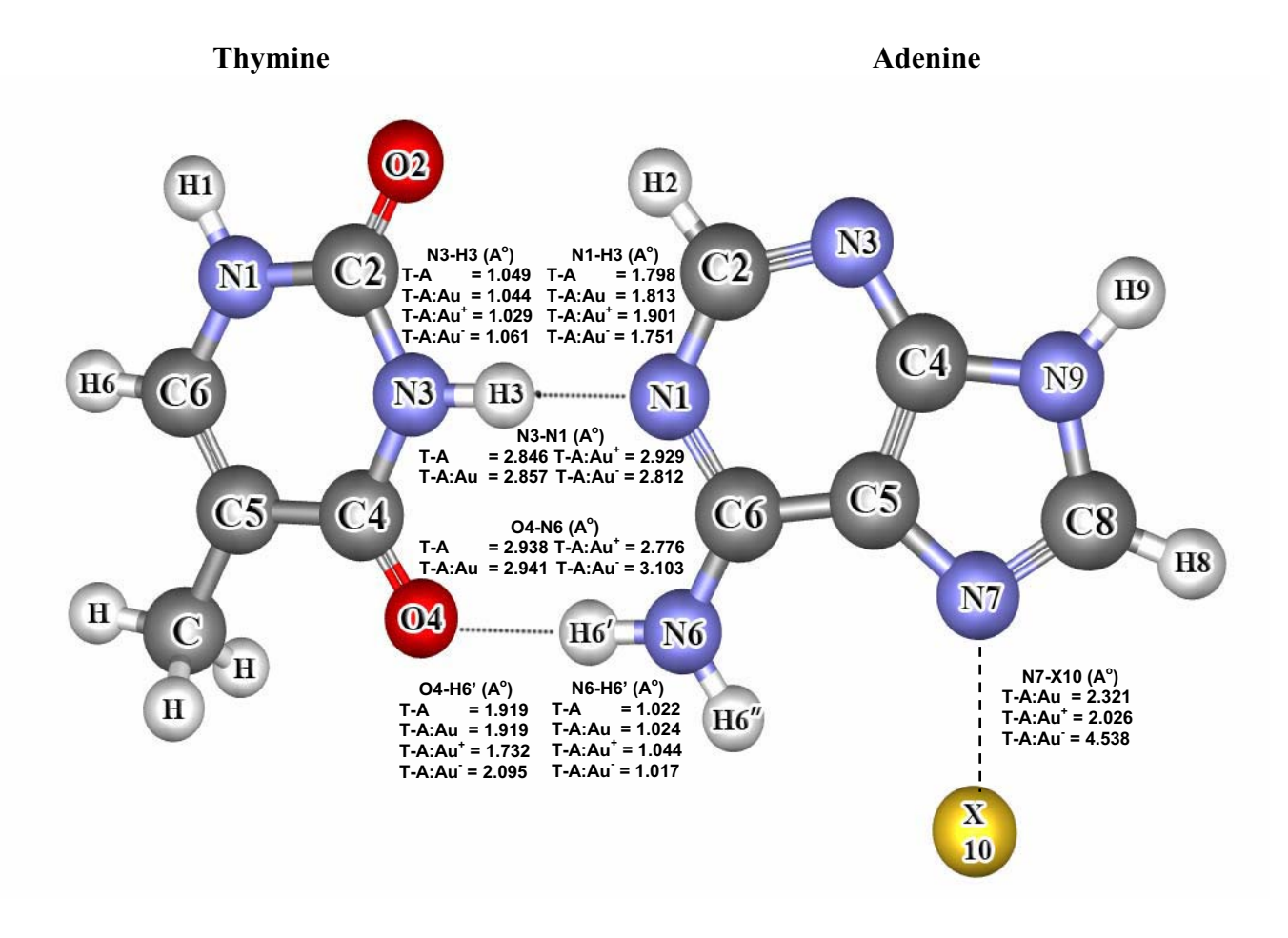


Fig. 1 The WC intermolecular H-bond lengths and the N-X distances of the T-A:X complexes in which X represents gold the species.

In compared to the original T-A complex, the changes of structural information infer that Au^+ weaken the strength of N1-N3 hydrogen bonding but strengthen the O4-N6 hydrogen bonding in the T-A base pairing. Conversely, Au^- makes the N1-N3 hydrogen bonding stronger but causes a weaker O4-N6 hydrogen bonding. In the T-A: Au° complex, even if a diminutive change (+0.003 Å) on an O4-N6 distance is detected, but the increasing of the N6-H6' bond distance would lead us to conclude that Au° performs in the same manner (but much weaker) with Au^+ .

The adsorption energies of the thymine base molecule with adenine bases bound with different kinds of gold species were also examined. Compared to the value of -13.741 kcal/mol for the thymine base interacting with an isolated adenine base, the interaction energies of the thymine base with the adenine base bound with Au°, Au⁺ and Au⁻ are -13.305, -18.216 and -9.666 kcal/mol, respectively. The three body interaction energies of the thymine base, the adenine base and the different gold species are -21.461, -91.572 and -19.005 kcal/mol, respectively. It should be noted that even if Au° modifes structural parameters in the T-A base pairing system it is insensitive to the binding energy. Moreover, Au⁺ ion enhances the T-A interaction by 32% and Au⁻ ion weakens the T-A interaction by 30%.

References:

- (1) Kryachko, E. S., and Remacle, F. (2005) *J. Phys. Chem. B* **109** (48), 22746-22757.
- (2) Daniel M.C. and Astruc D. (2004) Chem. Rev. 104, 293-346.

การศึกษากลไกการเกิดปฏิกิริยาไฮเดรชันของไซโคลเฮกซีนบนตัวเร่งปฏิกิริยา H-ZSM-5 ด้วย ระเบียบวิธี OM / MM

THE HYDRATION REACTION OF CYCLOHEXENE OVER H-ZSM-5 ZEOLITE: A QM/MM STUDY

<u>การันต์ บ่อบัวทอง</u>1,2, จำรัส ลิ้มตระกูล 1,2*

<u>Karan Bobuatong</u>^{1,2}, Jumras Limtrakul^{1,2*}

¹Laboratory for Computational & Applied Chemistry, Department of Chemistry, Faculty of Science, Kasetsart University, Bangkok 10900, Thailand ²Center of Nanotechnology, Kasetsart University Research and Development Institute, Kasetsart University, Bangkok 10900, Thailand ^{*}Corresponding author: Tel. 662-5705047, Fax 662-942-8900 ext 324, E-mail: jumras.l@ku.ac.th

บทคัดย่อ: ผลการศึกษาปฏิกิริยาไฮเดรชันของสารประกอบไซโคลเฮกซีนบนตัวเร่งปฏิกิริยาซี โอไลต์ชนิด H-ZSM-5 โดยระเบียบวิธี ONIOM2 (B3LYP/6-311G(d,p):UFF) พบว่ากลไก ปฏิกิริยาไฮเดรชันเกิดได้สองแบบคือกลไกปฏิกิริยาแบบขั้นเดียวและกลไกปฏิกิริยาเกิดเป็นแบบ 2 ขั้นตอน ขั้นตอนกลไกปฏิกิริยาแบบขั้นเดียวจะเกิดการถ่ายโอนหมู่ไฮดรอกซีจากโมเลกุลของน้ำ และการถ่ายโอนอะตอมไฮโดรเจน จาก H-ZSM-5 ไปยังโมเลกุลไซโคลเฮกซีน และการถ่ายโอนอะตอมไฮโดรเจน จาก H-ZSM-5 ไปยังโมเลกุลไซโคลเฮกซีน และการถ่ายโอนอะตอมไฮโดรเจนจากโมเลกุลของน้ำกลับไปยัง H-ZSM-5 พร้อมๆกัน จนเกิดสารประกอบไซโครเฮกซานอล ส่วนกลไกปฏิกิริยาเกิดเป็นแบบ 2 ขั้นตอนเริ่มจากการเคลื่อนย้ายโปรตอนจาก ซีโอไลต์ H-ZSM-5 ไปสู่ไซโคลเฮกซีนได้อัลคอกไซด์เกิดขึ้น จากนั้นอัลคอกไซด์จะทำปฏิกิริยากับน้ำเปลี่ยนเป็นไซโครเฮกซานอล ค่าพลังงานก่อกัมมันต์และค่าพลังงานการเกิดปฏิกิริยาของกลไกปฏิกิริยาแบบขั้นเดียวมีค่าเท่ากับ 16.26 และ -7.4 kcal/mol ตามลำดับ ซึ่งมีค่าใกล้เคียงจากการทดลอง 16.85 และ -8.9 kcal/mol ตามลำดับ

Abstract: The complete reaction mechanism for the hydration of cyclohexene over H-ZSM-5 zeolite was investigated theoretically by means of ONIOM2 (B3LYP/6-311G(d,p):UFF). The zeolite nanostructured pores included by the ONIOM method play an important role in regulating the orientation of the adsorbing molecule around the active site and significantly affect the energetic of the complexes. The hydration of cyclohexene catalyzed by H-ZSM-5 zeolites gives two different reaction mechanisms; both stepwise and concerted reaction mechanisms of the hydration reaction are considered. For the stepwise reaction mechanism, the hydration starts with the protonation of the adsorbed cyclohexene by the H-ZSM-5 zeolite leading to the formation of the alkoxide intermediate and, subsequently, the cyclohexanol can be generated by interaction with a water molecule. In the concerted reaction mechanism which is considered to be the reaction rate-determining step, the hydration of cyclohexene takes place in a single reaction step without prior alkoxide oxide formation. The estimated activation barrier of rate-determining step and the reaction energiy are 16.26 kcal/mol and -7.4 kcal/mol comparable with experimental results of 16.85 kcal/mol and -8.9 kcal/mol, respectively. The results of this study is to provide

data that will assist in understanding how the hydration of cyclohexene over H-ZSM-5 zeolite works.

Introduction: Cyclohexanol is one of the most important basic chemicals in the petrochemical industry, especially due to the new technology, where it can be manufactured through the hydration of cyclohexene. Its predominant use is as the raw material to produce the important fine chemicals such as adipic acid and carpolactam. Recently, Tatsumi et al. have investigated the cyclohexene hydration catalyzed by various zeolite catalysts. They found that ZSM-5 was the most effective of the zeolite catalyst for the cyclohexene hydration and showed the highest conversion and selectivity to cyclohexanol, but the reaction mechanism is not clearly understood. The objective of this present study is to clarify this problem, We have performed a theoretical study of the mechanism of hydration reaction of cyclohexene over H-ZSM-5 zeolite using the ONIOM method. We believe that the results obtained will achieve the aim of this study.

Methodology: The model of ZSM-5 zeolite, the 46T cluster, covering the 10T active region and three different channel structures (channel intersection, the straight channel, and the zigzag channel) where the reaction normally takes place, is taken from the lattice structure of ZSM-5 zeolite The ONIOM2 scheme in which the whole model is subdivided into two layers is adapted for computational efficiency. The active region consisting of the 12T cluster which is considered the smallest unit required to represent the reaction site of zeolite and the reactive molecules is treated with the B3LYP level of theory using 6-311G(d,p) basis set. The rest of the extended framework is treated with the UFF force field to reduce the computational time necessary and to practically represent the confinement effect of the zeolite pore structure. During the structure optimization, the 5T portion of the active site region [2(≡SiO)(FeO2)Al(OSi≡)2], and the adsorbate are allowed to relax while the rest is fixed at the crystallographic coordinates.

Results Discussion and Conclusion: The hydration reaction of cyclohexene over H-ZSM-5 zeolite has been investigated using the ONIOM2 model. The model is shown to be accurate in predicting the adsorption energies trend of the adsorbed reactants. The computed activation barrier and the reaction energies are comparable with experimental results. The hydration of cyclohexene catalyzed by H-ZSM-5 zeolites gives two different reaction mechanisms; both the stepwise and concerted reaction mechanisms of the hydration reaction are considered. For the stepwise reaction mechanism, the hydration starts with the protonation of the adsorbed cyclohexene by the H-ZSM-5 zeolite leading to the formation of the alkoxide intermediate and, subsequently, the cyclohexanol can be generated by interaction with a water molecule. In the concerted reaction mechanism which is considered being the reaction rate-determining step, the hydration of cyclohexene takes place in a single reaction step without prior alkoxide oxide formation. The estimated activation barrier of the rate-determining step and the reaction energy are 16.26 kcal/mol and -7.41 kcal/mol ,and are comparable with experimental results of 16.85 kcal/mol and -8.9 kcal/mol, respectively.

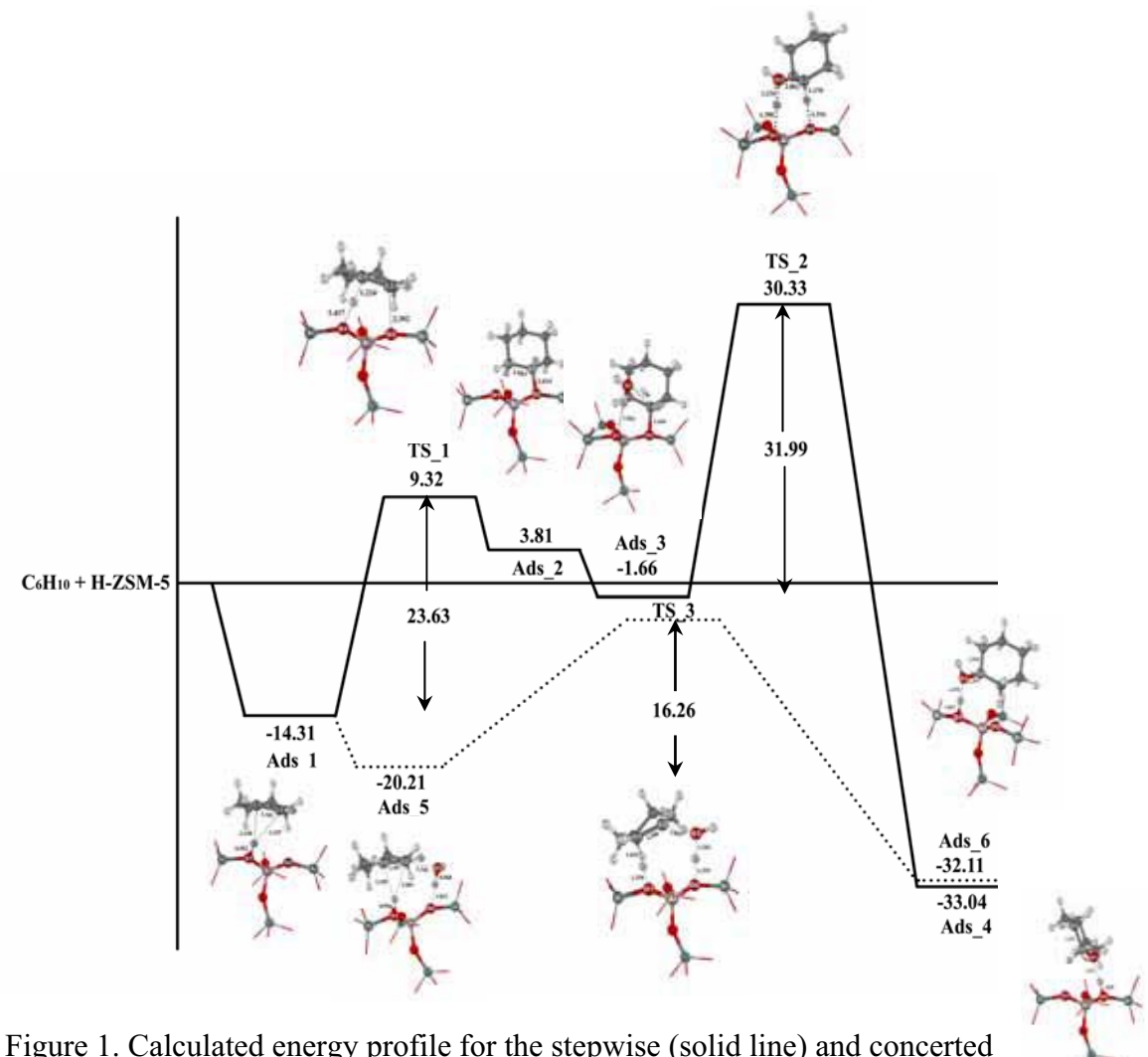


Figure 1. Calculated energy profile for the stepwise (solid line) and concerted (dash line) reaction mechanisms (kcal/mol).

References:

- (1) Jansang, B., Nanok, T., Limtrakul, J. (2006) J. Phys. Chem B. 110, 12626-12631.
- (2) Namuangruk, S., Pantu, P., and Limtrakul, J. (2004) J. Catal. 225, 523-530.
- (3) Namuangruk, S., Pantu, P., and Limtrakul, J. (2005) *ChemPhysChem* **6**, 1333-1339.

1

สึกษาอิทธิพลของความยาวและชนิดของท่อการ์บอนนาโนชนิดปลายปิดต่อคุณสมบัติทาง

อิเล็กทรอนิกส์ และคุณสมบัติทางเคมีโดยอาศัยปฏิกิริยาการเติมของโอโซน

THE EFFECT OF THE FINITE LENGTH AND TYPE OF SINGLE-WALLED CARBON NANOTUBES CAPPED WITH FULLERENE HEMISPHERES ON THEIR ELECTRONIC PROPERTIES AND CHEMICAL REACTIVITY VIA 1,3-DIPOLAR CYCLOADDITION OF OZONE

<u>มนตรี สว่างพฤกษ์</u>^{1,2}, ธานิน นานอก^{1,2}, สุภาวดี นาเมืองรักษ์^{1,2}, พิบูลย์ พันธุ^{1,2}, จำรัส ลิ้มตระกูล^{1,2,*}

<u>Montree Sawangphruk</u>^{1,2}, Tanin Nanok^{1,2}, Supawadee Namuangrak^{1,2}, Piboon Pantu^{1,2},

Jumras Limtrakul^{1,2,*}

บทคัดย่อ: ปฏิกิริยาการการเติมโอโซนบนตำแหน่งปลายปิดของท่อการ์บอนนาโนชนิด [5,5] และ [9,0] ได้ถูกศึกษา ด้วยระเบียบวิธี PBE/def-SV(P) และ ONIOM(B3LYP/6-31G(d):AM1) ผลปรากฏว่าเมื่อเพิ่มความยาวของท่อ การ์บอนนาโนได้นำไปสู่การเปลี่ยนแปลงคุณสมบัติทางอิเล็กทรอนิกส์ โดยค่า absolute chemical hardness ที่ถูก คำนวณด้วยวิธีที่เหมาะสมอย่าง PBE/def-SV(P) เปลี่ยนแปลงแบบพื้นๆ ลงๆ จาก 0.85 ถึง 0.15 อิเล็กตรอนโวลต์ เมื่อ ความยาวท่อเพิ่มจาก C_{60} ถึง C_{200} ในขณะที่เปลี่ยนแปลงแบบค่อยๆ ลดลง จาก 0.72 ถึง 0.28 อิเล็กตรอนโวลต์ สำหรับกรณีของ C_{78} ถึง C_{204} ในทำนองเดียวกันพลังงานที่เกิดจากอันตรกิริยาระหว่าง HOMO ของท่อการ์บอนนาโน และ LUMO ของโอโซน เปลี่ยนแปลงแบบขึ้นๆ ลงๆ จาก 0.05 ถึง -1.05 อิเล็กตรอนโวลต์ และ -0.02 ถึง -0.94 อิเล็กตรอนโวลต์ สำหรับกรณีของท่อการ์บอนนาโนชนิด [5,5] และ [9,0] ตามลำดับ แต่เมื่อพิจารณาอิทธิพลดังกล่าว ต่อคุณสมบัติทางเคมีโดยอาศัยปฏิกิริยาการเติมของโอโซนพบว่าความยาวและชนิดของท่อการ์บอนนาโนไม่มีผลต่อ ค่าพลังงานก่อกัมมันส์และค่าพลังงานการดูดซับทางเคมี โดยค่าพลังงานก่อกัมมันส์และค่าพลังงานการดูดซับทางเคมี โดยค่าพลังงานก่อกัมมันส์มีค่าเท่ากับ 2.29, 2.16-2.26 และ 2.15-2.18 กิโลแคลอรีต่อโมล และค่าพลังงานการดูดซับทางเคมีของโอโซนมีค่าเท่ากับ 44.56, 45.02-46.86 และ 48.21-48.53 กิโลแคลอรีต่อโมล สำหรับของ C_{60} , ท่อการ์บอนนาโนชนิด [5,5] และ [9,0] ตามลำดับ

Abstract: The 1,3-dipolar cycloaddition (1,3-DC) of ozone on the cap of [5,5]-armchair single-walled carbon nanotubes ([5,5]-ASWNTs) and [9,0]-zigzag single-walled carbon nanotubes ([9,0]-ZSWNTs) has been carried out using a PBE/def-SV(P) method as compared with an ONIOM(B3LYP/6-31G(d):AM1) approach. Increasing of the length of SWNTs leads to the change of electronic properties. The absolute chemical hardness of [5,5]-ASWNTs, calculated using the appropriate PBE approach, fluctuates and decreases from 0.83 eV to 0.15 eV for C₆₀ to C₂₀₀. This of [9,0]-ZSWNTs decreases without fluctuation from 0.72 eV to 0.28 eV for C₇₈ to C₂₀₄. Also, the FMO interaction energy of [5,5]-ASWNTs decreases with the fluctuation behavior from 0.05 eV to -1.05 eV. For [9,0]-ZSWNTs, it decreases from -0.02 to -0.94 eV. On the contrary, their activation and reaction energies are insensitive to the length and type of nanotubes. The basis set super position error (BSSE) corrected activation energies are 2.29, 2.16-2.26,

¹Laboratory for Computational & Applied Chemistry, Department of Chemistry, Faculty of Science, Kasetsart University, Bangkok 10900, Thailand

²Center of Nanotechnology, Kasetsart University Research and Development Institute, Kasetsart University, Bangkok 10900, Thailand

^{*}Corresponding author: Tel. 662-5705047, Fax 662-942-8900 ext 324, E-mail: jumras.l@ku.ac.th

and 2.15-2.18 kcal/mol and the chemisorption energies are exothermic by 44.56, 45.02-46.86, and 48.21-48.53 kcal/mol for C_{60} , [5,5]-ASWNTs, and [9,0]-ZSWNTs, respectively.

Introduction: The SWNTs are recognized as the ultimate nanomaterials due to their distinct chemical and electrical properties¹. Recently, Iijima et al. have performed the density functional theory on the study of the geometrical features of the finite-length carbon nanotubes capped with fullerene hemisphere. Their results showed that the geometries and HOMO-LUMO gaps of the [5,5]-ASWNT series depended on the nanotube length, but remained unchanged in the case of the [9,0]-ZSWNT series. These findings are encouraging to find out whether the chemical reactivity of the end caps of the capped SWNTs is sensitive to the nanotube type and length. Simultaneously, it is found that 1,3-DC of ozone with SWNTs is one of the most facile organic reactions with a small activation barrier of 2.8 kcal/mol². The FTIR studies of the oxidation of C_{60} using ozone have been reported at room temperature³. Two different surfaces bound functional groups, esters and quinines, as well as CO₂ and CO, were observed during the reaction³. Accordingly, the 1,3-DC of ozone is, in this work, chosen to study the nanotube length effect on the chemical reactivity. Furthermore, to our knowledge, the chemical reaction on the fullerene hemisphere of the capped nanotubes has not yet been reported. Therefore, this work may also predict the chemical reactivity at the cap site of SWNTs in comparison with the wall site of SWNTs.

Methodology: The 1,3-DC of ozone on the surface of C₆₀ and the caps of two series of [5,5]-ASWNTs and [9,0]-ZSWNTs has been carried out with; (1) the density functional Perdew-Burke-Ernzerhof (PBE) approach together with the standard def-SV(P) basis set; (2) the framework of a two-layer Our own N-layered Integrated Molecular orbital Molecular mechanics approach (ONIOM2) utilized in our previous study of the Diels Alder cycloadditions of SWNTs with electron-rich dienes³. The hybrid density functional B3LYP together with the standard 6-31G(d) basis set and the Austin model one (AM1) method were employed for the high-level (see the ball and stick atoms in Figure 1) and low-level treatments, respectively. Also, the counter poise correction method was used to correct the basis set superposition error (BSSE) for all apparent activation energies at the fully optimized geometries.

Results, Discussion and Conclusion: The absolute chemical hardness of [5,5]-ASWNTs, calculated by using an appropriate PBE method, fluctuates and decreases from 0.83 eV to 0.15 eV for C_{60} to C_{200} (see solid line in Fig 2(a)). Also, in the case of [9,0]-ZSWNTs, it decreases without fluctuation from 0.72 eV to 0.28 eV for C₇₈ to C₂₀₄ (see dash line in Fig 2(a)). The FMO interaction energy between the LUMO of ozone and HOMO of [5,5]-ASWNTs decreases with the fluctuation behavior from 0.05 eV to -1.05 and it is decreases from -0.22 to -0.94 eV for [9,0]-ZSWNTs (see Figure 2(b)). This implies that such electronic properties depend on the nanotube length, while their chemical reactivity is insensitive to the nanotube length. The BSSE corrected activation energies (E_a) of armchair and zigzag series are 2.16-2.26 kcal/mol and 2.15-2.18 kcal/mol, respectively. This is comparable with the experimental estimate of the 2.5 kcal/mol for 2-trans-butene. Also, a BSSE corrected E_a at the wall site of the armchair nanotube is found to be 6.03 kcal/mol. This leads to a conclusive proof that the most reactive site of the SWNTs is located on the fullerene hemisphere. A close inspection of the transition state structures reveals that, for the C₆₀, the reaction mechanism follows the synchronous pathway; whereas, for the armchair and zigzag nanotubes, the reaction

proceeds asynchronously. The exothermic chemisorption energies of armchair and zigzag series are 45.02-46.86 kcal/mol and 48.21-48.53 kcal/mol, respectively which are in a good agreement with that of 54.5 kcal/mol reported for 2-*trans*-butene. As a result, the type and length of nanotubes do not have a significant effect on the 1,3-DC of ozone on the cap site of SWNTs. By the way, although the ONIOM2 scheme can not present the electronic properties of SWNTS, it can still provide the activation and chemisorption energies. The BSSE corrected E_a are 2.07-2.78 kcal/mol and 2.11-2.30 kcal/mol as well as the chemisorption energies are 45.92-49.37 kcal/mol and 48.21-48.53 kcal/mol for [5,5] and [9,0] SWNTS, respectively.

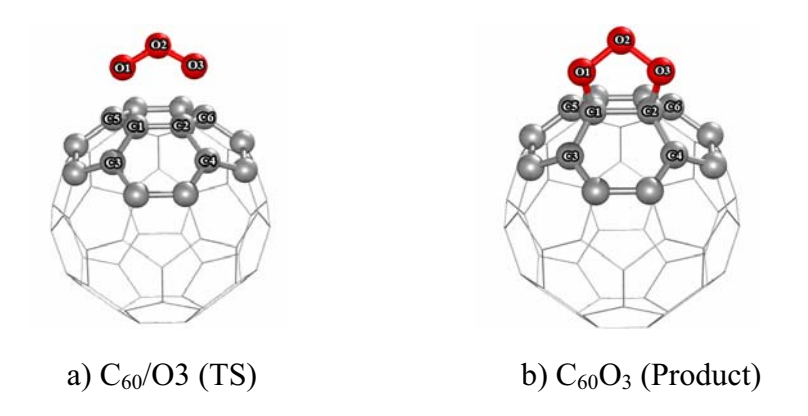


Fig 1 Optimized geometries of the $C_{60}O_3$ at transition state (TS) and product.

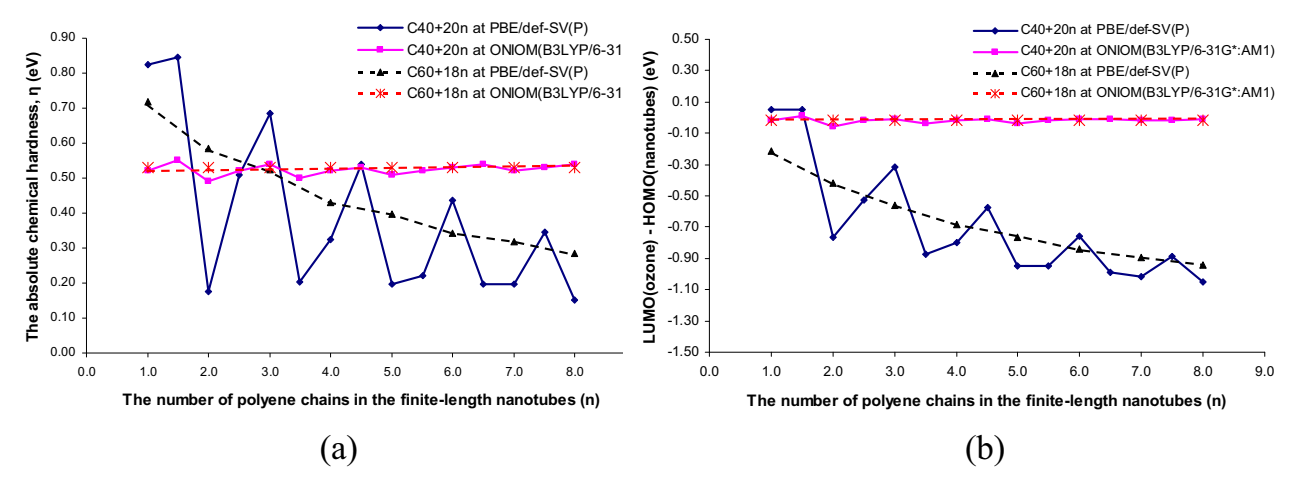


Fig 2 The absolute chemical hardness (η) and interacted Frontier Molecular Orbitals (FMOs) of SWNTs as a function of n.

References:

- (1) Iijima, S. (1991) *Nature* **354**, 56-58.
- (2) Lu, X., Tian, F., Xu, X., Wang, N., and Zhang, Q. (2003) *J. Am. Chem. Soc.* **125**, 10459-10464.
- (3) Mawhinney, D. B., Naumenko, V., Kuznetsova, A., Yates, J. T., Liu, J., and Smalley, R. E. (2000) *J. Am. Chem. Soc.* **122**, 2383-2384.
- (4) Warakulwit, C., Bumrungsap, S., Lumsirikul, P., Khongpracha, P., and Limtrakul, J. (2005) *Stud. Surf. Sci. Catal.* **156**, 823-828.

Keyword: 1,3-dipolar cycloaddition, single-walled carbon nanotubes, ozone

การศึกษาอันตรกิริยา และกลไลการเคลื่อนที่ของ 1-butene และ cis-2-butene บน H-FER ด้วยวิธี การ คำนวณ Combined Quantum Mechanics/Molecular Mechanics และ Molecular Simulation The Adsorption and Diffusion of 1-Butene and cis-2-Butene on H-FER: Combined Quantum Mechanics/ Molecular Mechanics and Molecular Dynamics Simulation บุญเดช เบิกฟ้า^{1,2}, จำรัส ลิ้มตระกูล ^{1,2*}

Bundet Boekfa^{1,2}, Jumras Limtrakul^{1,2*}

บทคัดย่อ: การศึกษาอันตรกิริยา และกลไลการเคลื่อนที่ของ 1-butene และ cis-2-butene ด้วยวิธี การคำนวณ combined Quantum Mechanics/Molecular Mechanics ได้พลังงานอันตรกิริยา เท่ากับ -16.55 และ -14.13 kcal/mol สำหรับ 1-butene และ cis-2-butene ตามลำดับ โดย สอดคล้องกับพลังงานที่ได้จากการคำนวณ Molecular Dynamics ซึ่งแสดงว่า 1-butene มีอันตร กิริยากับ H-FER สูงกว่า cis-2-butene และการคำนวณ diffusion activation energies สำหรับ 1-butene และ cis-2-butene มีค่า 5.11 และ 5.06 kcal/mol ตามลำดับ

Abstract: The adsorption and diffusion of 1-butene and cis-2-butene have been studied by means of combined Quantum Mechanics/Molecular Mechanics and Molecular Dynamics Simulation. The interaction energies are calculated to be -16.55 and -14.13 kcal/mol for 1-butene and cis-2-butene, respectively with combined Quantum Mechanics/Molecular Mechanics. This trend agrees with the interaction energies from MD simulation in the order 1-butene more than cis-2-butene. The diffusion activation energies from the MD simulation are 5.11 and 5.06 kcal/mol for 1-butene and cis-2-butene, respectively. The results correlate well to the experimental observation.

References:

- [1] Rungsirisakun, R., Nanok, T., Probst, M., and Limtrakul, J. (2006) *J. Mol. Graph. Model.* **24**, 373-382.
- [2] Namuangruk, S., Pantu, P., and Limtrakul, J. (2005) *ChemPhysChem* **6**, 1333-1339.
- [3] Namuangruk, S., Pantu, P., and Limtrakul, J. (2004) J. Catal. 225, 523-530.
- [4] Yoda, E., Kondo, J.N., and Domen, K. (2005) J. Phys. Chem. B 109, 1464-1472.

Keywords: FER zeolite, Density Funtional Theory (DFT), ONIOM, Molecular Dynamics Simulation, 1-butene, cis-2-butene, trans-2-butene

¹Laboratory for Computational & Applied Chemistry, Department of Chemistry, Faculty of Science, Kasetsart University, Bangkok 10900, Thailand

²Center of Nanotechnology, Kasetsart University Research and Development Institute, Kasetsart University, Bangkok 10900, Thailand

^{*}Corresponding author: Tel. 662-5705047, Fax 662-942-8900 ext 324, E-mail: jumras.l@ku.ac.th

ผลของ Confinement ที่มีต่อการดูดซับและการแพร่ของเฮกเซนในตัวเร่งปฏิกิริยาชนิด MCM-41 ที่มี ขนาดท่อต่างกัน: การศึกษาโดยระเบียบวิธีโมเลคิวลาร์ไดนามิคส์

Confinement Effects on Adsorption and Diffusion of Hexane in Nanoporous MCM-41 with Different Pore Sizes: a Molecular Dynamics Study

วิญญู แสงทอง^{1,2}, จำรัส ลิ้มตระกูล^{1,2*}

Winyoo Sangthong^{1,2}, Jumras Limtrakul^{1,2*}

¹Laboratory for Computational & Applied Chemistry, Department of Chemistry, Faculty of Science, Kasetsart University, Bangkok 10900, Thailand

²Center of Nanotechnology, Kasetsart University Research and Development Institute, Kasetsart University, Bangkok 10900, Thailand

*Corresponding author: Tel. 662-5705047, Fax 662-942-8900 ext 324, E-mail: jumras.l@ku.ac.th

บทคัดย่อ: ได้เสนอผลการศึกษาการดูดซับและการแพร่ของเฮกเซนในตัวเร่งปฏิกิริยาชนิด MCM-41 ที่มี ขนาดต่างกัน 4 ขนาด ที่อุณหภูมิ 300 เคลวิน โดยระเบียบวิธีโมเลคิวลาร์ไดนามิคส์ พบว่าค่าพลังงานการ ดูดซับสอดคล้องกับการทดลองสำหรับระบบที่มีขนาดท่อเท่ากัน ผลของ confinement พบว่าพลังงาน การดูดซับของเฮกเซนเพิ่มเมื่อขนาดท่อลดลง และพลังงานการดูดซับเพิ่มขึ้นเมื่อจำนวนเฮกเซนมากขึ้น ค่า สัมประสิทธิ์การแพร่ของเฮกเซนที่คำนวณได้สอดคล้องกับผลการทดลอง โดยค่าจะลดลงเมื่อเพิ่มปริมาณ เฮกเซนและขนาดท่อเล็กลง ระยะระหว่างโมเลกุลของเฮกเซนในท่อที่มีขนาดเล็กกว่าจะน้อยกว่าในท่อที่มี ขนาดใหญ่กว่าและน้อยกว่าเฮกเซนในสถานะของเหลว นอกจากนี้พบว่าที่ปริมาณเฮกเซนน้อยๆ เฮกเซน จะจัดเรียงตัวขนานกับท่อ และเมื่อปริมาณเฮกเซนเพิ่มขึ้นจะจัดเรียงตัวเป็นวงแหวนที่มีขนาดสอกคล้อง กับขนาดท่อ เฮกเซนในท่อที่มีขนาดใหญ่มีพฤติกรรมคล้ายคลึงกับเฮกเซนในสถานะของเหลว

Abstract: We report results of Molecular Dynamics (MD) simulations to study the adsorption and diffusion of hexane in four different pore sizes siliceous MCM-41 at 300K. It was found that the calculated adsorption energies are in good agreement with experimental ones for the same pore sizes. As a result of confinement in MCM-41, the free energies adsorption of hexane increase when the pore sizes decrease and increase also with the loadings. The calculated self-diffusion coefficients of hexane are reasonably close to the available experimental data. They decrease with increasing loadings and they decrease if the pore sizes decrease. The average distances between the centers of mass of hexane molecules in the smallest pores is only marginally less than in the larger pores and in the liquid phase. It was further found that for low loadings the hexane molecules lie parallel to the pore channel for every pore sizes. When the loadings are increased, they build up concentric rings with sizes depending on the pore channel diameters. Hexane molecules in the larger models behave in a similar manner to those in the liquid phase.

Introduction: MCM-41 is an innovative mesoporous material consisting of hexagonal, uniform, unidimensional mesopores that do not have a pore channel intersection. Their well defined structural characteristics and high thermal and hydrothermal stability makes the

MCM-41 family of materials an almost perfect model for the study of adsorption and transport properties of guest molecules in mesoporous systems. However, with experimental methods alone details of adsorption and diffusion at a microscopic level are very difficult to derive. In this study, the adsorption and diffusion of hexane in silanol-free high silica forms of MCM-41 is studied by MD simulations. Four MCM-41 frameworks with different sizes of their nanopores were used to study the dynamics of hexane molecules confined in these materials and to establish the confinement effect of pore sizes on the behavior of the probe molecules. We developed new semi-empirical intermolecular potential functions for the interaction between siliceous MCM-41 and hexane and tested them by comparing with some experimental quantities. The adsorption energies and diffusion coefficients of liquid hexane in these materials were calculated for various loadings from the simulated trajectories and are reported for the first time.

Methodology: Molecular dynamics simulations were performed using the DL_POLY 2.0 code. The systems studied were the periodic models of siliceous MCM-41 with four different pore diameters (they were denoted as A, B, C and D). Loadings started with one hexane molecule and were increased up to the point where the density of hexane calculated from pore volume and number of molecules equals the density of liquid hexane. For comparison, we also performed molecular dynamics simulations of liquid hexane in order to determine confinement effects of siliceous MCM-41 on the liquid structure. These simulations were performed with a time step of 1 fs within the NVE ensemble at room temperature (300 K). The resulting configurations were used as input for a 200 ps equilibration period with velocity rescaling. After this period, a simulation over 200 ps was performed without velocity rescaling to ensure that there were no further drifts. Then a 100 ps production run in which the coordinates and velocities of the atoms were stored every 10 fs for subsequent analysis.

Results Discussion and Conclusion: The adsorption and diffusion of hexane in simple models of siliceous MCM-41 at room temperature was studied by molecular dynamics simulations. New potential parameters were constructed from the existing values and experimental energetic data. The adsorption energies at a loading of one hexane molecule per supercell range between -9.09 and -13.65 kcal/mol. The variation of the molecular self-diffusion coefficients with loadings exhibits the normal trend of decreasing self-diffusion with increasing loadings and decreasing size of the pores. From the calculated radial distribution functions it can be seen that the hexane molecules are far from each other, about 6.3-6.6 Å which is slightly less in the liquid phase (6.7 Å). This is also a result of the confined space. We calculated the radial distribution of hexane molecules to the center of the pore channel and found that at low loadings they prefer locations parallel and close to the pore surface. With increased loadings the hexane molecules arrange themselves into concentric ring and chainlike structures inside the pores as shown in Fig. 1.

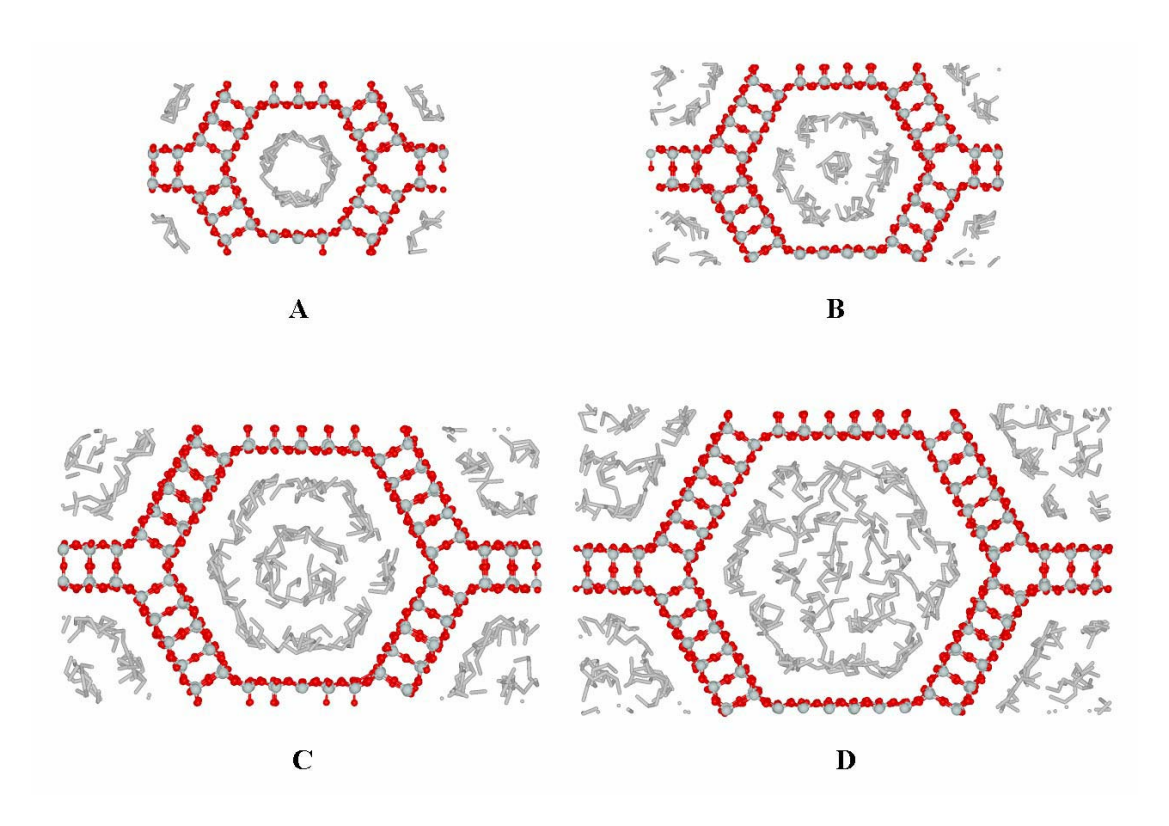


Fig. 1. Snapshot from the simulation showing a typical distribution of hexane molecules at saturated loading in models A-D.

References:

- (1) Rungsirisakun, R., Nanok, T., Probst, M., Limtrakul, J. (2006) *J. Molecular Graphics & Modelling* **24**, 373-382.
- (2) Trens, P., Tanchoux, N., Papineschi, P.M., Maldonado, D., di Renzo, F., Fajula, F. (2005) *Micropor. Mesopor. Mater.* **86**, 354-363.

การศึกษาอิทธิพลของการแทนที่ด้วยหมู่เอมีนในโครงสร้างของซีโอไลต์ชนิด ITQ-24 ในปฏิกิริยา

โปรโตเนชันของอัลคืน ด้วยระเบียบวิธีคำนวณ QM/MM

EFFECT OF AMINE SUBSTITUTED ITQ-24 ZEOLITE ON THE PROTONATION OF ALKENE: A QM/MM STUDY

บวรพล จันทร์แสง^{1,2} พิพัฒน์ คงประชา^{1,2} และ จำรัส ลิ้มตระกูล^{1,2*}

Bavornpon Jansang^{1,2} Pipat Khongpracha^{1,2} and Jumras Limtrakul^{1,2*}
¹Laboratory for Computational & Applied Chemistry, Department of Chemistry, Faculty of Science, Kasetsart University, Bangkok 10900, Thailand
²Center of Nanotechnology, Kasetsart University, Bangkok 10900, Thailand E-mail address: bavornpon@yahoo.com (B. Jansang), pipat_k@msn.com (P. Khongpracha) and fscijrl@ku.ac.th (J. Limtrakul).

บทคัดย่อ: ปัจจัยที่ควบคุมการเกิด alkoxide ในซีโอไลต์เป็นข้อมูลพื้นฐานที่สำคัญในการออกแบบ ตัวเร่งในปฏิกิริยาอัลคิลเลชันซึ่งเป็นปฏิกิริยาที่สำคัญในอุตสาหกรรมปีโตรเคมี ผลจากการคำนวณ ทางเคมีควอนตัมโดยใช้ระเบียบวิธีการคำนวณ ONIOM พบว่าค่าพลังงานที่ใช้ในปฏิกิริยาการเกิด alkoxide ในซีโอไลต์ชนิด ITQ-24 ที่มีหมู่เอมีนแทนที่ในโครงสร้างและที่ไม่มีหมู่เอมีนแทนที่มีค่า เท่ากับ 12.40 และ 17.34 kcal/mol ทำให้สามารถสรุปได้ว่าการแทนที่ด้วยหมู่เอมีนในโครงสร้าง ของซีโอไลต์มีส่วนช่วยให้ปฏิกิริยาการเกิด alkoxide ดีขึ้น นอกจากนี้ยังแสดงให้เห็นว่าการแทนที่ด้วยหมู่เอมีนในโครงสร้างของซีโอไลต์เป็นการเพิ่มความเป็นเบสให้กับระบบ

Abstract: The alkoxide formation of ethylene over amine-substituted and non-substituted in the ITQ-24 zeolite framework have been computed within the framework of the ONIOM approach utilizing the two-layer ONIOM scheme (B3LYP/6-31G(d,p):UFF). Amine substitution reduces the apparent activation energy of the reaction form 17.34 to 12.40 kcal/mol. The results imply that amine substitution in zeolite framework enhances the basicity of the system.

Introduction: Petrochemical processes make extensive use of zeolites, which are solid catalysts due to their unique properties of shape-selectivity. Normally, acidity of zeolite occurs via aluminum (Al) incorporated in zeolite framework which shows the characteristic of Brønsted acid. However, it is believed that a modification of zeolite framework by organic groups will improve the activity of the active site in zeolite. Recently, Yamamoto et al. directly substituted the methylene group (CH₂) for the ≡Si-O-Si≡ bridge of MFI and LTA zeolites framework directly. This alternative class of zeolite appears to be a novel application in base catalysis. However, periodic DFT calculation shows that not only the methylene group can be incorporated into the zeolite framework, but also the amine group (NH) can be incorporated. These results verify that amine which is doped in zeolite better shows characteristic Lewis base than methylene group. On the other hand, the ≡Si-NH-Si≡ bridge of amine substituted zeolite show weaker Brønsted acid properties than ≡Si-O-Si≡ bridge.

As for the alkylated reaction, the protonated step of the alkene molecule by the Brønsted proton is an initial step of the reaction to produce alkoxide species, an important intermediate for alkylating step. There are many theoretical studies on the investigation of this step. Namuangrak et al. calculated the apparent activation energy

of ethylene protonated in FAU zeolite by the ONIOM3 method, and estimated this to be 21.33 kcal/mol while the energy barrier was estimated to be 30.06 kcal/mol. For the amine substitution, Lesthaeghe et al. used a fully relaxed 16T cluster of H-ZSM-5 computed ethoxide formation. They found that the energy barrier of ≡Si-O-Al-O(H)-Si-NH-Si≡ bridge was higher than the ≡Si-O(H)-Al-O-Si≡ bridge. The activation barrier corresponding of ≡Si-O-Al-O(H)-Si-NH-Si≡ and ≡Si-O(H)-Al-O-Si≡ bridges were estimated to be 29.98 and 23.06 kcal/mol, respectively.

However, no literature has been found for a theoretical study examining the effect of amine-substituted on the \equiv Si-O(H)-Al-NH-Si \equiv bridge zeolite framework of ethoxide formation. Thus, we expect that the \equiv Si-O(H)-Al-NH-Si \equiv bridge will reduce the activation barrier of the system as the \equiv Si-NH-Si \equiv bridge is a stronger Lewis base than the \equiv Si-O-Si \equiv bridge. Therefore, in this present work we employ an advantage of the amine substituted zeolite in order to understand the catalytic, electronic and structure properties of alkoxide formation on a modification of the zeolite framework.

Methodology: Recently, Castaneda and co-worker synthesized a new threedimensional zeolite (ITQ-24). This zeolite has two types of cavity; a 12-membered ring (12MR) and a 10-membered ring (10MR). Moreover, it has two intersection cahnnels; 12MR and 10MR, which facilitate allowance for the bulky molecule. Up to the present time, there are only a few publications relating to this zeolite and we expect that in the future this zeolite will be a new candidate for petrochemical processes. Therefore, in this work we use ITQ-24 zeolite as a catalyst of ethoxide formation on a modification of zeolite framework. The two-layer ONIOM (ONIOM2) method has been carried out on cluster models representing ITQ-24 zeolite containing up to 169 tetrahedrally coordinated tetravalent atoms (see figure 1a). In terms of the ONIOM method, the 5T cluster represents the active part and the remainder has been described as the extended framework which was the van der Waals (vdW) contribution of zeolite framework. Previous studies reveal that the combination between the density functional theory B3LYP/6-31G(d,p) and the universal force field (UFF) provide high-quality information for evaluating the energetic and geometric structures of reaction.

Results, Discussion and Conclusion: We computed the ethoxide formation of ethylene on amine-substituted and non-substituted on zeolite framework of ITQ-24 using the ONIOM2(B3LYP/6-31G(d,p):UFF) method. In the first step, ethylene was adsorbed on the Brønsted proton of the active site. The second step is a transition state in which the Brønsted proton attacked at a primary carbon atom. In the final step, to stabilize the energy of system, a secondary carbon atom of ethylene formed a covalent bond with the oxygen bridge framework of zeolite for non-substituted, whereas for the amine-substituted, this formed on a nitrogen atom and lead to the ethoxide product. The adsorption energy of ethylene adsorbed on ITQ-24 zeolite of aminesubstituted and non-substituted was calculated to be -14.94 and -14.99 kcal/mol, respectively (see Figure 2.). The calculated apparent activation energies at the stationary point of both transition states are 17.34 and 12.40 kcal/mol, respectively. This result reveals that amine- or NH-substituted zeolite decrease the apparent activation energies by about 5 kcal/mol due to the fact that it has stronger Lewis base property when compare with oxygen atom. The energy barrier of the transition state of amine substitution was evaluated to be 27.34 kcal/mol. However, ethoxide product of amine substitution is more exothermic than non-substituted of -22.93 kcal/mol.

This result implied that it is possible to generate a stable organic functionalization in a modification of zeolite framework by organic groups.

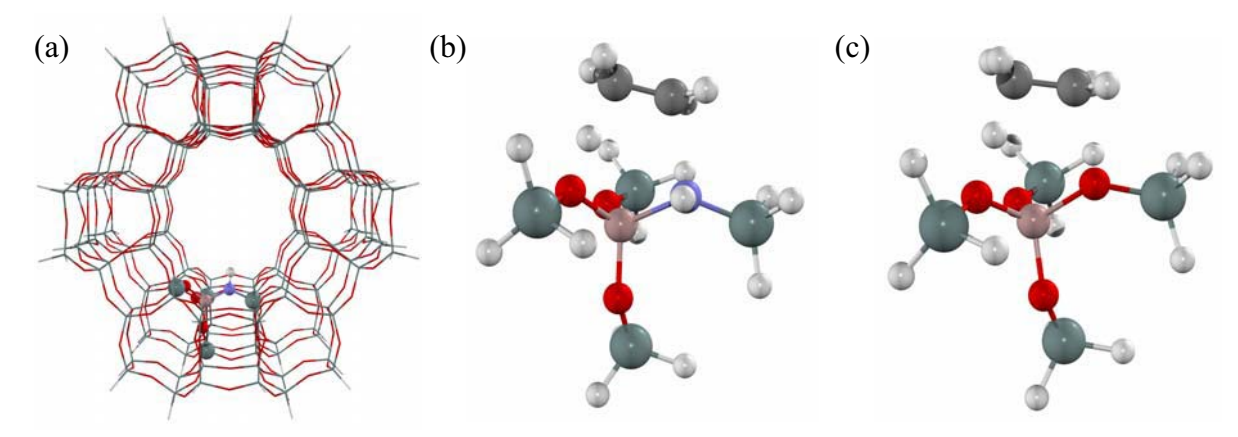


Figure 1. Illustration of the optimized geometry of ITQ-24 zeolite; (a) 5T/169T cluster model; (b) and (c) represent optimized transition states structure of amine-substituted and non-substituted zeolite, respectively.

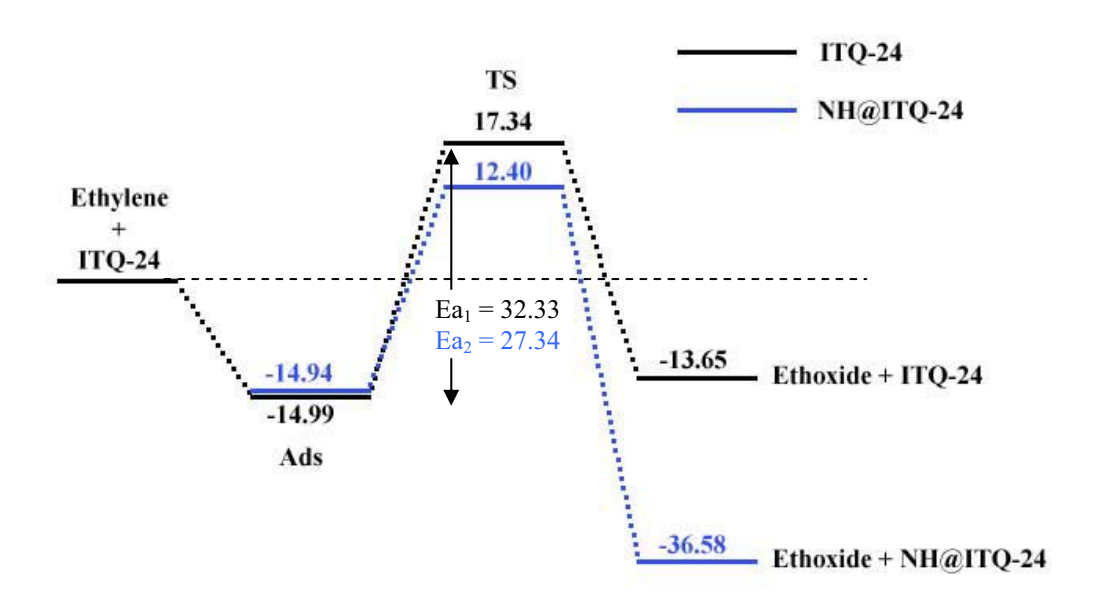


Figure 2. Optimized energetic profiles of ethoxide formation in amine-substituted (NH@ITQ-24) and non-substituted (ITQ-24) ITQ-24 zeolite.

References:

- (1) Yamamoto, K.; Sakata, Y.; Takahashi, Y.; Tatsimi, T. Science 2003, 300, 470.
- (2) Astala, R.; Auerbach, S. M. J. Am. Chem. Soc. 2004, 126, 1843.
- (3) Namuangrak, S.; Pantu, P.; Limtrakul J. J. Catal. 2004, 225, 523.
- (4) Lesthaeghe, D.; Speybroeck, Van. V.; Marin G. B.; Waroquier M. *J. Phys. Chem. B*, **2005**, *109*, 7052.
- (5) Castaňeda, R.; Corma, A.; Fornés, V.; Rey, F.; Rius, J. J. Am. Chem. Soc. 2003, 125, 7820.
- (6) Jansang, B.; Nanok, T.; Limtrakul, J. J. Phys. Chem. B 2006, 110, 12626.
- (7) Namuangrak, S.; Pantu, P.; Limtrakul J. ChemPhysChem 2005, 6, 1333.

Key words: ethylene, alkoxide, amine-substituted, ITQ-24; ONIOM

การศึกษาอันตรกิริยาระหว่างอนุภาค Au และพื้นผิว Rutile(110) โดยระเบียบวิธี DFT THE DFT STUDY OF INTERACTION OF Au CLUSTERS AND RUTILE (110) SURFACES

ปิติ ตรีสุกล l , จำรัส ลิ้มตระกูล 2 , และ Thanh N. Truong 3

Piti Treesukol¹, Jumras Limtrakul² and Thanh N. Truong³

² Faculty of Science, Kasetsart University, Bangkok, 10900, Thailand

บทคัดย่อ: อนุภาคขนาดเล็กของทองจะแสดงสมบัติความเป็นตัวเร่งปฏิกิริยาเมื่อถูกดูดซับบนพื้นผิว TiO_2 ในงานวิจัยนี้จึงได้ทำการศึกษาอันตรกิริยาระหว่างอนุภาคของทองและพื้นผิว TiO_2 – Rutile (110) โดยใช้ การคำนวณด้วยระเบียบวิธี Density functional theory (DFT/B3LYP) จากการศึกษาพบว่าอนุภาค ขนาดเล็กของทองจะเสถียรเมื่อดูดซับบนตำแหน่ง O-vacancy ของพื้นผิว TiO_2 โดยพลังงานยึดเหนี่ยว ระหว่างอนุภาคทองและตำแหน่ง O-vacancy มีค่าสูงกว่าเมื่อดูดซับที่ตำแหน่งอื่นถึง 18 kcal/mol อนุภาค ทองจะมีความหนาแน่นของอิเล็กตรอนเพิ่มขึ้นอย่างชัดเจนเนื่องจากมีการถ่ายเทอิเล็กตรอนจาก O-vacancy ในขณะเดียวกันอนุภาคทองมีผลกระบบต่อสมบัติทางอิเล็กทรอนิกส์ของพื้นผิว TiO_2 ในบริเวณกว้าง โดย ความหนาแน่นของอิเล็กตรอนบนตำแหน่งอะตอม Ti ที่อยู่ถัดไปจาก O-vacancy จะเพิ่มขึ้นอย่างชัดเจน ปรากฏการณ์นี้อาจมีส่วนในการเร่งกระบวนการแยกสลายโมเลกุล O_2 ซึ่งเป็นขั้นตอนที่สำคัญใน กระบวนการ oxidation ของ CO

Abstract: Highly dispersed gold particles on reducible TiO₂ can exhibit surprisingly high catalytic reactivity for CO oxidation reaction. The interaction of Au clusters with TiO₂ rutile (110) surface has been studied by an embedded cluster model at DFT/B3LYP level of calculation. Small Au clusters, which have been proposed to function as an active center for CO oxidation, can be stabilized on the TiO₂ surface by O-vacancy. The binding energy of an Au atom to the defective surface is 50 kcal/mol while that to the perfect surface is about 18 kcal/mol less. The electron density of the Au atom increases significantly due to the electron-transfer from the vacancy site. The electronic properties of the TiO₂ surface is found to be perturbed by the Au cluster as well. The electron density of the surface 5-fold Ti atoms next to the vacancy site increases significantly due to the adsorption of Au, which can enhance the ability in activating adsorbates such as O₂ which is the reason why Au/TiO₂ interface has an important role in the oxidation of CO.

¹ Faculty of Liberal Arts and Science, Kasetsart University, Kampaeng Saen, Nakorn Pathom, 73140, Thailand

³ Henry Eyring Center for Theoretical Chemistry, Chemistry Department, University of Utah, Salt Lake City, UT 84112

Introduction: Despite the inertness of gold metal compared to other transition metals, highly dispersed gold particles on reducible metal oxides can exhibit surprisingly high catalytic reactivity for many reactions. Several factors, such as size and shape of the cluster, metal-support interaction between Au clusters and the surface, have been suggested as the reason for the enhanced reactivity of small gold clusters. The Au clusters as small as three atoms are found to exhibit substantial activity for CO oxidation. Effects of the types of supports on catalytic activity are clearly seen from previous experimental studies. Au clusters on reducible oxide supports (e.g. F₂O₃, TiO₂) possess higher catalytic activity that those on non-reducible oxide supports (e.g. MgO, Al₂O₃, SiO₂) The strong interaction between Au particles and the defective surface and the notably high catalytic activity of Au/TiO₂ could be the results of electron transfer from the O-vacancy site to the metal particles. In this study, we are focusing on the interaction between Au and TiO2 surface and its consequence on the electronic properties of the surface and the Au cluster. By using ab initio calculation with an embedded cluster, calculations of adsorptions at low coverage and the orbital analysis can be achieved. These could provide more insight in interaction between metal clusters and the metal oxide surface.

Methodology: A stoichiometric cluster of Ti₁₇O₃₄, terminated by a set of pseudo-potentials, has been used to represent the surface of TiO₂ rutile (110). A defective surface was created by removing one neutral bridging oxygen (O_B) at the center of the perfect surface. These clusters are considered to be large enough to cover all the short range and medium range interactions. The effect of the Madelung potential from the remaining lattice was represented by a set of surface charges derived from the surface charge representation of the electrostatic embedding potential (SCREEP) methodology. Structures and energetics of TiO₂ surfaces, Au/TiO₂ systems and CO adsorption complexes were optimized at DFT/B3LYP level of calculation with mixed basis sets. A single Au atom and diatomic Au particle were placed on the stoichiometric and partial reduced TiO₂ surfaces at different possible sites. All calculations have been carried out by using Gaussian03[®] software.

Results, Discussion and Conclusion: The optimized structures of Au/TiO₂ systems have been determined by using SCREEP embedded cluster model at DFT/B3LYP level of calculation. On the perfect TiO₂ surface, the most stable site for an Au atom is on the bridging oxygen where the binding energy is 39 kcal/mol. The O-vacancy site of the defective surface has excess electron localized in the vacancy region, which can be

transferred to adsorbed Au atom. The Au atom can bind stronger to the O-vacancy site of the defective surface, with the binding energy of 57 kcal/mol. The adsorption of Au atom causes some changes in electron density of the TiO₂ surface. The Mulliken charge of the next-nearest Ti_{5f} atom is 0.2 au more negative. This phenomenon could enhance an ability of TiO₂ surface in activating the adsorbate species such as O₂ and to increases the catalytic activity of Au/TiO₂. The binding energy of CO on Au/TiO₂ is 8.3 kcal/mol. The supported Au withdraws electron slightly from CO molecule and cause the contracting of CO bond length. The Au clusters, on the other hand, provide electron to CO and consequences in the elongation of CO bond length. The small size of Au cluster or it negative charge may not be all the reasons for extraordinary properties of supported Au clusters but the TiO₂ surface may have other subtle effects that needed to be examined further.

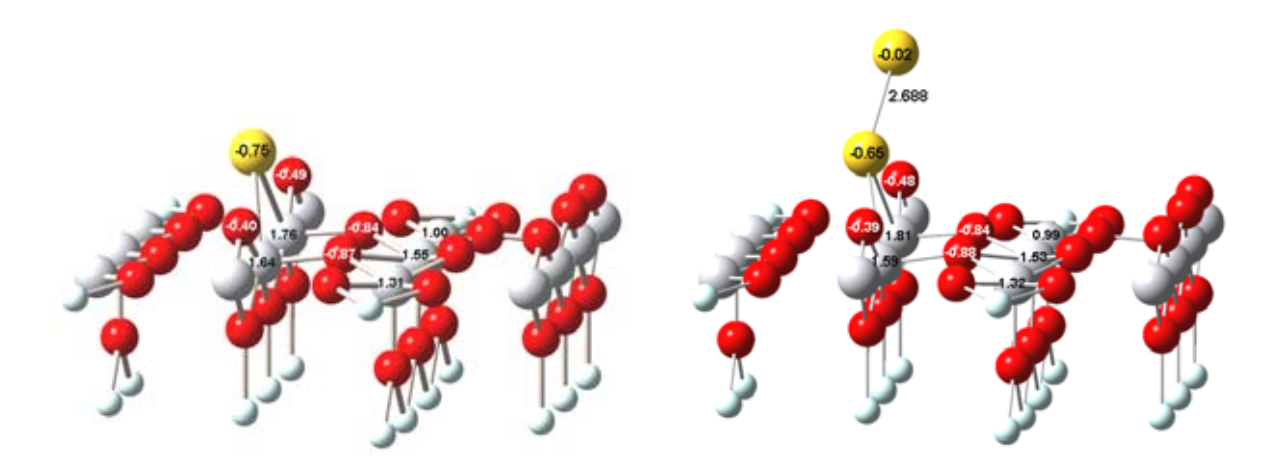


Figure 1 An optimized structure of Au atom supported on O-vacancy defective TiO₂ surface

Figure 2 Diatomic Au cluster adsorbed on the defective surface

References:

- (1) Haruta, M., Yamada, N., Kobayashi, T., and Iijima, S. J. Catal. 1989, 115, 301.
- (2) Wahlstrom, E., Lopez, N., Schaub, R. et al. *Phys. Rev. Lett.* **2003**, 90, 026101/1.
- (3) Mavrikakis, M., Stoltze, P., and Norskov, J. K. Catal. Lett. 2000, 64, 101.
- (4) Lee, S., Fan, C., Wu, T., and Anderson, S. L. J. Am. Chem. Soc. **2004**, 126, 5682.

Keywords: Density Functional theory (DFT), Au cluster, Rutile, TiO₂(110), O-Vacancy, Metal-support interaction

Nanotech 2007 จำนวน 4 เรื่อง



Over 5,000 attendees and 250 exhibitors expected!



> Nanotech 2007 Home > Program > Expo / Sponsors

> Press Room

Sessions

Monday Tuesday Wednesda_\

Adsorption of glycine and phenylalanine in H-ZSM-5 zeolite: an embedded QM/MM study At-a-Glance Sunday

B. Boekfa, J. Sirijaraensre, P. Limtrakul, P. Pantu and J. Limtrakul Kasetsart University, TH

Keywords:

Thursday Index of Authors

glycine, phenylalanine, H-ZSM-5, zeolite, adsorption, QM/MM, ONIOM

Abstract:

Confirmed Speakers

Index of Keywords

Conferences & Symposia

zeolites, providing detailed understanding of molecular behavior and interactions within the nanocavity of the Zeolites are crystalline aluminosilicate microporous materials whose pore diameters are in the range of 2 to 10 Å. Zeolites have numerous important applications in catalysis, adsorption, drug delivery, and chemical separations. Recently, zeolites have received attentions as an alternative adsorption medium for the separation stability. Molecular modeling and simulations are important tools in the study of the adsorption properties of zeolite pore network. While previous studies have been mainly focused on the adsorption of small inorganic and organic molecules within zeolites, in this study we will investigate adsorption of amino acids in zeolite as an alternative adsorption medium for amino acid separation. To the best of our knowledge there has been no theoretical study of amino acid adsorption within the nanocavity of zeolite. This work is, therefore, a first of amino acids since zeolites have advantages of size and shape selectivity, resistance to swelling and thermal theoretical investigation reporting the molecular behavior of amino acids interacted with H-ZSM-5.

Back to Program

Tuesday Wednesday Monday Sunday Sessions

Keywords

Authors

Thursday

Vanotech 2007 Conference Program Abstract

Technical Conferences | Business Conferences | Nano Impact Workshop | Venue / Hotels | Site Map Nanotechnology Conference | Terms of use | Privacy policy | Contact | NSTI Home | Nanotech 2007 Home | Program | Expo / Sponsors | Press Room | © Nano Science and Technology Institute, all rights reserved.

Names, and logos of other organizations are the property of those organizations and not of NSTI.

This event is not open to the general public and NSTI reserves the right to refuse admission and participation to any individual.



Over 5,000 attendees and 250 exhibitors expected!

ITSN >



Over 5,000 attendees and 250 exhibitors expected!



> Nanotech 2007 Home > Program > Expo / Sponsors

> Press Room

Keywords: At-a-Glance Sunday Confirmed Speakers Sessions Monday Index of Authors Index of Keywords Tuesday Wednesday Thursday

Capped-end of a Single-walled Carbon Nanotube: The Theoretical Studies on the Ozonization at the Effect of the Finite Length

M. Sawangphruk, J. Sirijaraensre, P. Pantu and J. Limtrakul Kasetsart University, TH

single-walled carbon nanotube, ozone, ONIOM, ozonization

Conferences & Symposia

carried out to understand this reaction. Yumura et al. revealed that the geometrical and electronic properties of the finite-length armchair SWNTs exhibit an oscillatory behavior depending on the length of the nanotubes. In contrast, the properties of the zigzag SWNTs are not dependent on the length of the tubes. It is, therefore, of been no reported theoretical studies on the effect of finite-length carbon nanotubes on the chemical reaction of Since the discovery in 1991, single-walled carbon nanotubes (SWNTs) have been investigated for numerous potential applications in nanotechnology. However, the insolubility and high chemical stability obstruct the purification and the applications of the nanotubes. The key to solve this problem may be the chemical interest to investigate the reactivity of finite-length carbon nanotubes. To the best of our knowledge, there have functionalization of SWNTs by introducing new physical and chemical properties and increasing solubility. Many reactions have been reported experimentally and theoretically for the functionalization of the carbon nanotubes. One of the most facile reactions is the 1,3-dipolar cycloaddition of ozone. Several theoretical works have been

Back to Program

Tuesday Wednesday Monday Nanotech 2007 Conference Program Abstract Sunday Sessions

Keywords

Authors

Thursday

Technical Conferences | Business Conferences | Nano Impact Workshop | Venue / Hotels | Site Map © Nano Science and Technology Institute, all rights reserved.

Nanotechnology Conference | Terms of use | Privacy policy | Contact | NSTI Home
Nanotech 2007 Home | Program | Expo / Sponsors | Press Room |

Names, and logos of other organizations are the property of those organizations and not of NSTI.

This event is not open to the general public and NSTI reserves the right to refuse admission and participation to any individual.



Over 5,000 attendees and 250 exhibitors expected!





Over 5,000 attendees and 250 exhibitors expected!



> Nanotech 2007 Home > Program > Expo / Sponsors

po / Sponsors > Press Room

.

At-a-Glance

Sessions

Sunday

Monday

Tuesday Wednesday

2007 NSTI Nanotec

Conduction Properties of BN-doped Fullerene Chain Obtained by Density Functional Calculations

N. Krainara, P. Luksirikul, J. Sirijaraensre, P. Pantu and J. Limtrakul Kasefsart University, TH

Thursday Keywords:

BN-doped Fullerene, C60-dimer, Conduction Properties, DFT

Abstrac

Confirmed Speakers

Index of Keywords

Conferences & Symposia

Carbon-based molecules such as fullerenes and carbon nanotubes, have attracted the attention of researchers because of their unique mechanical, and electronic properties and potential applications in a wide variety of areas of nanotechnology. The substitution of carbon atoms by other elements is one of the most interesting modifications of fullerenes. The hetero-fullerenes, especially the hybrid B/C/N fullerene (or CBN ball) are expected to become a novel electronic device. There have been experiments reported about the synthesis of BN-substituted fullerenes. Furthermore, several theoretical investigations have addressed the electronic properties and structural patterns of substitution of C60 by BN moieties. From previous studies, it was found that the most stable position of a BN bond of single BN-substituted C60 is located at the bond between two hexagons of fullerene. In addition, the doped BN played a significant role in decreasing the HOMO-LUMO gap of fullerene. In this work, therefore, two carbon atoms located between two hexagons of C60 are substituted by BN moiety to represent the model of BN-doped fullerene. Moreover, to improve the conductance, two BN-doped C60 monomers are connected together to form a dimer of BN-doped C60. It has been reported that the C60 dimer does not possess good conductivity because the junction of the molecules forms a bottleneck for the conduction of the electron. Therefore, in this present study, we have attempted to connect two molecules of BN-doped C60 via a bridging molecule, 3,8-phenanthroline.

Back to Program

Sessions Sunday Monday Tuesday Wednesday Nanotech 2007 Conference Program Abstract

Authors Keywords

Thursday

© Nano Science and Technology Institute, all rights reserved.

Nanotechnology Conference | Terms of use | Privacy bolicy | Contact | NSTI Home
Nanotech 2007 | Home | Program | Expo / Sponsors | Press Room |
Rechnical Conferences | Business Conferences | Nano Impact Workshop | Venue / Hotels | Site Map

Names, and logos of other organizations are the property of those organizations and not of NSTI.

This event is not open to the general public and NSTI reserves the right to refuse admission and participation to any individual.



Over 5,000 attendees and 250 exhibitors expected!





Over 5,000 attendees and 250 exhibitors expected!



> Nanotech 2007 Home > Program > Expo / Sponsors

> Press Room

Sunday

Monday Tuesday **Wednesda**

At-a-Glance

Sessions

Nanotube" Systems: A Quantum Chemical Analysis Structure and Electronic Properties of "DNA-Gold-

P. Pannopard, J. Sirijaraensre, S. Nokbin, P. Khongpracha and J. Limtrakul Kasetsart University, TH

Keywords:

Thursday Index of Authors

A=T base pair, single-walled carbon nanotubes, SWNTs, gold, DFT

Abstract:

Index of Keywords

for the fabrication of a chemical sensing probe that integrates both recognition and transduction moieties into a carbon nanotubes (CNTs) that possess fascinating structural, chemical, mechanical and electrical manners as charge-transport centers for electronic transducers. Accordingly, it is the objective of this current work, to The idea of chemical sensing based on molecular recognition is known as one of the most promising concepts requires probes which hold a specific recognition of desired chemical species and a transduction ability of that single molecular assembly. The scheme has been examined in various disciplines, especially for a nature mitated detection of specific DNA sequences. The exclusive properties of gold nanoparticles (Au NPs) are high sensitivity, electrical conductivity, size-dependent optical capability and affinity to the biomolecules. The recent experimental and theoretical studies reported that adenine base has the highest affinity with gold and it preferentially binds to nitrogen atom at the N7 position. Furthermore, there is considerable interest in applying investigate the modulation of adenine-thymine(A:T) hybridization under the interaction with the hybrid structure of a neutral gold atom acts as the reactive sites for anchoring of the DNA bases and both types of Single-Walled Carbon Nanotubes (SWNTs), zigzag (8,0) and armchair (5,5) to be electron transfer supports. Finally, the for single-molecule detection, even though it still remains in an early developmental stage. The approach recognition incident into a quantitative response signal. Due to those indispensable functions, it is very versatile system's electronic responses are observed. Confirmed Speakers Conferences & Symposia

Back to Program

Sunday Sessions Vanotech 2007 Conference Program Abstract

Tuesday Monday

Wednesday

Thursday

Keywords

Authors

© Nano Science and Technology Institute, all rights reserved.

Nanotechnology Conference | Terms of use | Privacy policy | Contact | NSTI Home
Nanotech 2007 Home | Program | Expo / Sponsors | Press Room |

Names, and logos of other organizations are the property of those organizations and not of NSTI.

This event is not open to the general public and NSTI reserves the right to refuse admission and participation to any individual. Fechnical Conferences | Business Conferences | Nano Impact Workshop | Venue / Hotels | Site Map



Over 5,000 attendees and 250 exhibitors expected!

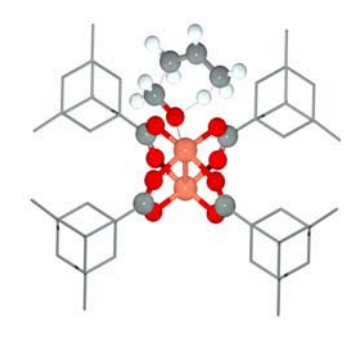


ACS National Meeting ครั้งที่ 236 จำนวน 4 เรื่อง

Quantum chemical analysis of reaction paths in carbonyl-ene reaction between formaldehyde and propene catalyzed with metal-organic framework MOF-11 **PETR 73**

Saowapak Choomwattana, saowapak_ch@hotmail.com¹, Thana Maihom, thanamai@hotmail.com¹, Pipat Khongpracha, jumras.l@ku.ac.th¹, Michael Probst, michael.probst@uibk.ac.at², and Jumras Limtrakul, jumras.l@ku.ac.th¹. (1) Department of Chemistry and Center of Nanotechnology, Faculty of Science, Kasetsart University, 50 Phaholyothin Rd., Ladyao, Jatujak, Bangkok, 10900, Thailand, (2) Institut für Ionenphysik, Universität Innsbruck, Technikerstrasse 25, 6020, Innsbruck, Austria

The interactions of formaldehyde and propene within the nanocavity of the Metal-Organic Framework have been investigated by ONIOM (B3LYP/6-31G(d,p):UFF) calculation. The influence of the Metal-Organic Framework leads to an energy barrier of the reaction ΔE_{act} of 24.1 kcal/mol as compared to the uncatalyzed system of ΔE_{act} of 34.4 kcal/mol. The carbonyl ene reaction of propylene using HCHO@MOF-11 takes place in a single concerted reaction step. The ΔE_{act} value for MOF-11 is similar to the one obtained for the zeolite catalyzed reaction (ΔE_{act} = 25.1 kcal/mol, HCHO@Na-Faujasite/CH₃CH=CH₂). These findings suggest that the MOF can be employed as one of the efficient catalysts for studying the adsorption property and reaction mechanism of the carbonyl-ene reaction.



<u>Chemistry of Petroleum and Emerging Technologies</u> 2:00 PM-4:15 PM, Wednesday, August 20, 2008 Doubletree -- Aria A/B, Oral

Division of Petroleum Chemistry

The 236th ACS National Meeting, Philadelphia, PA, August 17-21, 2008

QUANTUM CHEMICAL INVESTIGATION OF METHOXYBENZENE TRANSFORMATION TO ORTHO-, META- AND PARA-METHYLPHENOLS OVER ACIDIC FAUJASITE ZEOLITE: A MECHANISTIC STUDY

Bavornpon Jansang^{a,b,c}, Tanin Nanok^{a,b,c}, and
Jumras Limtrakul^{a,b,c*}

 ^aLaboratory for Computational & Applied Chemistry, Chemistry Department, Faculty of Science, Kasetsart University, Bangkok 10900, Thailand
 ^bCenter of Nanotechnology, Kasetsart University Research and Development Institute, Kasetsart University, Bangkok 10900, Thailand

^cNANOTEC Center of Excellence, National Nanotechnology Center, Kasetsart University, Bangkok 10900, Thailand

Introduction

Zeolites are one of the most versatile catalysts used in the petrochemical processing industry. One of the major properties which can promote a diverse range of catalytic reactions including acid-base and metal induced reactions. Moreover, zeolites, with their shape-selective properties, are the preferred choice for the realization of the desired end products. It is industrially relevant that zeolites have been found to be environmentally friendly and are, therefore, considered as green chemistry and they contribute towards the reduction of global warming. Faujasite zeolite, in particular, is attributed as one of the major catalysts used in petrochemical industries. Its protonic form has been found to be a significant active constituent for the catalytic cracking of hydrocarbons¹⁻³. In addition, its supercage with a diameter of approximately 13 Å enables it to operate in the same manner as a nanoreactor for the reactions of bulky molecules, including the alkylation of phenol and its family members⁴

Alkylation of phenol with methanol on zeolites undergoes two competitive reactions, i.e., the O- and C-methylation. The product of O-methylation is methoxybenzene or anisole, while the product of C-methylation is methylphenol or cresol. Experimental results revealed that the acid-base properties of the catalysts play an important role in the product selectivity in addition to the experimental factors 6,9,11-14. However, our previous calculation of the alkylation of phenol with methanol over nanostructured H-FAU catalyst demonstrated that the alkylation of phenol with methanol prefers to occur via the concerted pathway rather than via the stepwise pathway¹⁵. The O-methylation is faster than the C-methylation with estimated activation barriers of 28.3 and 32.6 kcal/mol for anisole and o-cresol, respectively. The rate-determining step is the step of surface methoxide. Moreover, it was found that

anisole is a kinetically primary product whereas o-cresol is the most thermodynamically stable product of the reaction. Nevertheless, many literatures suggested that anisole can be an intermediate in the formation of cresols during phenol methylation⁹⁻¹². On the other hand, anisole can transform to cresol. Various experimental information indicated that at higher temperatures and with a longer reaction time conditions, the selectivity of the product of C-methylation increases whereas O-methylation decreases. This point is comprehensively discussed in various literatures^{2,10,11}. In order to fulfill and understand the behavior of the alkylation reaction of phenol with methanol, the reaction mechanism of transformation of methoxybenzene to different isomers of methylphenol will be considered.

To the best of our knowledge, we are not aware of any experimental and theoretical reports on the mechanism of alkylation of phenol over zeolites and other porous materials. The elucidation of the reaction mechanisms does not only provide insights into the fundamental steps of the reaction, but also helps to optimize the reaction conditions and the design of catalysts for industrial production. The logical progression, which is the aim of our present work, is to of transformation mechanism accomplish the methoxybenzene to methylphenol on nanostructured H-FAU by employing the ONIOM method. The structures, energetic properties and thermal rate reaction along the reaction coordinates are presented.

Methods

The faujasite zeolite was modeled by the 178T nanocluster, 177 silicon (Si) and 1 aluminum (Al) atoms, taken from the lattice structure of faujasite zeolite¹⁶. The dangling bonds resulted from cutting the Si-O bonds which were terminated by the H atoms with the Si-H bond distances of 1.47 Å pointed in the same direction as the crystallographic Si-O bonds. This nanocluster covers an area of two supercages connected to each other through the 12T-membered ring window. To take advantage of the computational efficiency, the 178T cluster was subdivided into two layers of calculation methods according to the two-layer ONIOM (ONIOM2) scheme (Figure 1).

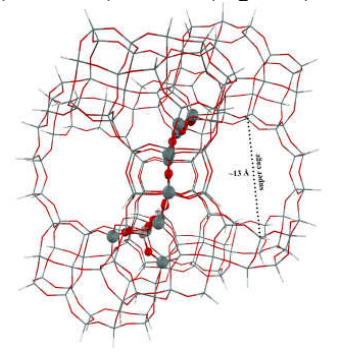


Figure 1. The 178T nanocluster of faujasite zeolite subdivided into two layers of calculation methods according to the two-layer ONIOM (ONIOM2) scheme.

The 14T cluster, including the 12T-membered ring window opening to two supercages and two additional basal T building units, was treated as the inner layer and computed with the hybrid density functional theory approach (B3LYP) combined with the 6-31G(d,p) basis set for describing the local active site of faujasite zeolite. The remainder of the 178T extended framework connected to the 14T active site was treated as the outer layer and computed with the universal force field (UFF). This force field has been found to provide a good description of the long-range van der Waals (vdW) interactions ¹⁷⁻²². All calculations were performed using the Gaussian 03 code²³. During optimization, only the basal 5T of the 14T inner layer, ≡SiO(Hz)Al(OSi≡)₂OSi≡, was permitted to relax while the remainder was fixed along the position of the crystallographic lattice. The frequency calculations were performed at the same level of theory to ensure that the obtained transition state structure has only one imaginary frequency that corresponds to a saddle-point of the required reaction coordinates. To obtain the kinetic behavior of this reaction, the kinetic analysis will be employed. For kinetic analysis of the transformation reaction, the thermal rate constant (k) was estimated by using the transition state theory (TST). Equation 1 is the formula for calculating the thermal rate constant:

$$k_r = \frac{k_B T}{h} \frac{q_{TS}}{q_{Int}} \exp(-\Delta E_a / RT)$$
 (1)

where ΔE_a is the activation energy, k_B is Boltzmann's constant, h is Plank's constant, T is the temperature, R is the universal gas constant and q_{TS} and q_{Int} are the total partition functions for the transition state and the intermediate complex, respectively, which include electronic, translation, rotational and vibrational partition functions. The total partition functions were calculated from the vibrational frequencies. All forward and reverse thermal rate constants were calculated at 298, 423 and 473K, which are the experimental temperatures of reaction for giving the kinetic details of the reaction.

Results and Discussion

Reaction mechanism. The transformation of methoxybenzene to different isomers of methylphenol on nanostructured H-FAU zeolite was presented via direct transformed pathways as shown in Figure 2.

$$\begin{array}{c} H \\ O \\ O \\ O \end{array}$$

Figure 2. Schematic diagram showing the reaction mechanism of the transformation of methoxybenzene to methylphenol in which phenol as a coadsorbed molecule.

The first step is the adsorption complex of methoxybenzene on the active region or Brønsted acid site of faujasite zeolite, **Ads_Methoxybenzene**. The adsorption complex will be adsorbed via the H-bonding complex between the oxygen of phenolic ring (O_{ani}) and the oxygen bridge

framework of the Brønsted acid site (O1). The corresponding intermolecular distance of the H-bonding complex O...O_{ani} is estimated to be about 2.58 Å whereas the O1-Hz-O_(ani) was estimated to be about 174.2 degrees. This compares well with an experimental report for the O1...O_{met} distance in the methanol adsorption on H-ZSM-5 using multinuclear solid-state NMR spectroscopy²⁴, which was in the range of 2.5 to 2.6 Å. This adsorption complex has an effect with the Brønsted acid site of zeolite. The O-Hz bond was lengthened from 0.97 to 1.03 Å whereas the Al-O1 and Si-O2 bonds were contracted by about 0.03 and 0.01 Å, respectively. The Al-O1-Si bond angle was decreased about 1 degree. At this point of the methoxyphenol adsorption complex with the Brønsted acid site of FAU zeolite the calculated relative energies profile was set to be 0 kcal/mol, as illustrated in Figure 3.

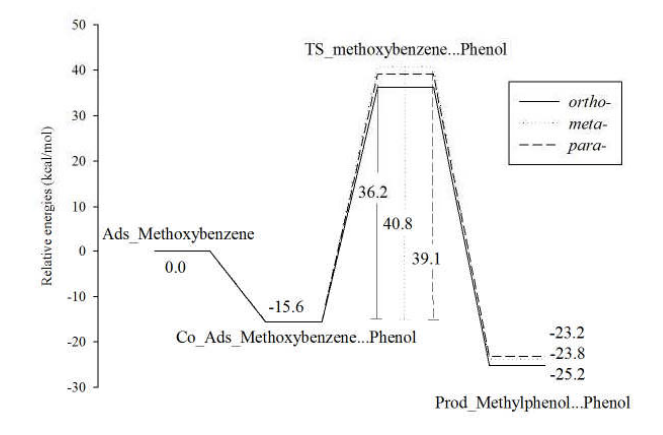


Figure 3. Calculated relative energies of the transformation of methoxybenzene to *ortho-*, *meta-* and *para-*methylphenols over nanostructured H-FAU zeolite by using the ONIOM2 method.

In the second step, another phenol molecule was inserted and located in the supercage of faujasite zeolite by placing it nearby the methoxybenzene, Co_Ads_Methoxybenzene...Phenol. With respect to the methoxybenzene adsorption complex, the corresponding adsorption energy was predicted to be -15.6 kcal/mol. However, this coadsorption between methoxybenzene and phenol was a weak interaction due to the size and steric hindrance of the two molecules. The estimated intermolecular distances of the methyl group of methoxybenzene with *ortho-*, *meta-* and *para-*isomers of phenol on the phenolic ring, C_(met_ani)...C_(phe), were 7.11, 6.11 and 6.39 Å, respectively. These distances will be contracted in the transition state step.

In the transition state of the transformation of methoxybenzene to methylphenol, **TS_Methoxybenzene**, the key of this step is the methoxy group (CH₃). After the methoxybenzene is adsorbed on the Brønsted acid site as a result of the acidic proton of zeolite, it attaches with the $O_{(ani)}$ and the $C_{(met_ani)}...O_{(phe)}$ bond length is lengthened at the same time with the phenol drawn closer. At this point, the

Table 1. Selected parameters of optimized structures, (Ads_Methoxybenzene, Co-Ads_Methoxybenzene...Phenol and TS Methoxybenzene) in the transformation of methoxybenzene to *ortho-, meta-* and *para-*methyphenols

Parameters	Ads Methoxybenzene	Co-Ads_MethoxybenzenePhenol			TS_Methoxybenzene		
r at affecters	Aus_wiethoxybenzene	ortho- meta-		para-	ortho-	meta-	para-
Distances							
O1-Hz	1.03	1.03	1.03	1.03	1.63	1.69	1.67
Hz-O(ani)	1.55	1.53	1.53	1.53	1.01	1.00	1.00
O1-O(ani)	2.58	2.57	2.57	2.57	2.63	2.67	2.65
C(met_ani)-O(ani)	1.44	1.44	1.44	1.44	2.17	2.26	2.15
C(met_ani)-C(phe)	-	7.11	6.11	6.39	2.09	2.04	2.14
C(phe)-H(phe)	-	1.08	1.09	1.09	1.09	1.09	1.09
Angles							
O1-Hz-O(ani)	174.2	178.1	178.1	178.1	174.3	168.9	164.3
O(ani)-C(met_ani)-C(phe)	-	100.6	101.2	109.6	173.4	172.6	172.9

configuration of CH3 will be altered from the tetrahedral to the trigonal planar structure or changed from sp³ to sp² hybridizations. This mechanism is likely to be the S_N2 type reaction. In order to stabilize the transition state structure, the methoxy will form a covalent bond with the phenolic ring, dependent on the favorable positions of the ortho- or meta- or para-isomers. The $C_{(met_ani)}...C_{(phe)}$ bond length of the ortho-, meta- and para-isomers were decreased to 2.09, 2.04 and 2.14 Å, respectively, whereas the $C_{(met_ani)}...O_{(phe)}$ bond lengths were increased to 2.63, 2.67 and 2.65 Å, respectively. The corresponding $O_{(ani)}$ - $C_{(met_ani)}$ - $O_{(phe)}$ bond angle of all configurations were estimated to be 173.4, 172.6 and 172.9 degrees for ortho-, meta- and paraisomers, respectively. All distances and angles of optimized structures are tabulated in Table 1. Moreover, it might be expected that the ortho-isomer should have the lowest activation barrier as compared to the other isomers. The corresponding activation energies (Ea) of ortho-, meta- and para-isomers were estimated to be 36.2, 40.8 and 39.1 kcal/mol, respectively. These results indicate that the requirement of the activation barrier of transformation of methoxybenzene to ortho-isomer of methylphenol is lower than that for other isomers. On the other hand,

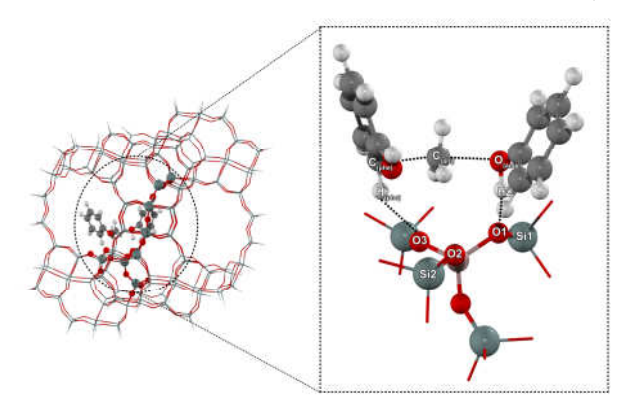


Figure 4. Configuration of the transition state structure and labeled parameters of *ortho*-methylphenol.

they demonstrate that *ortho*-methyphenol is the most preferential product in the transformation of methoxybenzene due to kinetically favorable control. This result agrees well with previous experimental reports on the methylation of phenol with methanol on H-Y zeolite^{6,10}. The calculated relative energies of all species involved in this reaction are illustrated in Figure 3.

The final step is the formation of methylphenol in different isomers. The methoxy specie moves toward the carbon position of the phenolic ring and forms a covalent bond. However, this step will be completed after the proton of the phenol back-donation to the Brønsted acid site of zeolite. And then the methylphenol will be created and another phenol will also be generated. This phenol was the result of the decomposition of methoxybenzene, subsequently, it can combine with methanol to form methoxybenzene or otherwise with another methoxybenzene to form methylphenol. With respect to the coadsorption complex of methoxybenzene with phenol, the reaction energy (E_r) for the production of ortho-, meta- and paramethylphenols were exothermic by 9.6, 8.2 and 7.6 kcal/mol, respectively. This result confirms that orthomethylphenol which was confined in nanostructured H-FAU zeolite was more stable than *meta*- and *para*-methylphenols.

Kinetic analysis. For kinetic analysis, the thermal rate constant (k) can be directly evaluated via Arrhenius equation by using the transition state theory. With comparison of the thermal rate constant between forward (k_f) and reverse (k_r) at 298K, the calculated forward thermal rate constants for *ortho-*, *meta-* and *para-*isomers, are estimated to be 7.141 x 10^{-13} , 8.565x 10^{-17} and 3.479 x 10^{-16} s⁻¹, respectively, whereas the estimated reverse thermal rate constants are predicted to be 7.227x 10^{-21} , 9.827 x 10^{-24} and 3.050 x 10^{-22} s⁻¹, respectively. These results indicate that the forward thermal rate constant is faster than the reverse thermal rate constant. On the other hand, the reaction will proceed or be driven via the forward thermal rate constants more so than by the backward ones.

Table 2. The calculated thermal rate constant (k) of forward (k_t) and reverse (k_t) by transition state theory at 298, 423 and 473 K.

Temperatures	Forward thermal rate constants: $k_f(s^{-1})$		Reverse thermal rate constants: k_r (s ⁻¹)			
(K)	ortho-	meta-	para-	ortho-	meta-	para-
298	7.141 x 10 ⁻¹³	8.565 x 10 ⁻¹⁷	3.479×10^{-16}	7.227×10^{-21}	9.827 x 10 ⁻²⁴	3.050 x 10 ⁻²²
423	1.118 x 10 ⁻⁰⁴	1.250×10^{-07}	2.199 x 10 ⁻⁰⁷	8.575×10^{-11}	5.401×10^{-13}	8.035×10^{-12}
473	1.410×10^{-02}	2.779 x 10 ⁻⁰⁵	3.971 x 10 ⁻⁰⁵	3.064×10^{-08}	2.849×10^{-10}	3.612×10^{-09}

Moreover, the rate constant of *ortho*-isomer has four and three times more rather than *meta*- and *para*-isomers,respectively.All calculations of forward and reverse thermal rate constants at different temperature are tabulated in Table 2. Considering the forward rate constant after the temperature was increased to 423 and 473K, it contrasts with the rate constant at 298K. Our result shows that the thermal rate constant of *meta*- and *para*-isomers will be reversed (1.250 x 10⁻⁰⁷ s⁻¹ vs. 2.199 x 10⁻⁰⁷ s⁻¹ for 423K and 2.779 x 10⁻⁰⁵ s⁻¹ vs. 3.971 x 10⁻⁰⁵ s⁻¹ for 473K). Although there is a reversal of the rate constants of *meta*- and *para*-isomers after increasing the temperature, this reversal is, however, very small. It occurs, perhaps, from the small difference of the activation barriers or from the steric hindrance of each isomer.

The reverse constants at 298K of *ortho-*, *meta-* and *para-*isomers are 7.227 x 10^{-21} , 9.827 x 10^{-24} and 3.050 x 10^{-22} s⁻¹, respectively. These indicate that the orders of the fastest reverse rate constant are *ortho->para->meta-*, even though the temperature is increased to 423 and 473K. These results are also in good agreement with the corresponding E_a+E_r of *ortho-*, *meta-* and *para-*isomers, which are estimated to be 45.8, 49.0 and 46.7 kcal/mol, respectively.

Conclusions

The combined methodology of the density functional theory and molecular mechanics by employing an ONIOM approach, ONIOM(B3LYP/6-31G(d,p):UFF), has been investigate performed to the transformation methoxybenzene to ortho-, meta- and para-methylphenols over nanostructured H-FAU zeolite. It was found that the ortho-isomer is the most preferential product compared to other isomers. The corresponding activation barriers are 36.2, 40.8 and 39.1 kcal/mol for ortho-, meta- and paraisomers, respectively. The reaction occurs via direct transformation between methoxybenzene and phenol. Taking into account the thermal rate constant, the forward thermal rate constant is faster than the reverse thermal rate constant. The ortho-methylphenol is the thermodynamically stable product of reaction, which agrees well with a previous experimental report on alkylation of phenol with methanol.

Acknowledgment. This work was supported in part by grants from the Thailand Research Fund (to J.L.) and the Kasetsart University Research and Development Institute (KURDI), the National Nanotechnology Center (NANOTEC Center of Excellence and CNC Consortium) and the Commission on Higher Education (Postdoctoral

Research Scholar to T.N.), Ministry of Education under Postgraduate Education and Research Programs in Petroleum and Petrochemicals, and Advanced Materials. The support from the Graduate School Kasetsart University is also acknowledged.

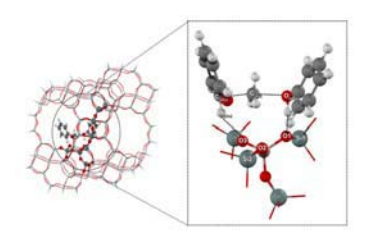
References

- (1) Corma, A. Chem. Rev. 1995, 95, 559.
- (2) Li, J.; Xiong, G.; Feng, Z.; Liu, Z.; Xin, Q.; Li, C. Microporous Mesoporous Mater. 2000, 39, 275.
- (3) van Santen, R. A.; Kramer, G. J. Chem. Rev. 1995, 95, 637.
- (4) Balsama, S.; Beltrame, P.; Beltrame, P. L.; Carniti, P.; Forni, L.; Zuretti, G. *Appl. Catal.* **1984**, *13*, 161.
- (5) Barman, S.; Pradhan, N. C.; Basu, J. K. Catal. Lett. 2006,
- (6) Borodina, I. B.; Pomakhina, E. B.; Ramishvili, T. M.; Ponomareva, O. A.; Rebrov, A. I.; Ivanova, I. I. Russ. J. Phys. Chem. 2006, 80, 892.
- (7) Garcia, L.; Giannetto, G.; Goldwasser, M. R.; Guisnet, M.; Magnoux, P. Catal. Lett. 1996, 37, 121.
- (8) Ivanova, I. I.; Pomakhina, E. B.; Rebrov, A. I.; Hunger, M.; Kolyagin, Y. G.; Weitkamp, J. J. Catal. 2001, 203, 375.
- (9) Marczewski, M.; Bodibo, J. P.; Perot, G.; Guisnet, M. J. Mol. Catal. 1989, 50, 211.
- (10) Wang, W.; De Cola, P. L.; Glaeser, R.; Ivanova, I. I.; Weitkamp, J.; Hunger, M. Catal. Lett. 2004, 94, 119.
- (11) Chantal, P. D.; Kaliaguine, S.; Grandmaison, J. L. *Appl. Catal.* **1985**. *18*, 133.
- (12) Pierantozzi, R.; Nordquist, A. F. Appl. Catal. 1986, 21, 263.
- (13) Samolada, M. C.; Grigoriadou, E.; Kiparissides, Z.; Vasalos, I. A. J. Catal. 1995, 152, 52.
- (14) Xu, J.; Yan, A.-Z.; Xu, Q.-H. React. Kinet. Catal. Lett. 1997, 62, 71.
- (15) Jansang, B.; Nanok, T.; Limtrakul, J. J. Phys. Chem. C 2008, 112, 540.
- (16) Olson, D. H.; Dempsey, E. J. Catal. 1969, 13, 221.
- (17) Rungsirisakun, R.; Jansang, B.; Pantu, P.; Limtrakul, J. J. Mol. Struct. 2004, 733, 239.
- (18) Kasuriya, S.; Namuangruk, S.; Treesukol, P.; Tirtowidjojo, M.; Limtrakul, J. J. Catal. 2003, 219, 320.
- (19) Namuangruk, S.; Pantu, P.; Limtrakul, J. *Journal of Catalysis* **2004**, *225*, 523.
- (20) Panyaburapa, W.; Nanok, T.; Limtrakul, J. J. Phys. Chem C 2007, 111, 3433.
- (21) Jansang, B.; Nanok, T.; Limtrakul, J. J. Phys. Chem. B 2006, 110, 12626.
- (22) Namuangruk, S.; Khongpracha, P.; Pantu, P.; Limtrakul, J. *J. Phys. Chem. B* **2006**, *110*, 25950.
- (23) Frisch, M. J. T., et al. Gaussian03; Gaussian, Inc.: Wallingford, CT, 2004.
- (24) Hunger, M.; Horvath, T. J. Am. Chem. Soc. 1996, 118, 12302.

Quantum chemical investigation of methoxybenzene transformation to ortho-, metaand para-methylphenols over acidic faujasite zeolite: A mechanistic study PETR 74

Bavornpon Jansang, bavornpon@yahoo.com, Tanin Nanok, g4384022@ku.ac.th, and Jumras Limtrakul, jumras.l@ku.ac.th. Department of Chemistry and Center of Nanotechnology, Faculty of Science, Kasetsart University, 50 Phaholyothin Rd., Ladyao, Jatujak, Bangkok, 10900. Thailand

Mechanistic investigations of the transformation of methoxybenzene (anisole) to *ortho-, meta-* and *para-*isomers of methylphenol (cresol) on nanostructured zeolite, H-FAU, was studied with the combined methods of the density functional theory (DFT) and molecular mechanics (MM) by employing an ONIOM approach. The two-layer ONIOM(B3LYP/6-31G(d,p):UFF) scheme demonstrated that the transformation of anisole to *ortho-*isomer is the most thermodynamically and kinetically preferential product. The corresponding activation barriers are predicted to be 36.2, 40.8 and 39.1 kcal/mol for *ortho-, meta-* and *para-*isomers, respectively. The calculated forward thermal rate constants at 298K, derived by using the transition state theory (TST) for *ortho-, meta-* and *para-*isomers, are 7.141 x 10⁻¹³, 8.565 x 10⁻¹⁷ and 3.479 x 10⁻¹⁶ s⁻¹, respectively, whereas the estimated reverse thermal rate constants are 7.227 x 10⁻²¹, 9.827 x 10⁻²⁴ and 3.050 x 10⁻²² s⁻¹, respectively. Our results, which are in good agreement with the experimental observations, indicate that our ONIOM model can be employed for studying the reaction mechanism on nanocatalysts.



<u>Chemistry of Petroleum and Emerging Technologies</u> 2:00 PM-4:15 PM, Wednesday, August 20, 2008 Doubletree -- Aria A/B, Oral

Division of Petroleum Chemistry

The 236th ACS National Meeting, Philadelphia, PA, August 17-21, 2008

QUANTUM CHEMICAL ANALYSIS OF REACTION PATHS IN CARBONYL-ENE REACTION BETWEEN FORMALDEHYDE AND PROPOENE CATALYZED WITH METAL-ORGANIC FRAMEWORK MOF-11

S. Choomwattana^{a,b}, T. Maihom^{a,b}, P. Khongpracha^{a,b}, M. Probst^c and J. Limtrakul^{a,b*}

^aDepartment of Chemistry and Center of Nanotechnology, Kasetsart University, Bangkok 10900, Thailand, fscijrl@ku.ac.th ^bNANOTEC Center of Excellence, National Nanotechnology Center, Kasetsart University, Bangkok 10900, Thailand ^cInstitute of Ion Physics and Applied Physics, University of Innsbruck, Innsbruck, Austria

Introduction

The carbonyl-ene reaction is the enantioselective reaction between all-carba-ene components and hetero-enophiles¹⁻⁴. Various industrial and biosynthetic processes⁵, including tetrahydrofuran (THF) synthesis⁶, are based on the carbonyl-ene reaction.

3-buten-1-ol is acquired as a monomer in polymerization reactions and as an intermediate for tetrahydrofuran (THF) synthesis⁶. Because of the disadvantages of a low boiling point of –19.5 °C and the tendency to self-polymerize to solid paraformaldehyde and trioxane, pretreatment with thermal or Lewis acid for formaldehyde is needed. These processes unfortunately involve problems concerning corrosion, handling and toxic waste.

Environment-friendly porous materials such as zeolites were found to be candidates for storage of formaldehyde⁷. Subsequently, the production of 3-buten-1-ol has been studied. More recently, the carbonyl-ene reaction between formaldehyde encapsulated in Na-faujasite and propylene has been investigated theoretically⁸. For the reaction with larger molecules, porous materials like Metal-Organic Frameworks (MOFs) become more advantageous because of the accessible variation of pore dimension and chemistry inside the cavity.

MOFs are known as crystalline porous materials with remarkable properties. They consist of three-dimensional clusters of metal oxide held together by organic linkers forming a systematic network with nanoscale periodic channels and cavities. The pore structure can be customized to satisfy various applications by using appropriate linkers. With their inorganic joints and assorted organic linkers, MOFs are promising catalysts, gas separators, molecular sensors, and so forth. MOF-11 has an open metal site of Cu₂(CO₂)₄ paddlewheel units and a spongy network of adamantine, illustrated in Fig. 1. Similar to zeolites, its porosity can be shape-selective. Its open metal sites can play a central role in highly selective and specific molecular transformations, as well as transport and storage⁹⁻¹². We want to investigate if its open metal site can be used to catalyze the ene-reaction in a way similar to Na cation in Na-FAU as described above.

We approach the reaction mechanisms on a molecular level by means of quantum chemical calculations. Since both zeolites and MOFs are micro-mesoporous materials, the computational methods and schemes used for MOFs can be adopted from the ones used in the study of zeolites. Like in

zeolites¹³⁻¹⁶, only a small part of the framework affects the electronic properties of the reactive site, thus facilitating modeling using quantum chemical methods. On the other side, because of the role of the MOF framework in the adsorption of the reactants¹⁷, it cannot be completely neglected. Hybrid methods such as embedded cluster or combined quantum mechanics/molecular mechanics (QM/MM) method¹⁸⁻²⁵ as well as the ONIOM scheme are well suited to such systems. We decided to use the ONIOM (Our-own-N-layer Integrated molecular Orbital + molecular Mechanics) method^{24,25} since it is frequently exploited to study extended systems²⁶⁻³⁰, and has also been applied to the adsorption of ethylene, benzene and ethylbenzene over acidic and alkaline faujasite and ZSM-5 zeolites^{29,31-33}.

In this work, we study the mechanism of the carbonyl-ene reaction between MOF-11 encapsulated formaldehyde and propylene. To our knowledge there is no experimental data for this reaction, but by comparison with the zeolite-based system we hope to predict the MOF-11 case correctly.



Figure 1. MOF-11 structure generated from XRD Data. The cavity dimensions (width, height, and depth) of the structure are $14.44 \times 6.00 \times 8.47 \text{Å}^3$. The metal open site of the paddlewheel cluster is magnified.

Theoretical Methods

The MOF-11 structure was obtained from XRD data³⁴. MOF-11 is based on a 3-D channel system with a diameter of 6.0-6.5 Å. It consists of square-shaped Cu₂(CO₂)₄ paddlewheel building units connected to 1,3,5,7-adamantane tetracarboxylate (ATC) linkers in PtS topology³⁴, where each admantane is bound to four Cu₂O₄C₈ squares. The active paddlewheel unit is the effective part to the molecules of the system, since formaldehyde can easily enter between the adamantine units. This region makes up the inner ONIOM layer and is treated on the B3LYP/6-31G(d,p) level of theory. The framework environment constitutes the outer ONIOM layer. In it, mostly van der Waals interactions due to confinement in the mesoporous materials play a role and are considered with the universal force field (UFF)³⁵. Earlier comparisons between calculations using UFF experimental results in organic-inorganic systems 35-39 indicate that UFF is reliable for this purpose.

In our calculations, the MOF framework was kept at the crystallographic geometry, while the upper part of the paddlewheel active site (CuO₄C₄, see Fig. 1) and the adsorbates (HCHO and CH₃CH=CH₂) were fully optimized.

Normal mode analyses were performed to confirm the transition state to have one imaginary frequency whose mode corresponds to the reaction coordinate. All quantum chemical calculations were performed with the Gaussian 03 code⁴⁰.

Results and Discussion

We separate the discussion into two sections. First, we discuss the structure of MOF-11 and the existence of encapsulated formaldehyde in MOF-11 (HCHO@MOF-11) in order to study the reactivity of this species. Then, we report the study of their interactions with propylene using the ONIOM model. A symbol like in M@S signifies that a molecule M adsorbed on an active site S of MOF.

MOF-11 and MOF encapsulated formaldehyde (HCHO@MOF-11) As previously found for zeolites^{31-33,41-47}, current works^{17,48} show that interactions of hydrocarbons adsorbate with the MOF network play a vital part in the structures and energetics of the adsorption process.

The MOF-11 model used in the study is illustrated in Fig. 1. Key optimized geometrical parameters are listed in Table 1. Fig. 2a exhibits the structure of formaldehyde stabilized in the MOF-11 framework. The Cu unit (Cu1-Cu2) is barely changed upon the adsorption of formaldehyde (0.085 Å and 5° for changes in Cu1-Cu2 bond distance and O-Cu-O bond angles, respectively), which is a smaller adjustment than has been found in Na-faujasite. The distance between formaldehyde and MOF-11 is found to be 2.3 Å. The carbonoxygen bond of formaldehyde is elongated from 1.207 to 1.215 Å. According to the interaction between the hydrogen atoms of formaldehyde and the oxygen atoms of the framework, the corresponding distance between the formaldehyde oxygen and the Cu atom of MOF-11 active site is 2.318 Å. and the resulting adsorption energy for the HCHO@MOF-11 complex is -12.3 kcal/mol. The C-O... Cu/MOF angle is 115.0°.

Carbonyl-ene reaction between MOF-11 encapsulated formaldehyde and propylene (HCHO@MOF-11/CH₃CH=CH₂) For the carbonyl-ene reaction, a concerted mechanism was proposed in which the bond between the carbon atom of formaldehyde (C) and the propylene carbon (C1) is formed and the propylene proton (H) is transferred. Assuming the same mechanism for the reaction in Na-faujasite and the calculated energy profile, we propose the reaction in the following steps:

In step (1), formaldehyde adsorbs over the paddlewheel active site of MOF-11 via lone pair electron interaction with an adsorption energy of -12.3 kcal/mol. Then, in step (2), the earlier encapsulated formaldehyde interacts with diffusing propylene via a π -interaction with a coadsorption energy of -19.0 kcal/mol, followed with the chemical reaction in order to produce 3-buten-1-ol. The required activation energy is 24.1 kcal/mol. The calculated transition state confirms the

proposed concerted pathway (Fig. 2c). Its imaginary frequency belongs to the mode in which the C-C bond is formed and H being transferred. The product formation is exothermic by -28.1 kcal/mol. The product needs 11.9 kcal/mol to desorb from the active site in the final step (3). The key geometrical parameters of the carbonyl-ene reaction between propylene and MOF-11 encapsulated formaldehyde from the geometric optimizations are presented in Table 1. The energetics of the reaction is illustrated in Fig. 3.

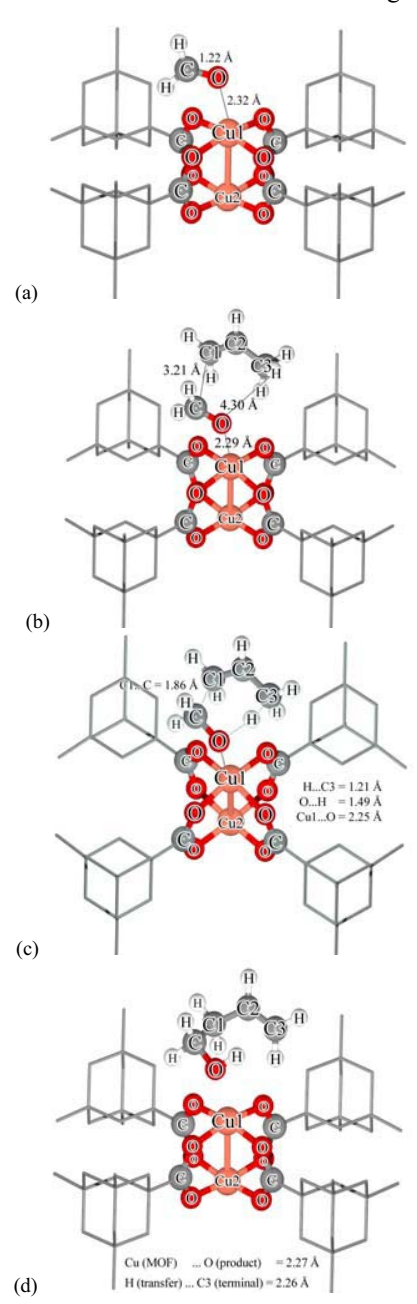


Figure 2. Structures of the HCHO@MOF-11/CH₃CH=CH₂ complexes: (a) HCHO@MOF-11; (b) coadsorption; (c) transition state and (d) product.

Table 1. Optimized geometric parameters of reactants, transition state and product of the carbonyl-ene reaction between formaldehyde and propylene on MOF-11 using the ONIOM (B3LYP/6-31G(d,p):UFF) method.

Parameters	Isolated molecul e	Ads- HCHO	Coads	TS	Prod.
Distances (Å)					
C-O	1.217	1.215	1.218	1.310	1.436
C1-C2	1.333	-	1.334	1.403	1.507
C2-C3	1.501	-	1.498	1.424	1.341
С3-Н	1.097	-	1.095	1.211	2.258
C-C1	-	-	3.213	1.864	1.543
О-Н	-	-	2.995	1.486	0.972
Cu1-O	-	2.318	2.285	2.248	2.265
Cu1-O1	1.936	1.940	1.937	1.944	1.944
Cu1-O2	1.936	1.941	1.949	1.980	1.968
Cu1-O3	1.936	1.959	1.965	1.973	1.958
Cu1-O4	1.936	1.958	1.949	1.939	1.934
Cu1-Cu2	2.506	2.591	2.595	2.652	2.599
Angles (degrees)				
∠O1-Cu1-O3	173.0	168.0	167.7	164.1	167.2
∠O2-Cu1-O4	173.0	168.0	167.6	164.3	167.1

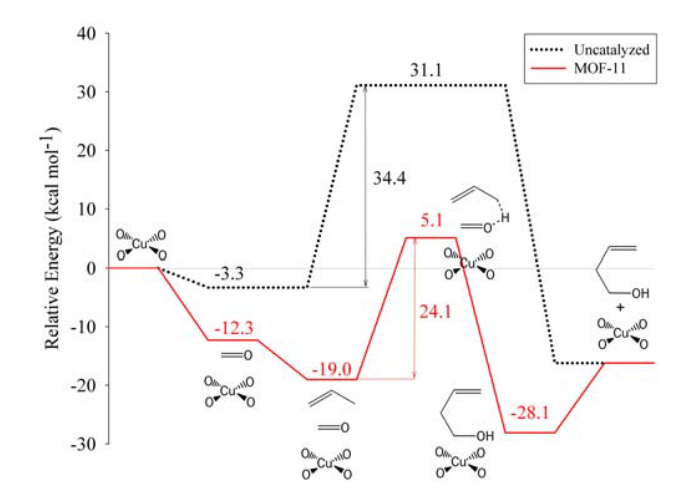


Figure 3. Calculated energy profiles (kcal/mol) for the carbonyl-ene reaction between HCHO and CH₃CH=CH₂ in MOF-11 system (solid line) and the bare system (dotted line).

The Cu atom is slightly moved away from the lower plane toward the reacting molecules. Specifically, the following geometric parameters of the reactants are changed: The propylene C3–H bond length is stretched from 1.095 to 1.211 Å and the distance between the propylene proton (H) and the formaldehyde oxygen (O) is shortened from 2.995 to 1.486 Å. The C–O double bond of formaldehyde is changed from 1.218 to 1.310 Å as the distance between the propylene carbon (C1) and formaldehyde carbon (C) is contracted from 3.213 to 1.864 Å. The C1–C2 and C2–C3 bond lengths are stretched from 1.334 and 1.498 to 1.403 and 1.424 Å, respectively. Due to the steric effect from the paddlewheel framework, the

overall activation energy is 5.1 kcal/mol. These results show that the electrostatic contribution from the Cu also stabilizes the transition state structure inside MOF-11. The product formation is illustrated in Fig. 2d. The adsorbed 3-buten-1-ol product is subsequently desorbed endothermically.

The results indicate that MOF-11 can be used as a catalyst in the carbonyl-ene reaction and that it stabilizes all species in the carbonyl-ene reaction systems. The apparent activation energy of 5.1 kcal/mol is higher than in Na-faujasite, but is lower than in the noncatalyzed reaction (31.1 kcal/mol). As the activation energy for this transition state is 24.1 kcal/mol, which is comparable to the reaction on Na-faujasite (25.1 kcal/mol), it is likely that the open site Cu atom can catalyze the reaction in a similar way to that of Na(I) in the faujasite. Both Na@FAU and MOF-11 catalysts can lower the activation energy compared to the uncatalyzed reaction (34.4 kcal/mol). The advantage of MOF over FAU is the adjustable size of the active MOF cavity by using different organic linkers to form the network structure of the framework.

Conclusions

Density-functional theory and the ONIOM approach are used for investigating the Molecular Organic Framework structures interacting with formaldehyde and their reaction with propylene. The reaction mechanism is proposed to be intermediate-free concerted, consisting of proton transfer and carbon-carbon bond formation. The energy barrier and the apparent activation energy for the MOF-11 system are 24.1 and 5.1 kcal/mol, respectively. It was found that inclusion of the extended Metal Organic Framework has an effect on the structure and energetics of the adsorption complexes and leads to a lower energy barrier ($\Delta E_{act} = 24.1 \text{ kcal/mol}$) of the reaction as compared to the bare model system ($\Delta E_{act} = 34.4$ kcal/mol). The result derived for MOF-11 is similar to the one for the zeolite catalyst ($\Delta E_{act} = 25.1$ kcal/mol obtained for faujasite zeolite in HCHO@Na-FAU/CH $_3$ CH=CH $_2$) suggesting that MOF-11 might be a good candidate material for use in catalysis.

Acknowledgement This work was supported in part by grants from the Thailand Research Fund, the National Nanotechnology Center (NANOTEC Center of Excellence and CNC Consortium), Kasetsart University Research and Development Institute (KURDI) and the Commission of Higher Education, Ministry of Education under Postgraduate Education and Research Programs in Petroleum and Petrochemicals, and Advanced Materials.

References

- Maruoka, K.; Hoshino, Y.; Shirasaka, T.; Yamamoto, H. Tetrahedron Lett. 1988, 29, 3967.
- (2) Mikami, K.; Terada, M.; Nakai, T. J. Am. Chem. Soc. 1989, 111, 1940.
- (3) Carreira, E. M.; Lee, W.; Singer, R. A. J. Am. Chem. Soc. 1995, 117, 3649.
- (4) Johannsen, M.; Joergensen, K. A. J. Org. Chem. 1995, 60, 5757.
- (5) Hoffmann, H. M. R. Angew. Chem., Int. Ed. Engl. 1969, 8, 556.
- (6) Squire, E. N. Synthesis of tetrahydrofuran; (du Pont de Nemours, E. I., and Co., USA). Application: US, 1981; pp 4.
- (7) Okachi, T.; Onaka, M. J. Am. Chem. Soc. 2004, 126, 2306.
- (8) Sangthong, W.; Probst, M.; Limtrakul, J. J. Mol. Struct. 2005, 748, 119.

- Holm, R. H.; Kennepohl, P.; Solomon, E. I. Chem. Rev. 1996, 96, 2239.
- (10) Davis, M. E. Stud. Surf. Sci. Catal. 1999, 121, 23.
- (11) Thomas, J. M. Angew. Chem., Int. Ed. 1999, 38, 3589.
- (12) Ramprasad, D.; Pez, G. P.; Toby, B. H.; Markley, T. J.; Pearlstein, R. M. J. Am. Chem. Soc. 1995, 117, 10694.
- (13) Sauer, J. Chem. Rev. 1989, 89, 199.
- (14) Sauer, J.; Ugliengo, P.; Garrone, E.; Saunders, V. R. Chem. Rev. 1994, 94, 2095.
- (15) Limtrakul, J. Chem. Phys. 1995, 193, 79.
- (16) Limtrakul, J.; Treesukol, P.; Ebner, C.; Sansone, R.; Probst, M. Chem. Phys. 1997, 215, 77.
- (17) Choomwattana, S.; Khongpracha, P.; Limtrakul, J. Adsorptions of CH₄ and C₂H₄ on MOP-28: A Combined QM and QM/MM study. In *Nanoporous Materials-V*; Sayari, A., Jaroniec, M., Eds.; World Scientific Publishing: Vancouver, Canada in press.
- (18) Limtrakul, J.; Jungsuttiwong, S.; Khongpracha, P. *J. Mol. Struct.* **2000**, *525*, 153.
- (19) Sinclair, P. E.; De Vries, A.; Sherwood, P.; Catlow, C. R. A.; van Santen, R. A. J. Chem. Soc., Faraday Trans. 1998, 3401.
- (20) Braendle, M.; Sauer, J. J. Am. Chem. Soc. 1998, 120, 1556.
- (21) Greatbanks, S. P.; Hillier, I. H.; Burton, N. A.; Sherwood, P. J. Chem. Phys. 1996, 105, 3770.
- (22) Khaliullin, R. Z.; Bell, A. T.; Kazansky, V. B. J. Phys. Chem. A 2001, 105, 10454.
- (23) Limtrakul, J.; Nanok, T.; Jungsuttiwong, S.; Khongpracha, P.; Truong, T. N. Chem. Phys. Lett. 2001, 349, 161.
- (24) de Vries, A. H.; Sherwood, P.; Collins, S. J.; Rigby, A. M.; Rigutto, M.; Kramer, G. J. J. Phys. Chem. B 1999, 103, 6133.
- (25) Svensson, M.; Humbel, S.; Froese, R. D. J.; Matsubara, T.; Sieber, S.; Morokuma, K. *J. Phys. Chem.* **1996**, *100*, 19357.
- (26) Tang, H. R.; Fan, K. N. Chem. Phys. Lett. 2000, 330, 509.
- (27) Roggero, I.; Civalleri, B.; Ugliengo, P. Chem. Phys. Lett. 2001, 341, 625.
- (28) Sillar, K.; Burk, P. J. Mol. Struct. (Theochem) 2002, 589-590, 281.
- (29) Kasuriya, S.; Namuangruk, S.; Treesukol, P.; Tirtowidjojo, M.; Limtrakul, J. J. Catal. 2003, 219, 320.
- (30) Torrent, M.; Vreven, T.; Musaev, D. G.; Morokuma, K.; Farkas, O.; Schlegel, H. B. *J. Am. Chem. Soc.* **2002**, *124*, 192.
- (31) Raksakoon, C.; Limtrakul, J. J. Mol. Struct. (Theochem) 2003,
- (32) Panjan, W.; Limtrakul, J. J. Mol. Struct. 2003, 654, 35.
- (33) Bobuatong, K.; Limtrakul, J. Appl. Catal., A 2003, 253, 49.
- (34) Chen, B.; Eddaoudi, M.; Reineke, T. M.; Kampf, J. W.; O'Keeffe, M.; Yaghi, O. M. *J. Am. Chem. Soc.* **2000**, *122*, 11559
- (35) Rappe, A. K.; Casewit, C. J.; Colwell, K. S.; Goddard, W. A., III; Skiff, W. M. *J. Am. Chem. Soc.* **1992**, *114*, 10024.
- (36) Casewit, C. J.; Colwell, K. S.; Rappe, A. K. J. Am. Chem. Soc. 1992, 114, 10035.
- (37) Casewit, C. J.; Colwell, K. S.; Rappe, A. K. J. Am. Chem. Soc. 1992, 114, 10046.
- (38) Rappe, A. K.; Colwell, K. S.; Casewit, C. J. *Inorg. Chem.* 1993, 32, 3438.
- (39) Kern, A.; Nather, C.; Studt, F.; Tuczek, F. Inorg. Chem. 2004, 43, 5003.
- (40) Gaussian 03, R. B.; M. J. Frisch, G. W. T., H. B. Schlegel, G. E. Scuseria, ; M. A. Robb, J. R. C., J. A. Montgomery, Jr., T. Vreven, ; K. N. Kudin, J. C. B., J. M. Millam, S. S. Iyengar, J. Tomasi, ; V. Barone, B. M., M. Cossi, G. Scalmani, N. Rega, ; G. A. Petersson, H. N., M. Hada, M. Ehara, K. Toyota, ; R. Fukuda, J. H., M. Ishida, T. Nakajima, Y. Honda, O. Kitao, ; H.

- Nakai, M. K., X. Li, J. E. Knox, H. P. Hratchian, J. B. Cross, ; C. Adamo, J. J., R. Gomperts, R. E. Stratmann, O. Yazyev, ; A. J. Austin, R. C., C. Pomelli, J. W. Ochterski, P. Y. Ayala, ; K. Morokuma, G. A. V., P. Salvador, J. J. Dannenberg, ; V. G. Zakrzewski, S. D., A. D. Daniels, M. C. Strain, ; O. Farkas, D. K. M., A. D. Rabuck, K. Raghavachari, ; J. B. Foresman, J. V. O., Q. Cui, A. G. Baboul, S. Clifford, ; J. Cioslowski, B. B. S., G. Liu, A. Liashenko, P. Piskorz, ; I. Komaromi, R. L. M., D. J. Fox, T. Keith, M. A. Al-Laham, ; C. Y. Peng, A. N., M. Challacombe, P. M. W. Gill, ; B. Johnson, W. C., M. W. Wong, C. Gonzalez, and J. A. Pople, ; Gaussian, I., Pittsburgh PA. 2003.
- (41) Namuangruk, S.; Pantu, P.; Limtrakul, J. *ChemPhysChem* **2005**, *6*, 1333.
- (42) Pelmenschikov, A.; Leszczynski, J. J. Phys. Chem. B 1999, 103, 6886.
- (43) Wesolowski, T. A.; Parisel, O.; Ellinger, Y.; Weber, J. J. Phys. Chem. A 1997, 101, 7818.
- (44) Derouane, E. G.; Chang, C. D. Microporous Mesoporous Mater. 2000, 35-36, 425.
- (45) Clark, L. A.; Sierka, M.; Sauer, J. J. Am. Chem. Soc. 2003, 125, 2136.
- (46) Vos, A. M.; Rozanska, X.; Schoonheydt, R. A.; Van Santen, R. A.; Hutschka, F.; Hafner, J. J. Am. Chem. Soc. 2001, 123, 2799.
- (47) Rozanska, X.; Van Santen, R. A.; Hutschka, F.; Hafner, J. J. Am. Chem. Soc. 2001, 123, 7655.
- (48) Boekfa, B.; Choomwattana, S.; Wattanakit, C.; Limtrakul, P.; Pantu, P.; Limtrakul, J. Effect of the Framework on the Adsorption of Methane on IRMOF-1, IRMOF-2, and IRMOF-6 Metal-Organic Frameworks: A Combined QM and QM/MM study. In *Nanoporous Materials-V* Sayari, A., Jaroniec, M., Eds.; World Scientific Publishing: Vancouver, Canada, in press.

Structures and reaction mechanisms of ethylene oxide hydration over H-ZSM-5: An embedded ONIOM approach

PHYS 501

Thana Maihom, thanamai@hotmail.com¹, Supawadee Namuangruk, supawadee@nanotec.or.th², Pipat Khongpracha, jumras.l@ku.ac.th¹, Tanin Nanok, g4384022@ku.ac.th¹, and Jumras Limtrakul, jumras.l@ku.ac.th¹. (1) Department of Chemistry and Center of Nanotechnology, Faculty of Science, Kasetsart University, 50 Phaholyothin Rd., Ladyao, Jatujak, Bangkok, 10900, Thailand, (2) National Nanotechnology Center (NANOTEC), NSTDA, Khong 1, Khongluang, Pathumthani, 12120, Thailand

Stepwise and concerted mechanisms of ethylene oxide hydration reaction within a cluster model covering nanocavity, where the straight and zigzag channels intersect, of H-ZSM-5 have been proposed and investigated by means of the embedded ONIOM(B3LYP/6-31G (d,p):UFF) methods. For the stepwise mechanism, the hydration reaction of ethylene oxide starts from the ring-opening of ethylene oxide by breaking of the C-O bond to form the alkoxide intermediate followed by the hydration of the alkoxide intermediate to produce ethylene glycol as the product of the reaction. The calculated activation energies are computed to be 30.8 and 10.6 kcal/mol for the ring-opening and hydration steps, respectively. For the concerted mechanism, the ring-opening and hydration take place in simultaneously with a small activation barrier of 9.2 kcal/mol. This reaction is suggested as a more economical alternative to the present non-catalytic hydration of ethylene oxide via the concerted mechanism for the production of ethylene glycol, a versatile intermediate in a wide range of applications, and should be of particular interest to industry.

PHYS Poster Session - General Theory
7:30 PM-10:00 PM, Wednesday, August 20, 2008 Pennsylvania Convention Center -- Hall C, Poster

Division of Physical Chemistry

The 236th ACS National Meeting, Philadelphia, PA, August 17-21, 2008

Interaction of glycine on gold nanocluster decorated on single-wall carbon nanotube: Theoretical investigation

PHYS 515

Pipat Khongpracha, jumras.l@ku.ac.th¹, Supawadee Namuangruk, supawadee@nanotec.or.th², Chompunuch Warakulwit, w_chompunuch@yahoo.com¹, and Jumras Limtrakul, jumras.l@ku.ac.th¹. (1) Department of Chemistry and Center of Nanotechnology, Faculty of Science, Kasetsart University, 50 Phaholyothin Rd., Ladyao, Jatujak, Bangkok, 10900, Thailand, (2) National Nanotechnology Center (NANOTEC), NSTDA, Khong 1, Khongluang, Pathumthani, 12120, Thailand

The deposition of a gold nanocluster on an open end of a single-wall carbon nanotube (SWNT) was designed by employing high accurate density functional theory calculations. The hybrid system that contains Au34 and C126H9 clusters was treated by Perdew-Wang 91 (PW91) functional using double-numerical with polarization (DNP) basis set. Interaction energies and electronic properties, i.e., energy gaps, charge redistribution and electronic densities of states (DOS), were carefully examined. The quantum population analysis by taking into consideration of electronic chemical potential so called Fermi energy reveals that the open end of SWNT has very high potential to absorb electron density and the gold nanocluster shows very promising electron donating characteristic. In the joining process, an electron transfer with a considerable magnitude of 0.84 e was observed from the gold nanocluster to the SWNT counterpart causing several bond formations between gold and carbon atoms. These findings are corresponding well with large interaction energy of -366.3 kcal/mol and supporting the creative concept in the hybrid assembly of a pair of these nanomaterial systems. In order to verify the possibility of applying the designed material in molecular bioassembly and biosensing fields of application, the interactions of a simple glycine amino acid were investigated. It should be noted that glycine molecule can bind firmly on the gold nanocluster by both amino (N-bound) and carboxylic (C-bound) functional groups. However, the N-bound interaction was found to be the more preferable configuration.



PHYS Poster Session - Electronic Structure of Transition Metal Systems and Organometallics 7:30 PM-10:00 PM, Wednesday, August 20, 2008 Pennsylvania Convention Center -- Hall C, Poster

Division of Physical Chemistry

The 236th ACS National Meeting, Philadelphia, PA, August 17-21, 2008

Nanoporous Materials ครั้งที่ 5 จำนวน 3 เรื่อง

ADSORPTIONS OF CO AND NO MOLECULES ON MOF-11: A QM/MM STUDY

PIPAT KHONGPRACHA^{1,2,3}, SUPAWADEE NAMUANGRUK⁴ JUMRAS LIMTRAKUL^{1,2,3,*}

(1) Physical Chemistry Division, Department of Chemistry, Faculty of Science,
Kasetsart University, Bangkok 10900, Thailand
(2) Center of Nanotechnology, Kasetsart University Research and Development Institute,
Kasetsart University, Bangkok 10900, Thailand
(3) NANOTEC Center of Excellence, National Nanotechnology Center,
Kasetsart University, Bangkok 10900, Thailand
(4) National Nanotechnology Center (NANOTEC), The National Science and
Technology Development Agency, 130 Phaholyothin Rd., Klong Luang,
Pathumthani 12120, Thailand

The chemistry of metal-organic frameworks (MOFs) has been extensively studied, with particular attention being paid to these porous compounds due to their many potential applications: such as gas storage; molecular sieves; and catalysis. In this work we studied the adsorptions of a molecule of the CO and NO gases on the open form of a copper dimer cluster, called the "paddlewheel" configuration, taken from the framework of the MOF-11 compound. The quantum cluster consisting of the paddlewheel and adamantine ligands was treated at the UB3LYP/6-31G(d) level of theory. In order to represent the environmental effect of the MOF framework, we applied the universal force field (UFF) to the system via our Own N-layered Integrated molecular Orbital + molecular Mechanics (ONIOM) scheme. The interaction energies in the ONIOM calculation are -8.39 and -31.24 kcal/mol for the adsorptions of CO and NO molecules, respectively. The van der Waals contributions from the framework of the MOF-11 in both systems are found to be, at most, 7% and insensitive to their interactions. These results indicate that the MOF-11 is very selective to NO gas and can be applied to separate a mixture of gases.

1. Introduction

The design and assembly of metal-organic framework networks have gained ever increasing attention in recent years due to their many potential applications: such as gas storage; molecular sieves; and catalysis [1,2]. The porous metal-organic framework (MOF) consists of metal ion units and organic ligand linkages. There are numerous transition metal (Zn^{II}, Cu^I, Ag^I or Cd^{II}) ions that have been extensively selected for being a part of secondary building units (SBUs). The SBUs possess many coordination patterns, such as the copper-

^{*} To whom correspondence should be addressed. E-mail: jumras.l@ku.ac.th

carboxylate paddlewheel, $Cu_2(O_2C_-)_4$, and the octahedral basic zinc carboxylate, $Zn_4O(O_2C_-)_6$, which act as square and octahedral joints. In addition, a number of three-dimensional coordination polymers have been characterized and prepared for connecting each of the SBUs to form a three dimensional network.

Among a large number of porous metal-organic framework compounds, Cu₂(ATC) or MOF-11 is one of the more interesting structures [3]. The formation of Cu₂(ATC) 6H₂O crystal can be assembled from a copolymerization of 1,3,5,7-adamanatane tetracarboxylate (ATC) with Cu(II) metal ions, giving the paddle-wheel Cu-C-O shape with the adamanatane network. The paddle-wheel metal cluster motif is considered to be very active for the adsorption process as there is more open area near the metal center. This accessible space is available for capturing molecules of incoming gas.

One of the main targets in the development of metal-organic frameworks is the focus on applying them to trap and separate organics and small gas molecules. To date, many of the works on these compounds have concentrated mainly on applying them for hydrogen storage. Understanding the properties of the high porosity surface materials is a very important aspect of achieving the goal to use them for gas storage. Previous *ab initio* as well as force field calculations were also utilized to investigate the adsorption properties of the compounds at the metal and polymeric linkage sites. Among many types of small gases, carbon monoxide and nitrous oxide molecules are known as common choices for probe molecules. Here, we describe the adsorption of CO and NO molecules on an MOF-11 material by taking advantage of the density functional theory. The environmental influence due to the interactions of atoms in the framework pore with a probe molecule, named the 'confinement effect' was taken into consideration via the two-layer our Own N-layered Integrated molecular Orbital + molecular Mechanics (ONIOM) technique [4].

2. Computational Details

The MOF-11 framework was modeled by the $Cu_{36}O_{144}C_{152}H_{136}$ cluster taken from its lattice structure. This cluster holds a region of eighteen copper oxide paddlewheel units connected to each other through eight adamantane organic linkages. The dangling bonds resulted from cutting the C-C bonds that were terminated by the H atoms. In order to take advantage of the computational efficiency with a satisfactory degree of accuracy, the MOF-11 cluster was divided into two layers of calculation methods as in the Quantum mechanical/Molecular mechanical (QM/MM) concept via the two-layer our Own N-layered Integrated molecular Orbital + molecular Mechanics (ONIOM2)

scheme (Figure 1). The inner layer or the quantum mechanical (QM) cluster, including one copper oxide paddlewheel and four adamantane organic linkages, was treated by the hybrid density functional theory approach (UB3LYP) combined with the 6-31G(d) basis set to represent the active site of MOF-11. The remaining extended framework that surrounds the inner layer was treated as the molecular mechanical (MM) layer via the universal force field (UFF) [5]. The force field has been found to provide a good description of the short-range van der Waals (vdW) interactions in many systems [6]. All calculations were performed using the Gaussian 03 code [7]. During optimization, only atoms in the inner layer were allowed to relax while the remainders were fixed along the position of the crystallographic lattice. A probe molecule (CO or NO) was placed nearby the active paddlewheel unit and optimized to reach the minimum energy configuration. The QM/MM adsorption energy (ΔE_{ads}) for such a probe molecule was obtained from Equation (1) while the QM adsorption energy $(\Delta E_{ads}(QM))$ was calculated from Equation (2). Thus, the MM adsorption energy $(\Delta E_{ads}(MM))$ can be derived from the difference between ΔE_{ads} and $\Delta E_{ads}(QM)$.

$$\Delta E_{ads} = E_{MOF-11/CO}^{(QM/MM)} - E_{MOF-11}^{(QM/MM)} - E_{CO}^{(QM)}$$
 (1)

$$\Delta E_{ads}(QM) = E_{MOF-11/CO}^{(QM)} - E_{MOF-11}^{(QM)} - E_{CO}^{(QM)}$$
 (2)

3. Results and Discussion

The optimized structures of the MOF-11 and their complexation with CO and NO molecules are illustrated in Figure 1. Selected geometrical parameters of the complexes and their corresponding adsorption energies are tabulated in Table 1. The CO molecule adsorbs linearly on the Cu atom inside the MOF-11 nanopore with a C-bound direction. The adsorption energy for the CO molecule is -8.39 kcal/mol. The NO molecule also interacts linearly with Cu atom with the Cu₁-N distance of 1.926 Å. On the adsorption of the CO molecule, the Cu₁ atom moves away from the cluster toward the CO molecule. The Cu₁-Cu₂ bond is lengthened from 2.525 Å to 2.771 Å while those Cu₁-O bonds are lengthened from 1.958 Å to 2.063 Å in the CO adsorption adduct. As for the MOF-11/NO complex, its adsorption energy is -31.24 kcal/mol, which comes mostly from the QM calculation for -30.88 kcal/mol (see Table 1). The effect of the extended MOF-11s framework on the probe molecules is very weak, which is due mainly to the small sizes of the molecules. The distance between the NO molecule and the Cu₁ atom is 2.372 Å. Despite the high adsorption of the NO molecule, the bonds in the metal oxide cluster are contracted. On the adsorption of the NO molecule, the Cu_1 - Cu_2 bond is contracted from 2.525 Å to 2.503 Å and those Cu_1 -O bonds are shortened slightly from 1.958 Å to 1.952 Å.

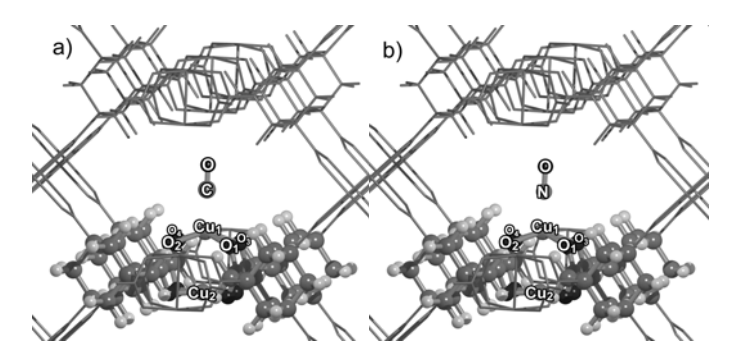


Figure 1. Models for the adsorptions of a) CO and b) NO molecules on MOF-11: the inner cluster (balls and sticks) was computed at the UB3LYP/ 6-31G(d) and the surrounding framework (lines) was treated with the universal force field (UFF).

The MOF-11/CO and MOF-11/NO adducts have been analyzed by calculating the differences of their electron densities compared to the noninteracting systems as shown in Figure 2. The results were compared to the Mulliken analysis. It is found that the electron density redistribution due to the interaction of the CO molecule with the paddlewheel cluster occurs mostly in the Cu₁ atom and CO molecule region. There is a small change of the electron density in the carboxylate groups and the Cu₂ atom. These findings are confirmed by the changes in the Mulliken charges. On the adsorption of the CO molecule, the positive charge of the Cu₁ atom decreases from 0.461 to 0.313 and the CO molecule gains a more positive charge by 0.110 while only few changes are found in the Cu_2 (+0.027) and those O_1 - O_4 (+0.016) atoms. In the case of the interaction of the NO molecule, it adsorbs on the MOF-11 framework at the same site as the CO molecule, the rearrangements of electron density are entirely different. There are much more electron density changes in both the paddlewheel and the NO molecule (Figure 2b). There are noticeable electron density reductions on both copper atoms along with electron density gatherings on those carboxylate oxygen atoms. Interestingly, there is no electron accumulation found in the intermolecular space between the paddlewheel cluster and the NO molecule. From the Mulliken population analysis, there is a very small net charge transfer (0.014 e) from the paddlewheel cluster to the NO molecule. The positive charges of copper atoms are increased from 0.461 to 0.635 and 0.553 for Cu₁ and Cu₂, respectively, while the negative charges of carboxylate oxygen atoms are also changed from -0.520 to -0.550 as well. These changes cause a higher ionicity in the metal oxide paddlewheel cluster and contract=those Cu-Cu and Cu-O bonds in the cluster.

Table 1. Optimized bond parameters (angstroms) of all isolated and adsorption complexes, adsorption energies (kcal/mol) and Mulliken populations (e). Values in parenthesis belong to isolated gas molecules.

	MOF-11	MOF-11/CO	MOF-11/NO
Cu ₁ -Cu ₂	2.525	2.771	2.503
Cu_1 - $O_{1,2,3,4}$	1.958	2.063	1.952
Cu_1 - C /- N	-	1.926	2.372
C-O/N-O	(1.137/1.159)	1.137	1.152
qCu_1	0.461	0.313	0.635
qCu_2	0.461	0.488	0.553
$qO_{1,2,3,4}$	-0.520	-0.504	-0.550
qC/qN	(0.174/0.112)	0.387	0.155
$q\mathrm{O}_{\mathrm{gas}}$	(-0.174/-0.112)	-0.277	-0.169
qCO/NO	0.000	0.110	-0.014
$\Delta Eads$	-	-8.39	-31.24
$\Delta Eads(QM)$	-	-7.82	-30.88
$\Delta Eads(MM)$	-	-0.57	-0.36

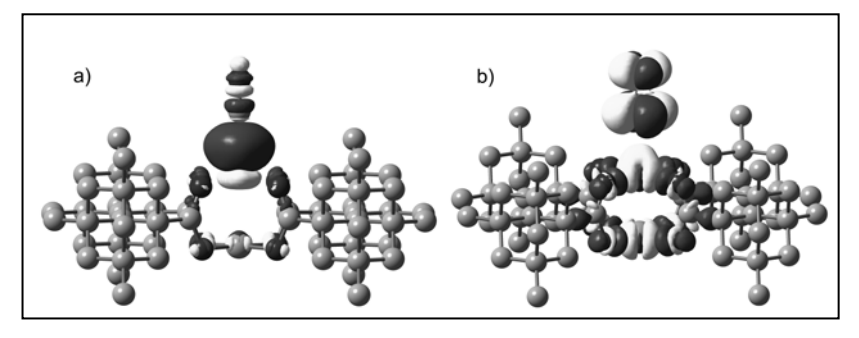


Figure 2. Electron density differences for the interactions of a) CO and b) NO molecules on the *model of the MOF-11 surface. Dark blue and light yellow surfaces refer to electron accumulating and electron depleting areas, respectively. Hydrogen atoms and the framework were excluded for clarification.

4. Conclusions

The density functional theory was used to study the adsorptions of CO and NO molecules on the open metal paddle-wheel cluster. To represent the influence of

the MOF framework on a guest molecule, we treated this issue by performing B3LYP/6-31G(d):UFF calculations through the ONIOM scheme. The adsorption energies for CO and NO molecules on MOF-11 are -8.39 and -31.24 kcal/mol, respectively. Although there is a very small amount of net electron density transfer (0.014 e) between the paddlewheel cluster and the NO molecule, the metal oxide cluster is polarized to hold a higher ionicity characteristic. Through the interaction of the NO molecule, copper atoms gain higher positive charges while those carboxylate oxygens have more negative charges, and the contractions of Cu-Cu and Cu-O bonds in the metal oxide cluster are noticeably observed. This induced ionicity causes the MOF-11/NO complex to have a much higher stability and a larger binding energy compared to the MOF-11/CO adduct. These results reveal that this type of nanoporous material is very selective to incoming guest molecules. Therefore, it can be used as a molecular sieve for separating a mixture of gases.

Acknowledgments

This work was supported in part by grants from the Thailand Research Fund and the Kasetsart University Research and Development Institute (KURDI), the National Nanotechnology Center (NANOTEC Center of Excellence and CNC Consortium) and the Commission on Higher Education, Ministry of Education under Postgraduate Education and Research Programs in Petroleum and Petrochemicals, and Advanced Materials.

References

- H. Li, M. Eddaoudi, M. O'Keeffe and O. M. Yaghi, *Nature* 402, 276 (1999).
- 2. M. Eddaoudi, D. B. Moler, H. Li, B. Chen, T. M. Reineke, M. O'Keeffe and O. M. Yaghi, *Acc. Chem. Res.* **34**, 319 (2001).
- 3. B. Chen, M. Eddaoudi, T.M. Reineke, J.W. Kampf, M. O'Keeffe, O.M. Yaghi, *J. Am. Chem. Soc.* **122**, 11559 (2000).
- S. Dapprich, I. Komiromi, K. S. Byun, K. Morokuma and M. J. Frisch, *Theochem* 461-462, 1 (1999).
- 5. A.K. Rappe, C.J. Casewit, K.S. Colwell, W.A. Goddard, W.M. Skiff *J. Am. Chem. Soc.* **114**, 10024 (1992).
- 6. S. Namuangruk, P. Khongpracha, P. Pantu, J. Limtrakul, *J. Phys. Chem. B.* **110**, 25950 (2006).
- 7. M.J. Frisch et al *Gaussian 03, revision B.05*; Gaussian, Inc.: Wallingford, CT, (2004).

ADSORPTIONS OF CH₄ AND C₂H₄ ON MOP-28 BASED CLUSTERS: A COMBINED QM AND QM/MM STUDY

SAOWAPAK CHOOMWATTANA 1,2 , PIPAT KHONGPRACHA 1,2,3 , JUMRAS LIMTRAKUL 1,2,3*

(1) Physical Chemistry Division, Department of Chemistry, Faculty of Science, Kasetsart University, Bangkok 10900, Thailand
(2) Center of Nanotechnology, Kasetsart University Research and Development Institute, Bangkok 10900, Thailand
(3) NANOTEC Center of Excellence, National Nanotechnology Center, Kasetsart University, Thailand

The adsorption properties of CH_4 and C_2H_4 on MOP-28 based clusters have been investigated by quantum mechanics (QM) and QM/MM approaches. The quantum clusters of the reaction center termed "paddlewheel" and "paddlewheel-ligand" are studied at the B3LYP/6-31G(d, p) level of theory. The environmental framework of the MOP-28 is included via a QM/MM model, where the QM has been represented by using the B3LYP while the MM is well represented by a well-calibrated universal force field, UFF. Thiophene as a ligand was found to polarize the paddlewheel. From the population charge analysis, thiophenes induced the electron transfer in the "paddlewheel" from its C atoms to O atoms, and passing over to Cu atoms. Their adsorption energies in both QM and QM/MM approaches are in the order of CH_4 (-1 kcal/mol) $< C_2H_4$ (-6 kcal/mol). The van der Waals contribution due to the environmental framework of the MOP-28 for all complexes can be accounted for up to, at most, 20% of their interactions. The combined interactions of the π -bond of the alkene molecule with Cu and backbonding of the metal to alkene have been nicely demonstrated by the natural bond orbital (NBO) analysis.

1. Introduction

Since the discovery of solids that have outstanding properties [1], such as high porosity, a new family of the porous materials, metal organic materials, has been investigated on its adsorption property, catalytic activity, and molecular storage capacity. The porous metal-organic polyhedra (MOP) is comprised of several metal clusters, each of which has two or more metal ions, and a sufficient number of capping ligands to inhibit polymerization of the metal organic polyhedra. The porous metal-organic polyhedra further includes multidentate linking ligands that connect adjacent metal clusters into a geometrical shape, describable as a

^{*} Corresponding authors: J. Limtrakul, email: fscijrl@ku.ac.th, Fax: (+66)2-562-5555 ext 2119

polyhedral, with metal clusters positioned at one or more vertices of the polyhedron [2].

MOP-28 [3] is a metal-organic truncated octahedron composed of six rigid square-shaped Cu₂(CO₂)₄ paddlewheel building units and twelve 2,2':5',2"-terthiophene-5,5"-dicarboxylate (TTDC) linkers. These linkers in the cis,cis conformation provide the critical 90° linkage for this unique construction. Previous studies showed that the MOP can trap and separate organics and small gas molecules. Till now, MOP-28 is the most porous molecular structure and stands among the first MOP to be characterized by gas sorption.

As observed in the zeolite framework, the interactions between the framework and any adsorbate molecule contribute remarkably to the sorption properties. These interactions, described by the term "confinement effect" [4, 5], consist dominantly of dispersive van der Waals interactions. For the adsorbed molecule with comparable in size to the pore dimension, the confinement effect should be considered [6].

Similar to zeolites, the MOP structure possesses a large number of atoms. To achieve the *ab initio* calculation for the paddlewheel active site with the effect from the framework taken into account, the recent development of hybrid methods, such as the embedded cluster or combined quantum mechanics/molecular mechanics (QM/MM) [7-12] methods. For very large systems, the ONIOM (our-Own-N-layered Integrated molecular Orbital + molecular Mechanics) method [13, 14], has been applied in order to reach a satisfactorily accurate result and, at the same time, with a sensible computational expense.

In this work, the adsorptions of CH_4 and C_2H_4 on MOP-28 models (QM and QM/MM) are examined to clarify the adsorption process and to address the confinement effect in the mesoporous materials. The ONIOM method enables us to use the density functional theory, for the precise treatment of the interaction between the absorbed molecule and the active site, and the universal force field (UFF) to account for the van der Waals interaction, which is found to be significant for the adsorption [15-20]. Since there is no experimental measurement for the adsorption of our chosen adsorbed molecules available now, this scheme should be only treated as a promising trend for the adsorption.

2. Methodology

The MOP-28 structure [4] is rhombohedral space group with unit cell parameters a=b=29.457(5)Å, c=54.236(20)Å. The framework consists of 6 Cu₂-(CO₂)₄ paddlewheel building blocks and 12 cis,cis-terthiophene linking units (see Figure 1). Two different strategies have been employed to model the alkane- and alkenes-

adsorbed metal-organic framework. First, the paddlewheel-ligand cluster model cut from the MOP-28 structure was used to represent the local active site of the MOP-28 framework. The quantum mechanical (QM) model with fixed terminating hydrogen atoms and probe molecules are fully geometrically optimized by employing the hybrid density functional theory (DFT) and B3LYP functional. The polarized double-ζ 6-31G(d,p) basis set was used for all light elements, while for Cu metal atoms, nonrelativistic effective core potential (ECP) was employed. The valence basis set used in connection with the ECP is essentially of double- ζ quality (the Stuttgart basis set). The QM/MM method with two-layer ONIOM (ONIOM2) scheme at B3LYP/6-31G(d,p):UFF was employed to study the adsorption. That is, for computational efficiency, only the small active region is treated quantum mechanically with the density functional theory method, while the contribution of interactions from the rest of the model is approximated by a less computationally expensive method. The B3LYP/6-31G(d,p) level of theory was applied for the paddlewheel-ligand cluster, which is considered to represent the active site. The rest of the framework was treated with the universal force field (UFF) [21]. This force field has been found to provide a good description of the short-range van der Waals interactions. All the calculations were accomplished by Gaussian 03 program package [22].

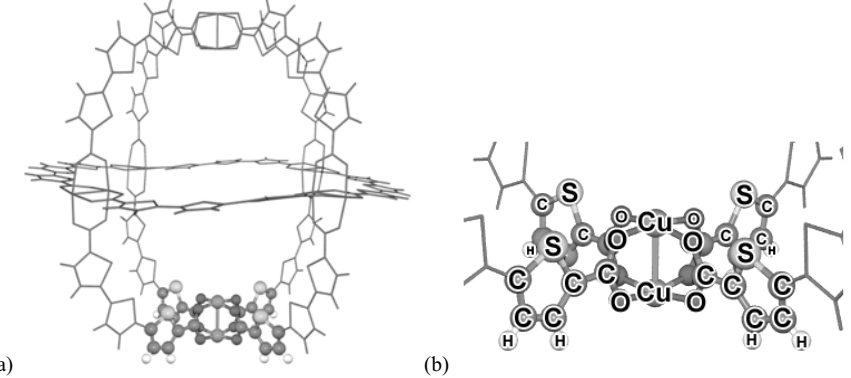


Figure 1. MOP-28 structure – (a) the framework system consists of 6 Cu₂-(CO₂)₄ paddlewheel building blocks and 12 cis,cis-terthiophene linking units (b) the closer view of paddlewheel block

3. Results and Discussion

For the purpose of clarity, the discussion is divided into three sections. First, the bare quantum mechanical (QM) model is compared to the bare quantum mechanical / molecular mechanical (QM/MM) model. Then, the adsorption of

ethylene to the clusters is discussed. In the last part, we also compare the adsorption of ethylene to those of methane with the clusters.

3.1 Comparison of the QM model to the QM/MM model

The XRD data are used to construct the paddlewheel cluster with four ligands of thiophene and the whole unit of MOP-28 which is used in the QM and QM/MM calculations, respectively (Fig.2).

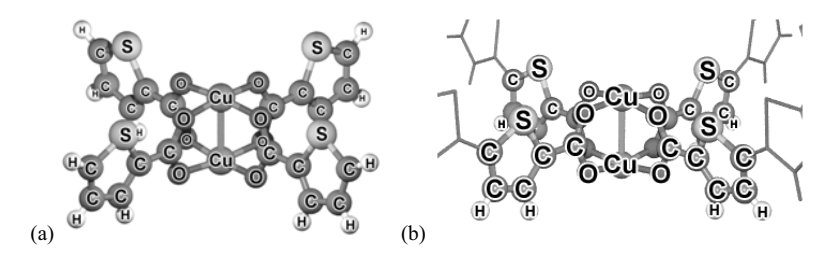


Figure 2. MOP-28 model used in the calculations. (a) For the model chosen for QM calculation, the region represented in ball-and-stick style is the active site. (b) For ONIOM approach, the active site and four linkers, calculated with B3LYP/6-31G(d,p) level of theory, is shown in ball-and-stick style. The rest of the structure is omitted for clarity.

To assess the sensitivity of the active site structure with varying environments, we optimized the active site, $[Cu_2(CO_2)_4]$ with four 2,2':5',2"-terthiophene-5,5"-dicarboxylate (TTDC) groups, known as the paddlewheel with four ligands], for all the clusters, while the remaining atoms were kept fixed at the crystallographic positions.

For the investigation on the spin state of the MOP-28 models, since the d-metal active site has a possibility not to be singlet, we investigated the spin state of the paddlewheel with four ligands quantum cluster and MOP-28 ONIOM scheme. It is found that both the quantum cluster and the ONIOM scheme are likely to be in a triplet state because the calculated energy for the triplet is lower than that for the singlet state (31.65 kcal/mol for both the quantum and ONIOM calculations). Therefore, the following discussion will be related to the bare optimized structures in the triplet state.

Regarding the geometries of the MOP-28 models, we compared the structure between the full quantum cluster of the active site and ONIOM scheme. The extended framework has the effect of insignificantly lengthening the Cu-Cu distance, as the distances are 2.512 Å and 2.519 Å for the quantum

cluster and MOP-28 ONIOM scheme, respectively, thus they have no effect on the activity of the paddlewheel active site.

3.2 The adsorption of ethylene with the clusters

The optimized structures of the adsorption complexes of C₂H₄ in both QM and ONIOM calculations are illustrated. There are two possible orientation of ethylene over the active site. It is found that the staggered orientation (Fig.3) is more stable. Then, the orientation is chosen to be studied in this work. Key geometrical parameters of the complexes and their analogous adsorption energies are shown in Table 1 and 2, respectively. We have observed C₂H₄ adsorption in different orientation. It is found to be adsorbed on the Cu atom in staggered orientation inside the cavity of MOP-28 via the π -complexation. The changes of the structural parameters that occurred in the adsorption are small. For both QM and ONIOM calculations, the Cu-Cu distance is elongated from 2.51 Å to 2.57 Å. It can be assumed that the inner Cu atom moved toward the ethylene to form an interaction. This assumption is supported by the lengthened C=C bond in the ethylene. In a detailed investigation, the combined interactions of the π-bond of C₂H₄ with Cu and backbonding of the metal to C₂H₄ is found and illustrated by natural bond orbital (NBO) analysis. It showed that π-bonding molecular orbital of C₂H₄ transfers electron to the unoccupied s orbital of the Cu atom, while the electron from d orbital of the Cu transfers back to the vacant p orbital in the C atom.

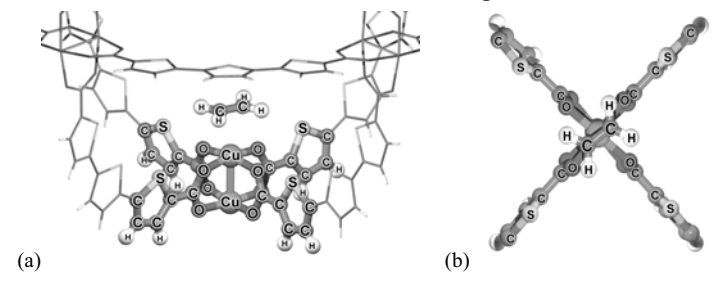


Figure 3. C_2H_4 adsorption in staggered orientation on MOP-28 in perspective (a) and top (b) view

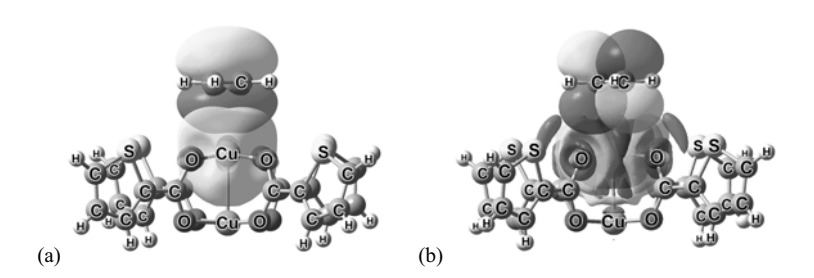


Figure 4. From NBO analysis, the C_2H_4 adsorption on MOP-28 model consists of (a) σ -donation from C_2H_4 to Cu atom (b) π -backbonding from Cu atom to C_2H_4

Analyzing the energetics, it is noted that the adsorption energy of C_2H_4 is -6.89 kcal/mol, while in the ONIOM calculation the energy is found to be -7.18 kcal/mol.

3.3 Comparison between the adsorptions of ethylene and methane with the clusters

Methane and ethylene adsorptions to the model and ONIOM scheme are performed by QM and QM/MM calculations, respectively.

Table 1. The key optimized geometrical parameters of the adsorption of CH_4 and C_2H_4 on MOP-28 models

Distance	Ql	QM		ONIOM2		
(Å)	CH ₄	C_2H_4	$\mathrm{CH_4}$	C_2H_4		
CuCu	2.520	2.571	2.518	2.572		
$CuC_{ads} \\$	3.230	2.687 2.687	3.222	2.683 2.694		
$Cu H_{\text{ads}}$	2.752 2.779	-	2.750 2.768	-		
C_{ads} - H_{ads}	1.094	-	1.094	-		
$C_{ads} = C_{ads}$	-	1.339	-	1.339		

In the bare cluster: For QM calculations, Cu...Cu = 2.512 Å

For ONIOM2 calculations, Cu...Cu = 2.519 Å

For isolated CH₄, C- H distance = 1.092 Å. For isolated C₂H₄, C=C distance = 1.330 Å

We compare the geometrical parameters in order to evaluate the interaction of adsorbents with MOP-28. As predicted, the Cu...Cu distance in the CH₄ adsorbed system is insignificantly different from the distance in the bare MOP-28, because of the molecular nonpolarity of the adsorbate. It is in the same trend with Cu...C_{ads} distances that the value in CH₄ adsorbed system is noticeably different from the distances in the C_2H_4 adsorbed system. Thus, it can be implied that the interaction of C_2H_4 is unlike the interaction of CH₄.

Since any distinction between the geometrical parameters from the QM and ONIOM calculations cannot be observed, it can hardly to be concluded that there is a confinement effect for the adsorptions of CH₄ and C₂H₄ on MOP-28 models. In the case of CH₄, the adsorption energy reveals the importance of the extended structure. Moreover, the effect would become essential if the loading is increased or size of absorbing molecules is comparable in size to the MOP nanocavity.

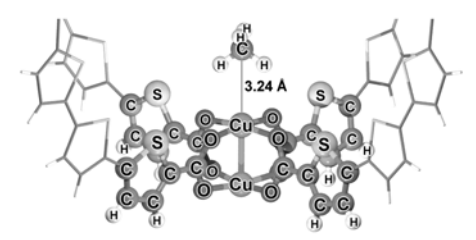


Figure 5. The adsorption of CH₄ on MOP-28 model in ONIOM calculation

Table 2. The adsorption of CH_4 and C_2H_4 on MOP-28 models at QM (B3LYP/6-31G(d,p)) and QM/MM at B3LYP/6-31G(d,p): UFF

Calculation	Adsorption Energy (kcal/mol)		
_	CH ₄	C_2H_4	
QM	-1.05	-6.89	
ONIOM2	-1.32	-7.18	

4. Conclusions

The adsorptions of CH₄ and C₂H₄ on MOP-28 were studied by using combined QM and QM/MM approaches. For the adsorption of CH₄ and C₂H₄ on MOP-28, the adsorption energies were predicted by ONIOM2 calculations to be -1.32 and -7.18 kcal/mol, respectively. The ONIOM model applied in this study can express the confinement effect of the MOP cavity. The van der Waals contribution due to the environmental framework of the MOP-28 for CH₄ adsorption and C₂H₄ adsorption complexes can be accounted for 0.27 kcal/mol (20%) and 0.29 kcal/mol (4%) respectively. The extended MOP framework that was represented by the UFF was found to be necessary for illustrating the confinement effect of the MOP and led to the further investigations on larger adsorbates.

Acknowledgements

This work was supported in part by grants from the Thailand Research Fund (to JL) and the Kasetsart University Research and Development Institute (KURDI), the National Nanotechnology Center (NANOTEC Center of Excellence and Computational Nanotechnology Consortium) and the Commission on Higher Education, Ministry of Education under Postgraduate Education and Research Programs in Petroleum and Petrochemicals, and Advanced Materials.

References

- 1. J.L.C. Rowsell and O.M. Yaghi Micropor. Mesopor. Mater. 73, 3-14 (2004).
- 2. O.M. Yaghi, A.C. Sudik, Patent, WO 028479, 2006.
- 3. Z. Ni, A. Yassar, T. Antoun, O.M. Yaghi *J. Am. Chem. Soc.*, 127, 12752 (2005).
- 4. E.G. Derouane, J.M. Andre, A.A. Lucus J. Catal. 110, 58 (1988).
- 5. C.M. Zicovich-Wilson, A. Corma, P. Viruela J. Phys. Chem. 98, 10863 (1994).
- 6. P. Pantu, B. Boekfa, J. Limtrakul *J. Mol. Catal. A* In Press, Accepted Manuscript, Available online 26 July 2007,
- 7. M. Brändle, J. Sauer J. Am. Chem. Soc. 120, 1556 (1998).
- 8. S.P. Greatbanks, I.H. Hillier, N.A. Burton, P. Sherwood *J. Chem. Phys.* **105**, 3770 (1996).
- 9. J. Limtrakul, S. Jungsuttiwong, P. Khongpracha J. Mol. Struct. 525, 153 (2000).
- 10. P. Treesukol, J.P. Lewis, J. Limtrakul, T.N. Truong *Chem. Phys. Lett.* **350**, 128 (2001).
- 11. R.Z. Khaliullin, A.T. Bell, V.B. Kazansky J. Phys. Chem. A 105, 10454 (2001).
- 12. I.H. Hillier, Theochem 463, 45 (1999).
- 13. S. Dapprich, I. Komiromi, K.S. Byun, K. Morokuma, M. J. Frisch *Theochem* **461-462**, 1 (1999).
- 14. M. Svensson, S. Humbel, R.D.J. Froese, T. Matsubara, S. Sieber, K. Morokuma *J. Phys. Chem.* 100, 19357 (1996).
- 15. P.E. Sinclair, A. de Vries, P. Sherwood, C.R.A. Catlow, R.A. van Santen *J.* Chem. Soc., Faraday **T 94**, 3401 (1998).
- 16. K. Sillar, P. Burk Theochem 589, 281 (2002).
- 17. X. Solans-Monfort, M. Sodupe, V. Branchadell, J. Sauer, R. Orlando, P. Ugliengo *J. Phys. Chem. B* **109**, 3539 (2005).
- 18. S. Kasuriya, S. Namuangruk, P. Treesukol, M. Tirtowidjojo, J. Limtrakul *J. Catal.* **219**, 320 (2003).
- 19. S. Namuangruk, P. Pantu, J. Limtrakul ChemPhysChem 6, 1333 (2005).
- 20. S. Namuangruk, P. Khongpracha, P. Pantu, J. Limtrakul *J. Phys. Chem. B* **110**, 25950 (2006).

- 21. A.K. Rappe, C.J. Casewit, K.S. Colwell, W.A. Goddard, W.M. Skiff *J. Am. Chem. Soc.* **114**, 10024 (1992).
- 22. M.J. Frisch et al *Gaussian 03, revision B.05*; Gaussian, Inc.: Wallingford, CT, (2004).

EFFECTS OF THE FRAMEWORK ON THE ADSORPTION OF METHANE ON IRMOF-1, IRMOF-2 AND IRMOF-6 METAL-ORGANIC FRAMEWORKS: A COMBINED QM AND MM STUDY

BUNDET BOEKFA 1,2 , SAOWAPAK CHOOMWATTANA 1,2 , CHULARAT WATTANAKIT 1,2 , PAILIN LIMTRAKUL 1,2 , PIBOON PANTU 1,2,3 , PIPAT KHONGPRACHA 1,2,3 , JUMRAS LIMTRAKUL 1,2,3*

The adsorption and interaction of methane on three different isoreticular metal-organic frameworks (IRMOFs) have been theoretically investigated at the ONIOM (MP2/6-31G(d,p):PM3) level of theory. Adsorption sites and various adsorbed structures were determined. Methane preferentially adsorbs at the corner region of the cubic structure of IRMOF by interacting with the three carboxylate groups of the 1,4-benzenedicarboxylate (BDC) linkers. The adsorption energy of methane on the IRMOF-1 is calculated to be -4.54 kcal/mol. The addition of a substituent on the linker molecule increases the adsorption energy to -6.75 and -5.00 kcal/mol for IRMOF-2 (BDC-Br) and IRMOF-6 (BDC-C₂H₄), respectively. The higher adsorption energy of methane in IRMOF-2 may be due to both the inductive and steric effects of the substituted Br atom.

1. Introduction

Metal-organic frameworks (MOFs) are new, important porous materials with potential applications in separation, catalysis, and gas storage [1,2]. These crystalline porous materials are composed of three-dimensional clusters of metal oxide held together by organic linkers forming into a systematic network with periodic channels and cavities in the nanoscale. The pore structure can be tailored to suit various applications by using suitable linkers.

The MOF-5 structure is composed of the oxide-centered Zn₄O tetrahedron attached to six edge-bridged carboxylate linkers to generate the octahedron-shaped secondary building unit (SBU) to reticulate the cubic structure of MOF-5. The series of frameworks based on the structure of MOF-5 have been designed without changing the cubic structure of MOF-5. By changing the linkers instead of the 1,4-benzenedicarboxylate (BDC) the various IRMOF structures were synthesized. Yaghi and coworkers [3] synthesized IRMOF

1

⁽¹⁾ Department of Chemistry, Faculty of Science, Kasetsart University, Bangkok 10900, Thailand

⁽²⁾Center of Nanotechnology, Kasetsart University Research and Development Institute, Bangkok 10900, Thailand

⁽³⁾NANOTEC Center of Excellence, National Nanotechnology Center, Kasetsart University, Bangkok 10900, Thailand

^{*}Corresponding authors: J. Limtrakul, email: fscijrl@ku.ac.th, Fax: (+66)2-562-5555 ext 2119

materials with pore sizes ranging from 3.8-28.8 Å. These materials also have the advantages of low density (1.0 to 0.20 g/cm³) and high surface areas (500 to 4,500 m²/g). Therefore, MOFs are excellent materials for molecular storage and molecular sieves [3,4]. The IRMOF-6 was reported to have the highest methane storage capacity. [3]

The methane storage on IRMOF-6 has been studied and compared with other materials such as FAU zeolite, silicalite zeolite, MCM-41 and carbon nanotubes [5, 6]. The IRMOF-6 is one of the best materials for methane storage due to its high free volume, low framework density, and strong energetic interaction between the framework and methane molecules. In addition to this, the simulations show that the linkers change to 1,4-tetrabromobenzene-dicarboxylate and 9,10-anthracenedicarboxylate, the amount adsorbed per volume can be increased [5].

One of the main targets in the development of metal-organic frameworks is the focus on applying them to trap and separate organics and small gas molecules, especially for hydrogen storage and methane storage. [3-10] Understanding the properties of the high porosity surface materials is a very important aspect of achieving the goals for being suitable for gas storage. The knowledge of adsorption sites and interactions with the adsorbed molecule would be of great benefit for the design of better metal-organic frameworks. In this study, the interactions of methane on IRMOF-1 (BDC-H), IRMOF-2 (BDC-Br) and IRMOF-6 (BDC-C₂H₄), are investigated with the ONIOM calculation. The aims of this paper are: 1) to investigate the adsorption behavior of methane on IRMOF; 2) to discuss the effect of the framework from the ONIOM calculation; and 3) to study the effect of the linker-BDC to the adsorption properties of methane via IRMOF-1, 2 and 6.

2. Methodology

The structures of IRMOF were generated from the crystallographic X-Ray pattern [2]. The smallest model consisted of Zn₄O(CO₂)₆ and one BDC linker (total of 39 atoms). The next model had the metal cluster and three BDC linkers to represent a corner of the cubic structure of MOF-5 (total of 59 atoms). Full quantum calculations were used for these two models. To include the extended framework of the MOF-5 structure, the ONIOM2 method was employed to take advantage of the computational efficiency with a satisfactory degree of accuracy. The IRMOF-1 cluster was divided into two layers of calculation methods. The inner layer was the cluster of 59 atoms modeled with density

functional theory B3LYP/3-21G. The extended structures up to 1215 were modeled with semi-empirical methods. The extended 251-atom model covered the six $\rm Zn_4O(CO_2)_6$ clusters around the quantum cluster. The extended 439-atom model covered one complete unit cell (see Fig. 1). The largest model of 1215 atoms covered the 8 unit cells. The structures of IRMOF-2 and IRMOF-6 were similar to the IRMOF-1 but with different linker molecules (see Fig. 2).

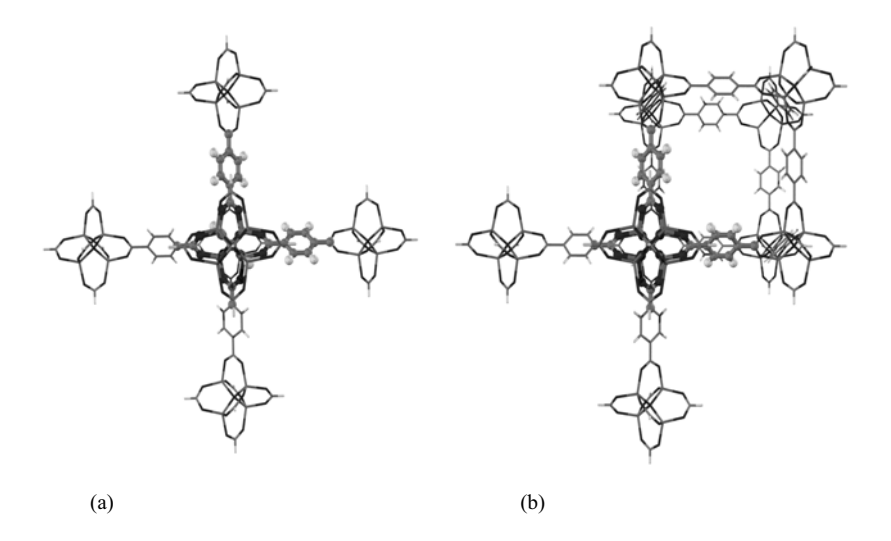


Figure 1. The IRMOF-1 structure represented with (a) 251 atoms and (b) 439 atoms. The high level region of one $Zn_4O(CO_2)_6$ unit and three BDC linkers (total of 59 atoms) at the center is illustrated by ball-and-stick and the extended framework is illustrated by wire frame.



Figure 2. Linker structure of various isoreticular metal-organic frameworks (MOFs).

The $Zn_4O(CO_2)_6$ cluster and the probe molecule were allowed to relax while the linkers were kept fixed along the crystalline coordinates. The single point energy calculations at MP2/6-31G(d,p) level of theory were performed to refine the adsorption energies since it is known that DFT does not take into account the dispersion force of the interactions. The extended frameworks are treated with 3 approaches: AM1; PM3; and UFF levels of calculation via ONIOM methodology [13]. All calculations were performed with the Gaussian 03 program [14].

3. Results and Discussion

3.1 The effect of the cluster size on the adsorption of methane

Adsorption of methane on IRMOF-1 was investigated on various sizes of fragment clusters. The smallest model consisted of Zn₄O(CO₂)₆ and one BDC linker (total of 39 atoms). The next model added two more BDC linkers to complete one corner of the cubic structure of MOF-5 (total of 59 atoms). Extended structures of the IRMOF-1 were included by using the ONIOM2 method. Semi-empirical methods were used to model extended structures up to 251 and 439 atoms. The structure optimizations were done at the BYLYP/3-21G. The single point energy calculations at MP2/6-31G(d,p) level of theory were performed to refine the adsorption energies since it is known that DFT does not take into account the dispersion force of the interactions. The calculated structures for Zn-O and O-C distances were close to experimental measurements of 1.91 and 1.30 Å, respectively. The O-C-O and Zn-O-C angles were also close to experimental measured values of 125.0 and 130.4 degrees, respectively [1, 10]. Methane adsorbed on the corner region having its three hydrogen atoms placed in the middle of each pair of carboxylate groups of the linkers (see Fig. 3). For example, the distances between the H1 atom of the adsorbed methane to O1 and O6 of the carboxylate groups are almost equal at 2.85, and 2.90 Å, respectively.

The calculated adsorption energies were tabulated in Table 1. The adsorption energy was -3.97 kcal/mol for the smallest cluster. Increasing the cluster size to 59 atoms increased the adsorption energy to -4.27 kcal/mol. Addition of the extended framework by semi-empirical methods slightly increased the overall adsorption energy by 0.2-0.4 kcal/mol. Although the effect of the extended framework is very little at this low loading condition, it may be important for the adsorption at high loading. All the semi-empirical methods

used in this study showed similar results. The PM3 method was selected for further study because this approach always provides more reliable results for structure and adsorption properties of the complexes involving metal-ligand as well as hydrogen bonding interactions as compared to the AM1 approach.

Table 1. Adsorption energies (kcal/mol) of methane on IRMOF-1 with MP2/6-31G(d,p)//B3LYP/3-21G.

	Size of framework (atoms)					
Methods	39	59	59/251	59/439	59/1215	
MP2	-3.97	-4.27				
MP2:AM1			-4.55	-4.60		
MP2:PM3			-4.52	-4.54		
MP2:UFF			-4.67	-4.69	-4.68	

Other adsorption structures were also studied. Methane can also adsorb on one of the carboxylate oxygen atoms, but with a smaller adsorption energy. Methane was found to have little interaction with the benzene ring, and an adsorption structure near the benzene ring was not found.

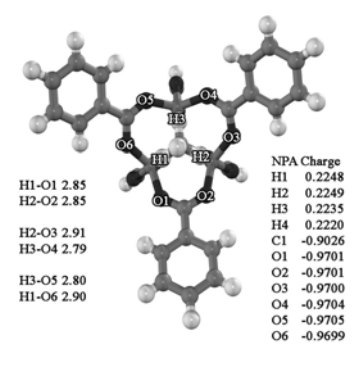


Figure 3. The optimized structure of the methane adsorption on IRMOF-1. Atoms near the adsorption site are labeled atomically and numerically and the extended framework is omitted for clarity. Selected distances (in Å) and NPA charge parameters are shown.

3.2 Methane adsorption on IRMOF-2 and IRMOF-6

The methane adsorptions on IRMOF- 1, 2 and 6 have been studied with ONIOM MP2/6-31G(d,p):PM3//B3LYP/3-21G:PM3. The optimized structures

are shown in Fig. 4. The adsorption energies of methane are -4.54, -6.75 and -5.00 kcal/mol for IRMOF-1, 2 and 6, respectively.

Table 2. The geometrical parameters of methane on IRMOF-1, 2 and 6 with MP2/6-31G(d,p):PM3//B3LYP/3-21G:PM3 (distances in Å and angles in radius).

	IRMOF-1 59/439		IRMOF-2 59/439		71/499	
	Bare	Complex	Bare	Complex	Bare	Complex
distances						
Zn-O1	1.88	1.88	1.86	1.86	1.86	1.86
Zn-O2	1.88	1.88	1.87	1.87	1.86	1.86
O1-C1	1.29	1.29	1.28	1.28	1.28	1.28
O2-C1	1.29	1.29	1.29	1.28	1.28	1.28
O1 H1		2.85		2.72		2.82
O2 H2		2.85		3.33		2.89
H1-C	1.09	1.09	1.09	1.09	1.09	1.09
Н2-С	1.09	1.09	1.09	1.09	1.09	1.09
O1 C		3.63		3.64		3.61
O2 C		3.63		3.89		3.74
angles						
O2-C1-O2	121.8	121.8	122.8	122.9	123.5	123.6
C1-O1-Zn1	132.8	132.6	138.1	138.3	131.7	132.1
C1-O2-Zn2	132.8	132.9	125.7	125.6	131.6	131.2
O1-H1-C		127.2		141.7		133.1
O2-H2-C		126.9		113.0		125.8

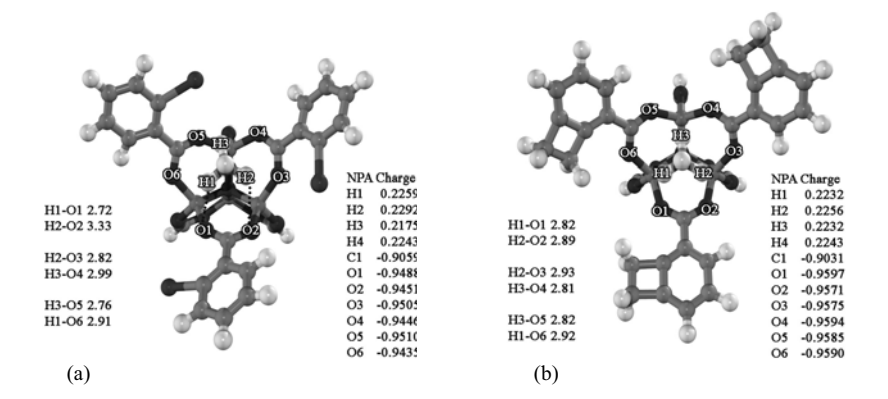


Figure 4. The optimized structure of the methane adsorption on (a) IRMOF-2 and (b) IRMOF-6. Atoms near the adsorption site are labeled atomically and numerically and the extended framework is omitted for clarity. Selected distances (in Å) and NPA charge parameters are shown.

The substituent groups on IRMOF-2 and IRMOF-6 caused unsymmetrical adsorption. The interaction between the hydrogen atom (H1) of methane to the O1 oxygen atom, that sits closer to the Br atom, appeared to be stronger than the interaction between the H2 and O2 atoms as indicated by the shorter distance of

O1--H1 (2.72 Å) than the O2--H2 distance (3.33 Å). Due to the electron withdrawing property of the Br atom, the atomic charges of oxygen atoms of the carboxlyate groups of IRMOF-2 (average of -0.95 e) are slightly less negative than on the other (average of -0.97 and -0.96 e for IRMOF-1 and IRMOF-6, respectively). The stronger adsorption energy for IRMOF-2 and IRMOF-6 as compared to the unsubstituted IRMOF-1 is due to the reduction in pore size that is well known to enhance the interaction energy and in the case of the IRMOF-2, to some extent, may be due to the inductive effect of the Br atom. The higher adsorption energy on IRMOF-6 compared to IRMOF-1 is in agreement with its better methane uptake [3]. Düren [5] also reported that the isosteric heat of adsorption at low loading of methane on IRMOF-6 was higher than that on IRMOF-1 and predicted that a higher adsorption heat for IRMOF-2 (than that of IRMOF-6), which used 1,4-tetrabromobenzenedicarboxylate as the linker molecule. In this study, we also observed the same trend of adsorption energies, IRMOF-1 < IRMOF-6 < IRMOF-2.

4. Conclusions

The influence of the extended metal-organic framework (MOF) on adsorption properties of methane interacted with various isoreticular MOFs, namely IRMOF-1, IRMOF-2, IRMOF-6 were carried out at the well-calibrated MP2/6-31G(d,p):PM3 theoretical level, the MP2/6-31G(d,p) is used for the high level, while the low level is treated with PM3. Although the effect of the extended structure at low loading amounts to only about 10%, it may, however, be essential if the loading is increased. The interactions of methane with three different MOF derivatives: IRMOF-1; IRMOF-2; and IRMOF-6 are predicted to be -4.54, -6.75 and -5.00 kcal/mol, respectively. The substituent groups on IRMOFs (X = H, Br, and C_2H_4) play a prominent role in the structure and adsorption properties of the complexes, which is due to their inductive and steric effects being in good agreement with experimental observations. This information is useful for diffusion properties, adsorption capacity, and reaction mechanisms, which is important for material development.

Acknowledgments

This work was supported in part by grants from the Thailand Research Fund (to JL) and the Kasetsart University Research and Development Institute (KURDI), the National Nanotechnology Center (NANOTEC Center of Excellence and Computational Nanoscience Consortium) and the Commission on Higher

Education, Ministry of Education under Postgraduate Education and Research Programs in Petroleum and Petrochemicals, and Advanced Materials.

References

- H. Li, M. Eddaoudi, M. O'Keeffe and O. M. Yaghi, *Nature* 402, 276 (1999).
- 2. M. Eddaoudi, D. B. Moler, H. Li, B. Chen, T. M. Reineke, M. O'Keeffe and O. M. Yaghi, *Acc. Chem. Res.* **34**, 319 (2001).
- 3. M. Eddaoudi, J. Kim, N. Rosi, D. Vodak, J. Wachter, M. O'Keeffe and O. M. Yaghi, *Science* **295**, 469 (2002).
- 4. N. L. Rosi, J. Eckert, M. Eddaoudi, D. T. Vodak, J. Kim, M. O'Keeffe and O. M. Yaghi, *Science* **300**, 1127 (2003).
- 5. T. Düren, L. Sarkisov, O. M. Yaghi and R. Q. Snurr, *Langmuir* **20**, 2683 (2004).
- 6. M. J. Rosseinsky, Microporous Mesoporous Mater. 73, 15 (2004).
- 7. J. L. C. Rowsell, E. C. Spencer, J. Eckert, J. A. K. Howard and O. M. Yaghi, *Science* **309**, 1350 (2005).
- 8. T. Sagara, J. Klassen, J. Ortony and E. Ganz, *J. Chem. Phys.* **123**, 014701 (2005).
- 9. M. Fuentes-Cabrera, D. M. Nicholson and B. G. Sumpter, *J. Chem. Phys.* **123**, 124713 (2005).
- 10. A. Samanta, T. Furuta and J. Li, J. Chem. Phys. 125, 084714 (2006).
- 11. D. Y. Siberio-Pérez, A. G. Wong-Foy, O. M. Yaghi and A. J. Matzger, *Chem. Mater.* **19**, 3681 (2007).
- 12. S. Pawsey, I. Moudrakovski, J. Ripmeester, L.-Q. Wang, G. J. Exarhos, J. L. C. Rowsell and O. M. Yaghi, *J. Phys. Chem. C* **111**, 6060 (2007).
- 13. S. Dapprich, I. Komiromi, K. S. Byun, K. Morokuma and M. J. Frisch, *Theochem* **461-462**, 1 (1999) .
- 14. M.J. Frisch et al *Gaussian 03, revision B.05*; Gaussian, Inc.: Wallingford, CT, (2004).

สรุปกิจกรรมที่เกี่ยวข้อง

การประชุมเมธิวิจัยอาวุโส สกว.

ในหัวข้อเรื่อง "การออกแบบ การวิเคราะห์สมบัติ การ ผลิต และการประยุกต์ใช้งานวัสดุในระดับนาโน"

> เมื่อวันที่ 10 กันยายน 2551 ณ โรงแรมรามาการ์เด้นส์ กรุงเทพฯ

รายงานสรุปการจัดประชุมวิชาการ เมธีวิจัยอาวุโส สกว.

"การออกแบบ การวิเคราะห์สมบัติ การผลิต และการประยุกต์ใช้งานวัสดุในระดับนาโน"

วัตถุประสงค์ของการจัดประชุมวิชาการฯ

- 1. เพื่อติดตามความก้าวหน้าของนักวิจัยภายในกลุ่ม ผ่านการนำเสนอผลงานวิจัยทั้งแบบโปสเตอร์ และแบบปากเปล่า
- 2. เพื่อเปิดโอกาสให้นักวิจัยของกลุ่มได้นำเสนอผลงานวิจัยที่ได้รับการสนับสนุนจาก สกว. อีกทั้งได้ แลกเปลี่ยนความรู้ความคิดเห็นซึ่งกันและกัน อันจะนำไปสู่การพัฒนาคุณภาพงานวิจัยต่อไป

ประโยชน์ที่ได้รับจากการจัดประชุมวิชาการฯ

- 1. ได้ทราบความก้าวหน้าของงานวิจัยที่อยู่ภายใต้แผนของโครงการฯ การติดตามสถานะงานวิจัย จะนำไปสู่การปรับปรุงการทำงานวิจัย เพื่อให้นักวิจัยสามารถผลิตผลงานได้ทันตามแผนที่วางไว้
- 2. ทำให้เกิดการพบปะแลกเปลี่ยนความคิดเห็น และรับฟังปัญหาในการดำเนินงานวิจัยระหว่าง หัวหน้าโครงการและนักวิจัยในโครงการได้อย่างใกล้ชิด ซึ่งการระดมความคิดจากนักวิจัยหลายๆ ท่านและจากหลายสาขาวิชาจะทำให้เกิดการพัฒนางานร่วมกันอย่างมีประสิทธิภาพ
- 3. เปิดโอกาสให้นิสิตทั้งที่มีและไม่มีส่วนร่วมในงานวิจัย ได้ทราบถึงทิศทางและความสำคัญของ งานวิจัยภายใต้แผนของโครงการฯ ซึ่งอาจสร้างแรงจูงใจให้นิสิตเหล่านี้เข้ามามีส่วนร่วมในการ ทำวิจัย โดยผู้ช่วยวิจัยในระดับบัณฑิตศึกษาถือเป็นกำลังสำคัญที่ผลักดันให้งานวิจัยสำเร็จลุล่วง ไปได้ด้วยดี

สรุป

การจัดประชุมวิชาการฯ ในครั้งนี้บรรลุวัตถุประสงค์เป็นอย่างดียิ่ง

ข้อเสนอแนะจาผู้เข่าร่วมประชุม

- 1. นักวิจัยต้องการให้มีการจัดประชุมมากกว่าหนึ่งวัน เนื่องจากต้องการนำเสนอเนื้อหาให้ครบถ้วน เพื่อให้ผู้เข้าร่วมประชุมสามารถติดตามการนำเสนอได้อย่างเข้าใจ ซึ่งจะนำไปสู่การเสนอแนะ ข้อมูลที่เป็นประโยชน์ได้อย่างมีประสิทธิภาพ
- 2. นักวิจัยต้องการให้มีการจัด workshop เพื่อให้เห็นภาพรวมในการทำงานวิจัยที่ชัดเจนขึ้น โดยเฉพาะงานวิจัยทางด้านเคมีคอมพิวเตอร์ ซึ่งนักวิจัยทางด้านการทดลองสามารถนำมาใช้ ศึกษาเพิ่มเติมเพื่อให้หัวข้อวิจัยที่ทำอยู่มีความสมบูรณ์มากขึ้น
- 3. นักวิจัยต้องการให้มีการเชิญผู้เชี่ยวชาญจากต่างประเทศในหัวข้อที่น่าสนใจมาบรรยายเพื่อให้ ได้รับความรู้ ประสบการณ์ และความคิดเห็นใหม่ๆที่จะนำมาพัฒนางานวิจัยต่อไป

อื่น ๆ

ได้แนบเอกสารเพิ่มเติมเพื่อการรายงานที่สมบูรณ์ขึ้นดังนี้

- 1. โปรแกรมและบทคัดย่อของการจัดประชุมวิชาการฯ
- 2. สำเนารายชื่อผู้เข้าร่วมการประชุมวิชาการฯ

บรรยากาศ การเข้าร่วมประชุมวิชาการฯ



































